UNIVERSITÀ DEGLI STUDI DI PALERMO
DIPARTIMENTO DI BIOMEDICINA SPERIMENTALE E NEUROSCIENZE CLINICHE

Dottorato in Medicina Sperimentale e Molecolare

APPLICATION OF NOVEL 3D CULTURE MODELS OF HUMAN MUCOSAE TO STUDY THE EFFECTS OF ENVIRONMENTAL FACTORS ON NON-COMMUNICABLE DISEASES

S.S.D. BIO/16 - Anatomia Umana

TESI DI

Dr. Alberto Fucarino

COORDINATORE DEL DOTTORATO

Chiar.mo Prof. G. Zummo

TUTOR

Chiar.mo Prof. F. Bucchieri

CICLO XXIV

List of Contents

LIST OF FIGURES

ABBREVIATIONS

AD	**Atopic Dermatitis**
AJ	**Adherens Junctions**
ALI	**Air Liquid Interface**
BEBM	**Bronchial Epithelial Basal Medium**
BEGM	**Bronchial Epithelial Growth Medium**
BSA	**Bovine Serum Albumine**
BSC	**Biological Security Cabinet**
CaCl2	**Calcium Chloride**
CAL	**Chronic Airflow Limitation**
CCR3	**Chemochine Receptor 3**
COAD	**Chronic Obstructive Airway Disease**
COLD	**Chronic Obstructive Lung Disease**
COPD	**Chronic Obstructive Pulmonary Disease**
CORD	**Chronic Obstructive Respiratory Disease**
CSE	**Cigarette Smoke Extract**
DMEM	**Dulbecco's Modified Eagle Medium**
ECM	**Extra Cellular Matrix**
EEM	**Epon Embedding Media**
EGTA	**Ethylene glycol tetraacetic acid**
EHS	**Engelbreth-Holm-Swarm**
ELISA	**Enzyme-Linked Immuno-Sorbent Assay**
EMTU	**Epithelial Mesenchymal Trophic Unit**

ER **Endoplasmatic Reticulum**

FCS **Fetal Calf Serum**

FEV1 **Forced Expiratory Volume in 1 Second**

FVC **Forced Vital Capacity**

GINA **Global Initiative for Asthma**

HBEC **Human Bronchial Epithelial Cells**

HBSS **Hank"s balanced salt solution**

HDM **House Dust Mite**

HH **Hygiene Hypothesis**

HRP **Horseradish perossidasi**

ICS **Inhaled CorticosteroidS**

IFN **Interferon**

Ig **Immunoglobulin**

IL **Interleukin**

MgCl2 **Magnesium Chloride**

moDC **monocytic Dendritic Cells**

NaCl **Sodium Chloride**

OVA **Ovalbumin**

PAOM **Pseudomonas Aeruginosa PAO1 conditioned Medium**

PBS **Phosphate Buffered Saline**

PCR **Polymerase Chain Reaction**

PET **PolyEthylene Terephthalate**

PO **Propylene Oxide**

PVDF	**Polyvinylidene Fluoride**
SCF	**Stem Cells Factor**
SEM	**Scanning Electron Microscopy**
SSCP	**Single-Strand Conformation Polymorphism**
TEM	**Transmission Electron Microscopy**
TER	**Transepithelial Electrical Resistance**
Th	**T-helper**
TJ	**Tight Junctions**
TNF	**Tumor Necrosys Factor**
TSLP	**Thymic Stromal Lymphopoietin**
WHO	**World Health Organization**

ACKNOWLEDGEMENTS

Perdonatemi questa libertà, ma penso che non sarei in grado di esprimere in maniera altrettanto precisa quanto segue, non usando la mia lingua natia. For Pieter and only for Pieter: Ask to Maria to translate it for you, and after that tell all the story to guys because I want they know how much I am profoundly grateful for all the attentions they had for me. Penso sia necessario partire dall'inizio, che questi ringraziamenti debbano iniziare dalla persona che involontariamente mi ha spinto a scegliere questa strada. È chiaro che comunque c'erano già la passione, la voglia e il desiderio di fare ricerca, ma c'erano anche tanti e tanti dubbi. Poi un giorno mi sono ritrovato a leggere, ultimo anno di università, uno di quegli stupidi giornaletti che distribuiscono a mensa: un insieme di pubblicità, annunci e raramente qualche raro articolo sulla vita accademica. All'interno di uno di questi articoli, un giovane ricercatore, un tale Francesco esponeva quanto segue: "Nella vita, i soldi vanno e vengono, la salute può andare e venire, la posizione lavorativa, gli affetti, i dispiaceri e tantissime altre cose sono soggetti a transitorietà, ma la conoscenza, tutto quanto è stato appreso da esperienze personali e con il piacere di sapere, quello rimarrà sempre". Penso che in quel momento sia scattata in me la molla di: "Io voglio far ricerca". Non solo per l'opportunità di ampliare smisuramente quanto già sapevo ma anche per l'opportunità di conoscere realtà diverse cosa che un ragazzo di quell'età, in Italia, non può certo farsi sfuggire. Mi sembra doveroso iniziare con il ringraziare le due persone che più mi hanno aiutato e sostenuto in questi tre anni di dottorato, non che siano stati gli unici, ma sicuramente fondamentali e insostituibili: Fabio e Maria. Inutile elogiare le loro qualità professionali, quanto mi abbiano trasmesso e quanto fondamentale il loro supporto tecnico sia stato, ma è il lato umano quello che è stato più importante per me. Sono stati in grado di rendere l'ambiente di lavoro come casa, a dire il vero anche meglio di casa, entrambi sono persone polivalenti, con interessi vari e incredibile curiosità. Se non fosse stato per loro, questi tre anni sarebbero stati sicuramente di ben altra fattura. Ancora grazie, spero di poter fare per voi la metà di quanto avete fatto per me. Ringrazio il Prof. Zummo, la cui operatività, umanità e meraviglioso modo di vedere il mondo della ricerca, permette una realtà altrimenti difficilmente realizzabile a Palermo. Ringrazio il Prof. Cappello che dedica al

nostro dottorato appena ventotto ore al giorno, maestro della tecnica "Bastone e Carota", e che ogni giorno mi permette di imparare qualcosa di nuovo. Ringrazio Francesca e Luigi, compagni di avventura, con cui ho condiviso gioie e dolori, patemi e successi, ma soprattutto incredibili esperienze. Un'altra menzione particolare va a Pieter e Letty che sono stati capaci di farmi sentire a casa immediatamente, che hanno reso un'esperienza inizialmente piena di paura, un ricordo magico e incredibile. Come essere lì da sempre, mi son sentito importante e immerso in un gruppo di amici. Famiglia e colleghi non possono essere scelti, mentre gli amici sì, e il sentirsi scelto è stata una sensazione impareggiabile. Ringrazio tutti i ragazzi del gruppo di polmonologia del LUMC, ognuno di loro ha dedicato ore e ore a sopportarmi, aiutarmi e guidarmi. Senza di voi, buona parte di questa tesi non sarebbe qui. In realtà ci sono ancora tante altre persone che dovrei ringraziare, da Antonella a Vanessa, da Ilenia a Gabriele, da Alessandro a Ettore, ma so già che mi sono dilungato troppo e concesso fin troppe licenze; permettetemi quindi di concludere ringraziando quanti invece qui non sono citati, quanti adesso nella mia vita non ci sono più o sono solo un aspetto marginale, e a voi, amici che ho perso in questi anni che dedico maggiormente questa tesi. Purtroppo il dedicare tanto al lavoro ha necessariamente tolto a qualche altro ambito, e il tempo da poter dedicare allo stare insieme, si è assottigliato sempre più. Un anno di lontananza ha influito, così come queste feste dedicate esclusivamente alla scrittura. E per quanto oggi, non siate più punti fermi nella mia vita, sappiate che vi voglio bene. Vi lascio alla lettura, ma era giusto che sapeste che senza il contributo di tutte queste meravigliose persone, questa tesi, oggi, non sarebbe qui.

1.INTRODUCTION

1.1 Respiratory system

The main functions of the respiratory system involve carrying out gas exchange, bringing oxygen into the body and removing carbon dioxide waste by metabolism. The system includes the nose, pharynx, larynx, trachea, bronchi, and lungs and pleurae. The respiratory system is divided into upper and lower segments. The nose and pharynx (throat) make up the upper respiratory system. Both of these structures are also part of the digestive system. The lower respiratory system consists of the larynx or voice box, trachea (windpipe), bronchi, and lungs and pleurae (serous membranes that cover the lungs), the upper surface of the diaphragm, and numerous other structures within the thoracic cage. Inhaled air is warmed, moistened, and initially filtered in the upper respiratory system. The nose has an internal nasal cavity with an olfactory region and a respiratory region. The pharynx begins at the posterior end of the nasal cavity. Inhaled air passes through the nasal cavity into the pharynx. A mucous membrane lines the nasal cavity and the pharynx. In the respiratory region of the nose, the epithelium covering the membrane contains glands that produce lubricating mucus, which, together with the epithelial cilia, help trap unwanted particles in inhaled air. The upper respiratory system also includes the nasal conchae, vocal cords, and eustachian tubes.

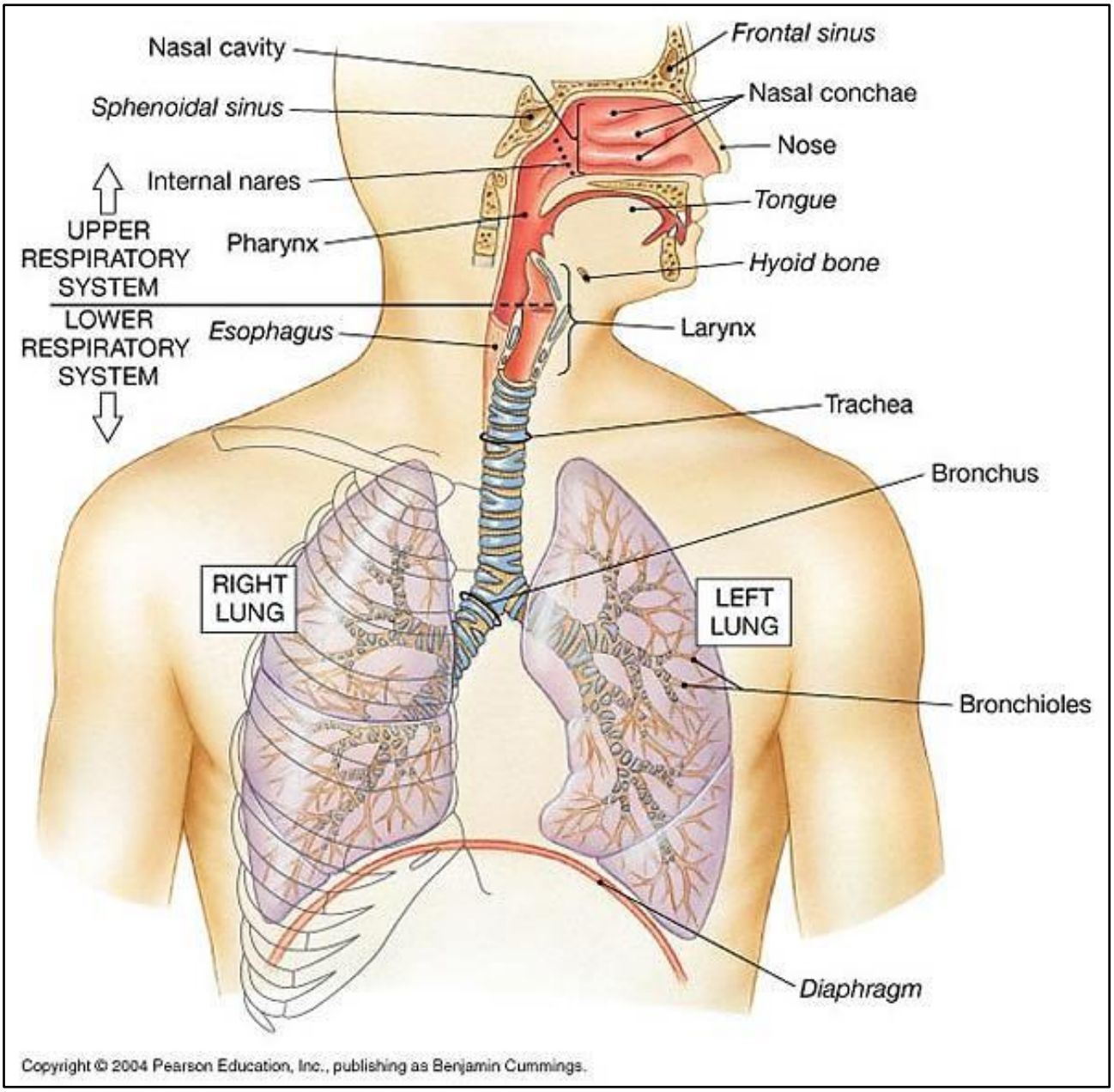

***Fig.1**: Schematic view of the human respiratory system.*

1.2.1 The lower respiratory system

The upper region continues into the lower respiratory system at the larynx. The lower respiratory system consists of the larynx, trachea, bronchi and lungs and pleural linings that enclose them. Inhaled air moves from pharynx through the larynx, then enters the right or left bronchi and passes through the branching airways (secondary bronchi, tertiary bronchi and higher order branches and bronchioles) into the lungs. These progressively smaller airways deliver oxygen rich air to the lungs, where gas exchange occurs in tiny air sacs called alveoli. Exhaled air containing carbon dioxide leaves the body by the same route in

reverse. The trachea is a major airway of the lower respiratory system. The trachea is a cartilaginous and membranous tube extending from the lower part of the larynx to the upper border of the fifth thoracic vertebra, where it divides into the two bronchi, one for each lung. The trachea is an almost cylindrical structure that measures about 11 cm in length, with a diameter of about 2.5 cm (Murray, 1986). The trachea is composed of rings of hyaline cartilage wrapped in elastic fibrous membrane; its interior is lined with a mucous membrane. The tracheal cartilages are stacked horizontally and separated by narrow intervals. They provide structural support that helps keep the airway open and are typically highly elastic until advanced age. The number of cartilages varies from 16 to 20; each forms an incomplete, crescent shaped ring around the frontal two thirds of the tube.

The bronchi and their subdivisions are major airways of the lower respiratory system. The bronchi begin at the right and left primary bronchus and divide into the secondary bronchi with a smaller diameter that enter the lungs. In the lungs, further branching results in yet narrower secondary and tertiary bronchi that in turn subdivide into bronchioles.

The primary bronchi have a similar composition to the trachea. In the right primary bronchus, the number of cartilaginous rings varies from six to eight, and in the left primary bronchus, from nine to twelve. The right bronchus is wider, shorter, and oriented more vertically than the left. The right bronchus divides into three main secondary bronchi that service the three lobes of the right lung. The left bronchus bifurcates into two secondary bronchi that service the two lobes of the lung.

The secondary bronchi, also termed lobar or intrapulmonary bronchi, are airways of the lower respiratory system. They branch from the paired bronchi to service the lobes of the right and left lungs, respectively. Within a lung, the lobar bronchi divide and subdivide throughout the entire organ, with the smallest subdivisions forming the narrow diameter tubes called bronchioles. In lieu of cartilaginous rings, secondary bronchi are supported by irregular plates of hyaline cartilage.

Tertiary bronchi are relatively narrow airways of the lower respiratory system. Each lung contains ten tertiary bronchi that arise from the secondary bronchi branching in the lung lobes, and their support structure contains only small

amounts of cartilage. As tertiary bronchi branch in turn, they give rise to even narrower bronchioles that contain no cartilage at all. Situated deep in the lungs, these lobular bronchioles are only about 0.2 mm in diameter. Each divides into two or more respiratory bronchioles, serving scattered alveoli. The division of these bronchioles forms further branches that service additional alveoli (Kuhn, 1978; Jeffrey, 2003).

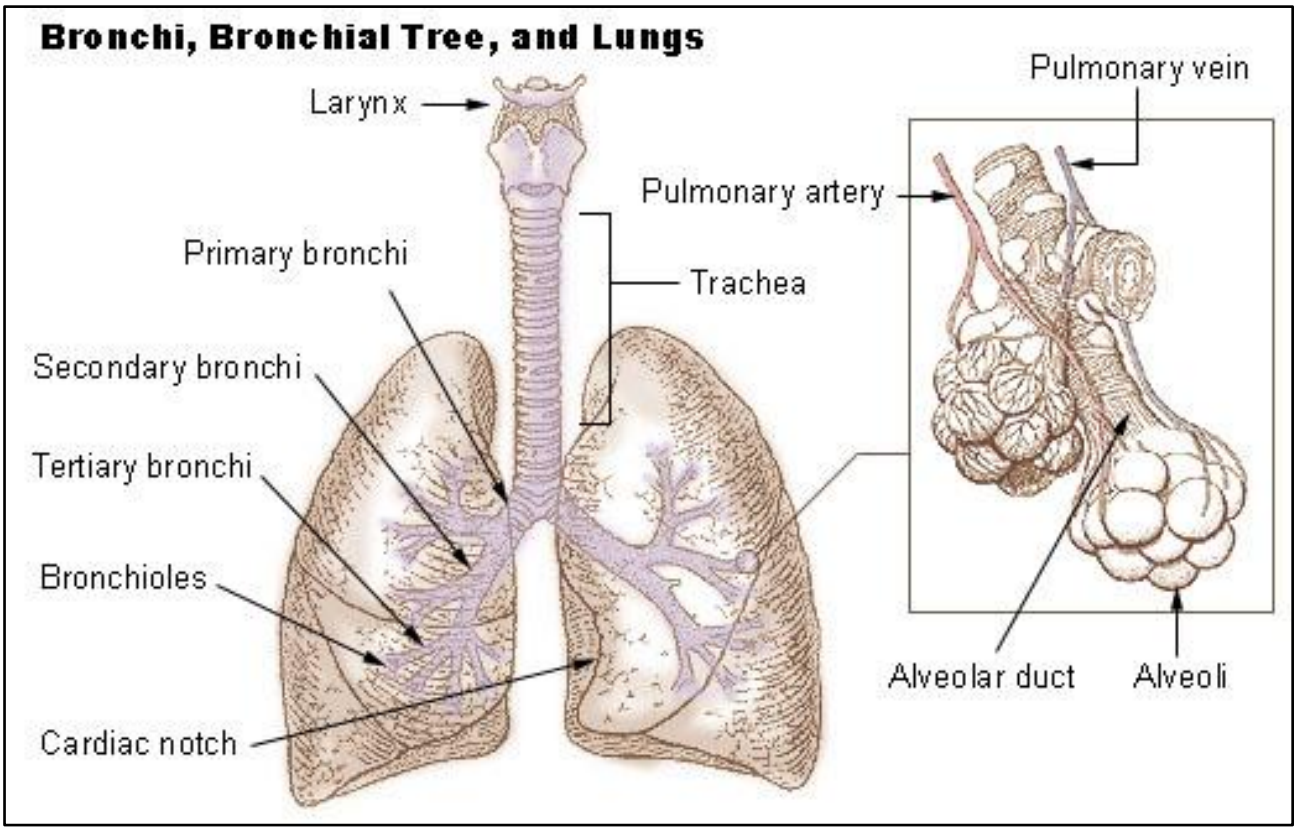

Fig.2: *Diagram of the lungs.*

1.2.2 Histology of the airways

While having displaying a similar general organization, the various sections of the airway show histological differences arising out of the function that the organ in question carries out.

The nasal mucosa is characterized by a highly differentiated neuroepithelium, the olfactory epithelium, equipped with cellular elements able to recognize a large number of odorous molecules through the activation of an electrical signal that is conveyed into the olfactory sensory areas of the cerebral cortex.

The larynx has, at the level of the mucosa, a pseudo-stratified epithelium with variations in height, which in some regions becomes columnar. The epiglottis is coated by a pavement composed epithelium to withstand the continuous and intense mechanical stresses caused by the passage of food (Standring, 2005).

The mucosae of the trachea and main bronchi consist of a pseudo-stratified epithelium and lamina propria separated from the tunica by an elastic lamina; the outermost tunica adventitia is rich in collagen. In detail, the pseudo-stratified epithelium is composed by different types of cells, including muciparous goblet cells, serous cells, ciliated columnar cells, basal cells, and stem cells that are able to divide asymmetrically to give rise to cells capable of differentiating into the other cytotypes of the epithelial lining. While the bronchial diameter decreases, the structure of the respiratory tree changes: the epithelium becomes more and more cubic, with loss of cilia and scarce goblet cells, and the alveoli becoming flattened (Gail, 1983).

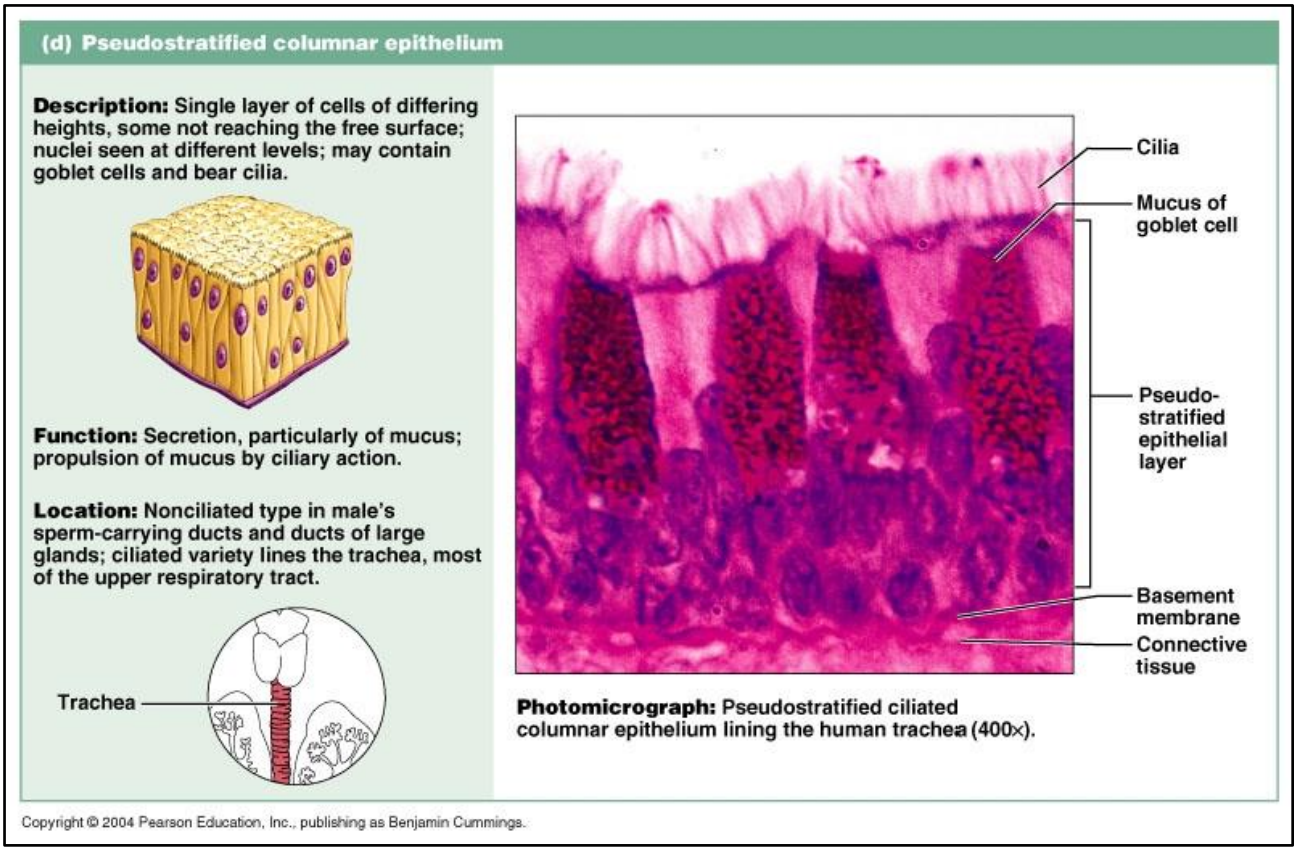

Fig.3: *Pseudostratified columnar epithelium.*

1.2.3 The protective role of airway epithelium

As stated before, the typical airway epithelium is a pseudo-stratified polarized structure that includes a columnar layer composed by different cell cytotypes (ciliated cells, secretory cells, and basal cells). It plays a key role in the protection of the internal milieu of the lungs from accidentally inhaled pollutants, infectious agents and other particulate matter (STCC Foundation Press, 2011). It acts not only as a physical barrier, but the bronchial epithelium also actively protects the airways by secreting mucus and other cytoprotective molecules that inactivate and block inhaled substances, which are subsequently removed by ciliary movement (Knight, 2003). Furthermore, there is an intense collaboration between the epithelial cells and the innate immune system cells to prevent damage caused by inhaled threats. Tissue regeneration can be improved by molecular signaling by the immune and inflammatory cells which can remove debris and provide a supply of local growth factors (Crystal, 2008). In addition to the cellular component, the extracellular matrix (ECM) also plays an important role in maintaining the equilibrium of the airways. ECM acts as a scaffold onto which tissue can organize; it stores large amounts of information used to modulate cell shape, cytoskeletal organization, cell polarity and motility, as well as cell proliferation and survival. Different observational and *in vitro* studies have shown the importance of the extracellular matrix. It is necessary to maintain the contractile phenotype of smooth muscle cells *in vitro*, or to regulate their differentiation. For example, the expression of specific integrins is indispensable for cell survival and differentiation, and for establishing cell polarity (Friedl, 2004).

1.2.4 Apical Accessory Epithelial Structures

On the apical side of epithelial layer, cells present different structures depending on functions they carry out. In particular, the apical side of airway epithelial cells presents microvilli and cilia.

Microvilli:

1. Closely packed, finger-like projections of cytoplasms that increase the surface area of the cell.
2. The number and shape on cell surface correlate with the absorptive and secretive capacity of the cell itself.
3. Can be seen with a LM (characterized by "brush" or "striated" borders).
4. Contain a core of actin filaments, which are anchored by villin at the tip.
5. Actin also extends downwards into the apical cytoplasm where it attaches to a terminal web described below:
    a. The web consists of a horizontal network of actin filaments lying just below base of the microvillus.
    b. These actin filaments are stabilized by spectrin. Spectrin anchors the terminal web to the apical membrane of the cell.
6. Also contain myosin II and tropomyosin filaments, which allow the microvillus to contract.
7. Usually present on the surface of microvilli is an amorphous cell coat of the "glycocalyx" glycoprotein.

The "Brush Cell" (pneumocyte III) is a particular type of cell that can be found in the airways. These cells present a columnar shape and squat microvilli (0.5-1 um in length and 150-180 nm in width) with 120-140 villi on each cell (Reid, 2005). Their functions are still unknown, but a concrete hypothesis is that these cells could have a chemoreceptor role. Chang and colleagues (Chang, 1986) suggested that they may play a role in detoxification or act as a sensor for alveolar fluid or alveolar air tension. Another possible function for brush cells that arises from their location in the lung is immune surveillance. All these theories emphasize the importance of these accessory structures in the complete functionality of the epithelial tissue, and the fact that the loss or modification of these structures affects the ability to carry out its functions.

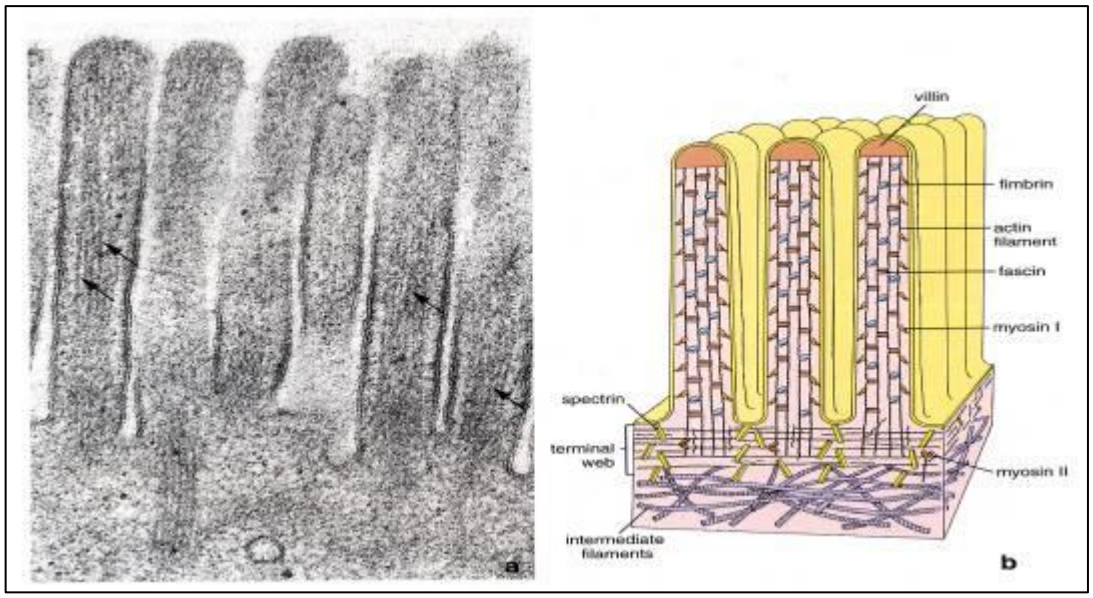

Fig. 4: *Microvilli* *(Ross, Histology: A Text and Atlas, 4th ed)*

Cilia:

1. Motile cytoplasmic structures capable of actively propelling particles along the cell surface.
2. Beat in a synchronous pattern and utilize ATP for movement.
3. Arranged into orderly rows (respiratory tract) OR occur as single structure (rete testis or vestibular cells of the ear).
4. With a LM, the cilia appear as hair-like structures emerging from the apical surface. They are anchored into the apical cytoplasm by a basal body:

   a. Modified centriole that contains nine microtubule triplets in its core forming a ring structure.

   b. Under a LM, the basal bodies appear as a thin, dark-staining band at the base of the cilia.

5. Each cilium contains an inner core of microtubules arranged in a 9+2 pattern. There are nine pairs or doublets of microtubules that are circularly arranged around 2 central microtubules.

   a. The microtubules composing each doublet are designated as the "A" microtubule and the "B" microtubule.

   b. "A" microtubule: 13 tubulin dimers arranged in a side-by-side manner.

c. "B" microtubule: 10 tubulin dimers that do not form a complete circle, instead "sharing" a portion of its wall with the "A" microtubule.

d. Each doublet contains a "pair of arms" that extends off the "A" microtubule to form cross-bridges with the "B" microtubule in the adjacent doublet. These arms contain dynein.

e. The nexin protein links the doublets together.

f. Radial spokes extend from the nine outer doublets to the central doublet.

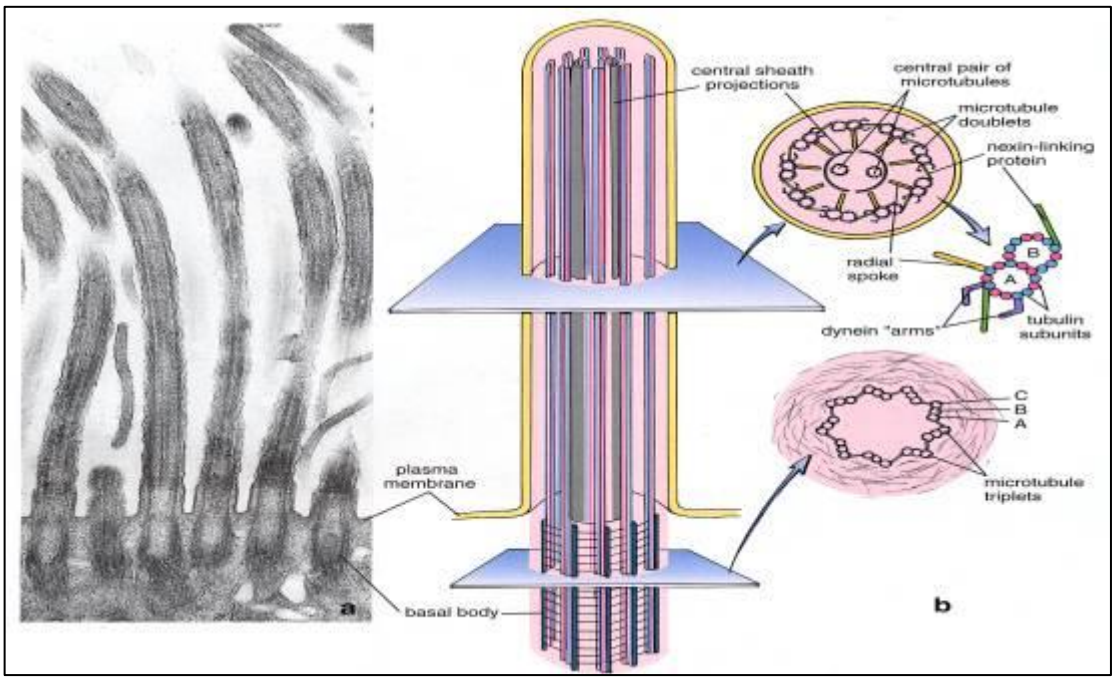

Fig.5: *Cilia.* *(From: Ross, Histology: A Text and Atlas, 4th ed)*

Motile or moving cilia are found in the lungs, respiratory tract and middle ear. These cilia have a rhythmic waving or beating motion. They work, for instance, to keep the airways clear of mucus and dirt, allowing us to breathe easily and without irritation. Another type of cilia is the "primary cilia" that shares has a structure similar to that of the other cilia, but these do not possess the motile ability, and instead carry out other functions. In humans, primary cilia are found on nearly every cell in the body. In contrast to the motile cilia, the primary or non-motile cilia are usually one per cell; nearly all mammalian cells have a single non-motile primary cilium. In addition, examples of specialized primary cilia can be found in human sensory organs such as the eye and nose. Previous studies have demonstrated the importance of the "ECM-Cilium-Golgi" axis in providing a

continuous signaling (Poole, 1997). More recent studies have investigated the key role of cilia in regulating the normal cell cycle and how timed resorption and reassembly of cilia are dynamic processes closely linked to execution of cell developmental programs, and how a deregulation of this pathway can lead to cancer (Plotnikova, 2008). The primary cilium is clearly a dynamic organelle whose assembly and disruption is implicated in the regulation of many cell functions with the association of various proteins and stimuli. Improving the understanding of this regulation may provide novel insights into the etiology (and therapy) of diverse ciliopathies, and into the mechanisms by which cells respond to a range of environmental influences (Santos, 2008). The signals that trigger assembly and disassembly of cilia in tissues are not yet well understood. It is likely that molecules that control the cell cycle are involved in these processes, at least in cells that form a primary cilium, given that the cilium is present only during a limited cell cycle window. Tight control of transcription and translation may be essential since many cilia proteins bind or regulate cytoskeletal elements, and may have a detrimental effect if released in large quantities into the cytosol (Dawe, 2006).

1.2.5 The Tight Junctions

Tight junctions, also known as occluding junctions or *zonula occludens*, could be defined as closely associated areas of two cells, whose membranes create a "continuum" of epithelium. They are multiprotein complexes that modulate the strength of cell-cell adhesion. Tight junctions are only found in epithelial cells. The other functions exerted by tight junctions are active transport of molecules through a multi-step process, and modulation of the cytoskeletal organization (Hartsock, 2008). The regulation of cell polarity also depends on the tight junction complexes (Shin, 2006). They maintain the apico-basal polarity (CRB3 and PAR3 complexes). The transmembrane proteins of tight junctions can bind surface antigens in bacteria and consequently alter the tightness of the connections (Coyne, 2003). This ability is significant because of the role signaling plays in the secondary immune response (Wan, 2000).

Three main transmembrane protein families constitute a tight junction complex; these are the occludin, claudin and junctional adhesion molecule families. The proteins of the first two families make contact, on the intra-cytoplasmic side,

with the *zonula occludens* proteins (ZO-1). The ZO-1 are a membrane-associated component of both tight junctions (TJ) and adherens junctions (AJ), found at the site of cell-cell interaction. ZO-1 has the role of an intracellular adaptor protein and is known to interact with claudins, occludin, cadherins, the actin cytoskeleton and downstream signaling pathways and transcription factors (Balda, 2009).

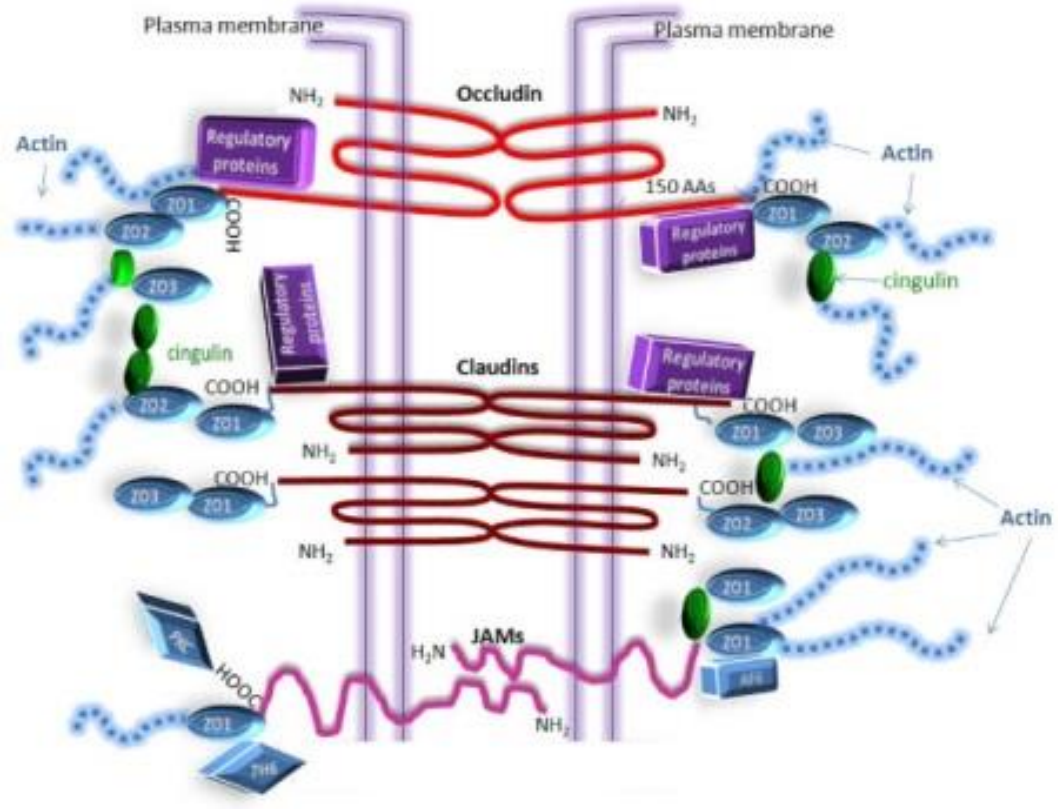

Fig.4: *Schematic representation of tight junctions.*
(Fluids Barriers CNS. 2011; 8: 3. Published online 2011 January 18. doi: 10.1186/2045-8118-8-3. Copyright ©2011 Redzic; licensee BioMed Central Ltd.)

1.3 Chronic inflammatory diseases of the airways

The term "chronic inflammatory diseases of the airways" stands for a set of disorders that are characterized by a progressive and rarely reversible obstruction of the airways. More in detail, they present with a massive inflammation, easily collapsible airways, exhaling problems and, with the progression of the disease, a worsening of the condition with an increasing number of medical clinic visits and hospitalizations. These diseases include: bronchiectasis, bronchitis, asthma and chronic obstructive pulmonary disease (COPD). The COPD shares similar characteristics with the other obstructive lung diseases, but it also presents some unique features in terms of disease onset, frequency of symptoms and airway obstruction reversibility.

The most relevant factor in diagnosing an obstructive lung disease is a decreased FEV1/FVC ratio (Forced expiratory volume in 1 second/Forced vital capacity), which measures the ability to exhale a certain percentage of the air inspired within one second (over 70% in a healthy individual). The patient may also be affected by one or more of the following symptoms: hyperplasia and hypersecretion by mucus glands, inflammation, constriction, smooth muscle hyperplasia, cough, wheezing, and/or dyspnea (Hargreave, 2009).

Chronic obstructive pulmonary disease is a heterogeneous group of chronic progressive diseases characterized by airflow limitation and a gradual loss of lung function that is not fully reversible. Also known as chronic obstructive lung disease (COLD), chronic airflow limitation (CAL), chronic obstructive airway disease (COAD), and chronic obstructive respiratory disease (CORD), this disease is caused by the simultaneous occurrence of emphysema and chronic bronchitis, a pair of commonly co-existing diseases of the lungs, in which the airway lumen become narrowed. The result is a limitation of the flow of air to and from the lungs. In clinical practice, COPD is defined by its characteristically low airflow in lung function tests. Unlike in asthma-related pathologies, this limitation is rarely (and poorly) reversible and normally gets progressively worse over time (Lee, 2009). A broader view of the causes of health disparities between populations, including socioeconomic status, race, ethnicity, and geography is necessary for finding better solutions to complex population health problems such as COPD (Rabe, 2007). The main cause of COPD development is noxious particles or gas,

most commonly from tobacco smoke or ambient pollution, which triggers a massive inflammatory response in the airways and lungs. The inflammatory response in the larger airways is known as chronic bronchitis, which is diagnosed clinically when a patient regularly coughs up sputum. In the alveoli, the inflammatory response causes a progressive modification of lung tissues, a process known as emphysema (Sun, 1995). The natural progression of COPD is characterized by occasional sudden worsening of symptoms, known as acute exacerbation, most of which are caused by infections or air pollution (Jeffrey, 2006).

1.3.1 Asthma

Asthma is a very common inflammatory disease of the airways. It causes a narrowing of the airways and its impact is growing across the world, by imposing burdensome liabilities to the public health systems. Cytokines play a key role in orchestrating the chronic inflammation and the structural changes in the respiratory tract, and have become an important target in the development of new therapeutic strategies against this disease. The most recent definition of asthma from GINA (the Global Initiative for Asthma) states that "Asthma is a chronic inflammatory disorder of the airways in which many cells and cellular elements play a role. The chronic inflammation is associated with airway hyper-responsiveness that leads to recurrent episodes of wheezing, breathlessness, chest tightness, and coughing, particularly at night or in the early morning. These episodes are usually associated with widespread, but variable, airflow obstruction within the lung that is often reversible either spontaneously or with treatment" (GINA report, 2008).

During an asthma attack, the lining of the bronchial tubes swell, causing the airways to narrow, thus reducing the flow of air into and out of the lungs. Recurrent asthma symptoms frequently cause sleeplessness, daytime fatigue, reduced activity levels and school and work absenteeism. Luckily, asthma has a relatively low fatality rate compared to other chronic diseases (Boushey, 1980; Chung, 2001).

The prevalence of asthma in the developed countries is about 10% in adults, and higher in children, while in the developing countries, the percentage is lower but constantly growing. The World Health Organization (WHO) estimates that 300

million people currently suffer from asthma. It is the most common chronic disease among children (WHO publication, 2003). Asthma often arises at a very young age and is characterized by a remodeling of the upper airways and an increased mucous secretion. This is the result of an inflammatory process that occurs at the expense of the airways themselves. But asthma is not only childhood pathology. Different studies have shown that the prevalence of asthma in the age group of patients above 65 years old has been increasing in the recent years. The asthma phenomenon in the elderly is much more complex than one might expect. The oxidative stress derived from the ageing process probably leads to immunological and inflammatory changes that have a significant impact on the respiratory system. Asthma is also often confused with other pathologies, in particular COPD, or chronic bronchitis or emphysema. (Pawankar, 2008).

The current guidelines for classifying asthma severity are based on two parameters: the FEV1 and the peak expiratory flow rate. According to the clinical classification system, asthma can be classified in terms of the frequency of symptoms which can be intermittent, mild persistent, moderate persistent and severe persistent. Asthma may also be classified as atopic or non-atopic, according to the presence (atopic) or absence (non-atopic) of reaction to allergens. Various cells play different roles in the pathogenesis of this disease, and like an orchestra, they have a crucial role in the evolution of the disease.

The inflammatory response in asthma involves primarily the larger airways. Bronchial biopsies obtained from asthmatic subjects show the infiltration of eosinophils, mast cells and activated T-cells, particularly Th2 cells. There are obvious structural changes, such as the deposition of collagen beneath the epithelial layer and a hypertrophy of airway smooth muscle cells. There is also an increase in angiogenic processes at the level of the hyperplastic areas.

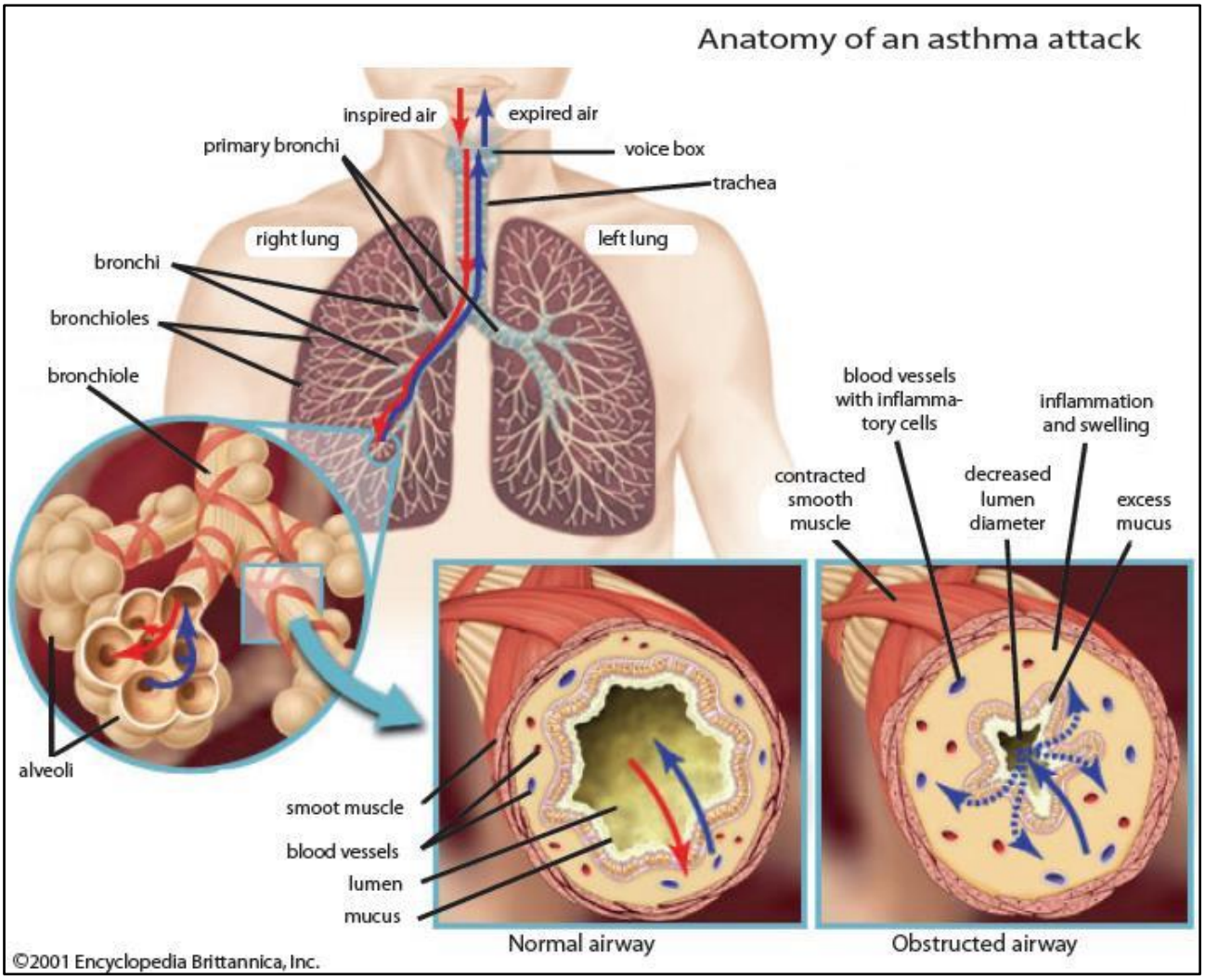

Fig.5: *Anatomy of an asthma attack.*

In asthma, epithelial cells are involved in the organization of the inflammation process (Hackett, 2011). They release many cytokines, including the SCF (which keeps the mast cells in an activated state at the level of the airways), the TSLP (that acts on dendritic cells and stimulates the release of Th2 chemoattractants CCL17 and CCL22) and various chemokines that attract eosinophils through the CCR3 receptor. The Th2 lymphocytes regulate the inflammatory process through the release of IL-4 and IL-13 (which stimulate B cells to synthesize IgE), IL-5 (that acts at the level of eosinophils) and THE-9 (that stimulates the proliferation of mast cells, which in turn release histamine and cysteinyl-leukotrienes that lead to bronchoconstriction).

Cytokines exert their pro-inflammatory action by recruiting, activating and promoting the survival of cells involved in inflammation of the respiratory tract.

Cytokines can be divided into: lymphokines (cytokines secreted by T cells that regulate the immune response), pro-inflammatory cytokines (that amplify and maintain the inflammatory state), and growth factors (that promote cell survival and lead to airway tissue remodeling), chemokines (that act as chemotactic agents for the inflammatory cells) and anti-inflammatory cytokines (that negatively modulate the inflammatory response).

The pro-inflammatory cytokines involved in asthma include TNF-α, IL-β 1 and IL-6, whose levels are increased in the BAL of asthmatic subjects, and lead to an amplification of inflammation through the activation of NF-kB. In other diseases, such as rheumatoid arthritis or inflammatory bowel disease, blocking the action of these cytokines has led to benefits for the patient, so it would be interesting to determine a similar approach to airway inflammation.

Interleukin 15 is an important mediator of chronic inflammation. An association between certain haplotypes of IL-15 and bronchial asthma has been described. An inappropriate activation of the immune system due to aero-environmental allergens and many other stimuli cause this disease, that is associated with a bronchial hyperreactivity and a massive presence of eosinophils and a high level of IgE present in the serum. The inflammatory response is initiated and supported by various cytokines, particularly IL-4, IL-5 and IL-13 (produced by T-helper type 2 lymphocytes). In contrast, it is likely that various mediators of the Th1 response, which inhibit the Th2 response, are deleted by the TH2 response itself. Such mediators include IL-2, IFN-γ and TNF-α (Barnes 2008).

IL-15 is a cytokine that mediates the Th-1 response, which in turn regulates the activation, proliferation and cytokine release by T-, NK- and mast cells, as well as B lymphocytes. IL-15 shares many biological functions with IL-2, but opposite effects have also been reported. This is because IL-15 interacts with the β and γ receptor chains of IL-2, but there is also a unique chain α for IL-15. Recently, an association between a haplotype based on five polymorphisms of the IL-15 gene and asthma outbreak in pediatric age has been reported (Bierbaum et al, 2006).

The genetics of asthma appear very complex. Due the complexity of asthma, it is difficult to understand the exact effect of each single component in the disease process, and how they contribute to the disease. Various studies have indisputably demonstrated that asthma has an important genetic component, but

there is no clear pattern of inheritance with a widely variable heritability rate between 36-79%

Multiple genome-wide linkage studies for asthma and allergy have been performed to date, and their results have shown that many of the genes involved in such pathologies are related to the immune system or involved in the modulation of inflammation or in the remodeling processes. Susceptibility to asthma can be influenced both by genes and environmental factors, which can have an impact at different stages in life.

1.3.1.1 Atopic Asthma

Atopic asthma (also known as allergic asthma or extrinsic asthma) affects a subpopulation of individuals that experience a worsening of symptoms upon exposure to allergens to which they are sensitized. Upon such exposure, the airways become constricted and inflamed, affecting breathing. The severity of symptoms is variable. This form of asthma is more common in children than in adults. The WHO estimates that more than 50% of patients with adult asthma suffer from Atopic asthma. There is an inherited tendency toward the development of extrinsic asthma. It is related to a hypersensitivity reaction of the immune response. The subject often has a family medical history that includes allergies of one kind or another, and a personal history of allergic disorders. Secondary factors affecting the severity of an attack or triggering its onset include events that produce emotional stress, environmental changes, for example in humidity or temperature, and exposure to noxious fumes or other airborne allergens. Common "activating" antigens include seasonal pollens (e.g., grass, tree and weed pollens), house dust mite, and domestic animals (e.g., cat, dog and horse), and multiple sensitivities are usually present. Atopy and asthma are not absolute co-morbidities; all individuals with asthma do not have allergies and all individuals with allergies do not have asthma.

There is no definitive cure, but avoiding the allergen will prevent symptoms from developing. A common precautionary measure is limiting outdoor activities when the pollen concentrations in the air are high, but this obviously greatly limits normal daily activities of the subject. It is possible to use various drugs and alternative therapies. Bronchodilators such as epinephrine and aminophylline may be used to enlarge the bronchioles, thus relieving respiratory distress. Other

drugs that thin the secretions and help in their ejection (expectorants) may also be prescribed.

1.3.1.2 The remodeling of airways in asthma

Chronic inflammation leads to the structural changes in the airways in asthma, collectively termed airway remodeling. These changes include changes in the epithelium and sub-epithelial layers, the latter including matrix abnormalities and alterations of the airway smooth muscle layer (Holgate, 2007). Asthma exacerbations are frequently characterized by sputum production and, furthermore, fatal asthma is commonly associated with mucus blocking the airways. The mechanism of mucus hypersecretion is probably multifactorial, but one consistent finding is that of goblet cell hyperplasia in the airway epithelium of patients with asthma (Holgate, 2008). Although inflammation undoubtedly plays a central role in asthma, it does not explain many of the characteristic features of this chronic and recurrent disease (Cockcroft, 2006).

The relevance of airway remodeling, the other main histologic characteristic of asthma, in the disease pathogenesis is still controversial, since traditionally inflammation was thought to be the sole foundation of asthma, causing airway remodeling to receive considerably less attention. Multiple studies have shown an increase in subepithelial fibrosis in asthmatic patients (Bousquet, 2000). The degree of subepithelial fibrosis correlates with the severity, but not with the duration of disease. Interestingly, although one study found that treatment with an inhaled corticosteroid (ICS) for four weeks had no effect on the thickness of the subepithelial layer, another study, in which the treatment with ICS was continued for 12 months, showed significant reductions in the thickness of the subepithelial layer, suggesting that subepithelial fibrosis is a consequence of airway inflammation (Dahl, 2006).

These alterations of the airways also provide an explanation for corticosteroid-resistant bronchial hyperresponsiveness, and for the accelerated decline in lung function observed in adults with asthma. The deposition of new extracellular matrix in the lamina reticularis could prove to be another marker of chronic epithelial damage. To explain these tissue changes and the continuous inflammatory loop, the "Epithelial Mesenchymal Trophic Unit" (EMTU) theory was proposed. Changes in the microenvironment that characterize the normal

connection between the epithelial and mesenchymal cells have been described (Zeisberg, 2009). These modifications promote tissue remodeling and support the inflammatory state (Vincent, 2009). During embryogenesis, signal exchange between the epithelium and mesenchyme trigger tissue morphogenesis. During asthma, there is likely to be a reactivation or a deregulation of these signals. Therefore, the resistance to treatment with corticosteroids could be explained by a tissue remodeling from some other origin.

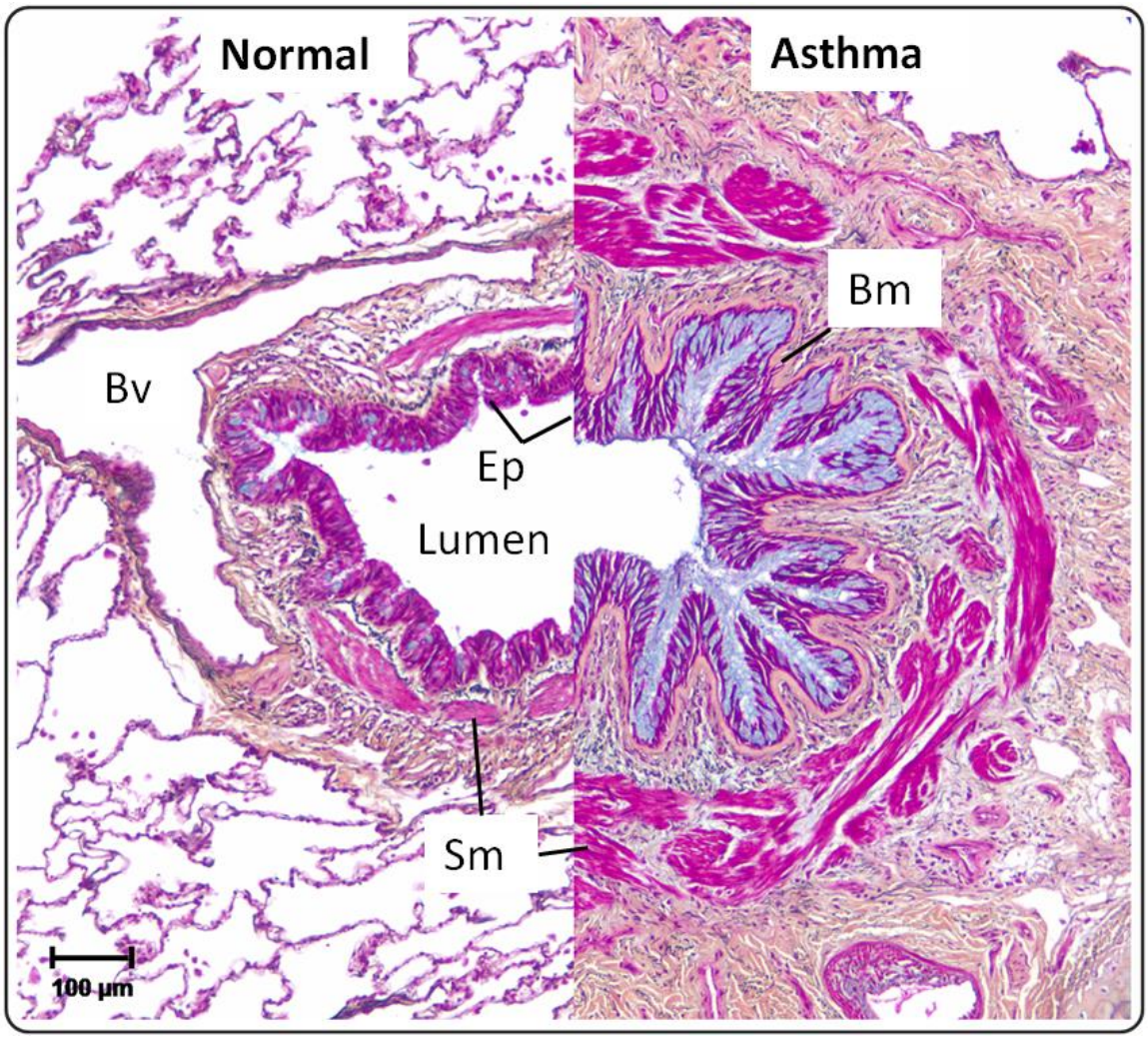

Fig.6: *The airways in asthma undergo significant structural remodeling. Medium-sized airways from a normal and severe asthmatic patient were sectioned and stained using Movat's pentachrome stain. The epithelium (Ep) in asthma shows mucous hyperplasia and hyper secretion (blue), and significant basement membrane (Bm) thickening. Smooth muscle (Sm) volume is also increased in asthma.*

Samuel J. Wadsworth, S. Jasemine Yang and Delbert R. Dorscheid (2012). IL-13, Asthma and Glycosylation in Airway Epithelial Repair, Carbohydrates - Comprehensive Studies on Glycobiology and Glycotechnology, Prof. Chuan-Fa Chang (Ed.), ISBN: 978-953-51-0864-1, InTech, DOI: 10.5772/51970.

(Available from: http://www.intechopen.com/books/carbohydrates-comprehensive-studies-on-glycobiology-and-glycotechnology/il-13-asthma-and-glycosylation-in-airway-epithelial-repair).

1.3.1.3 The hygiene hypothesis

Asthma is a complex pathology resulting from several genetic and environmental factors. In regards to the genetic factors, our genome contains a vast pool of candidate genes and loci. For example, an alteration in the ADAM 33 gene has been reported in several studies. ADAM 33 is a protein expressed in the smooth muscle cells, and alterations of this protein lead to an atypical response to inflammation. Alterations (or the presence of specific isoforms) of the interleukin genes are involved in the predisposition of an individual to develop asthma during his or her lifetime.

For example, IL-4 and its receptor and IL-13 are involved in Th2 response, and at the same time, other membrane proteins, such as the $F_c\varepsilon R_1$ receptor, are implicated in the Th1 response. It is clear that both kinds of responses may have an active role in the development of this pathology.

Focusing on the duality of the Th1- and Th2 pathways it is necessary to mention the "hygiene hypothesis" (HH). This theory was proposed by David P. Strachan at the end of the 80s to explain why hay fever and eczema were less common in children from large families, who were probably exposed to more infections through their siblings, than in children with no siblings. From that moment, the HH has been widely scrutinized and it has become an important theoretical framework for the study of allergic pathologies. It explains the increased prevalence in allergic diseases that has been seen since the industrialization era, in particular in the more developed countries. The theory, initially limited to allergic disorders, has been extended to other autoimmune diseases, like multiple sclerosis or diabetes. In summary, pathologies thought to be related both to the Th2- and Th1 pathways have been steadily increasing over the last 30 years, and even though this may seem like a contradiction initially, it can be considered as a further confirmation of the theory. The proposed mechanism acknowledges the fact that regulatory T cells are important in maintaining the balance between Th1- and Th2 responses, and states that a lack of microbial exposure early in life has a negative effect on the development of regulatory T cells. The central notion of the theory is that some parasitic agents that developed with mankind are able to protect us from a large spectrum of autoimmune disorders. The results of some more recent studies have confirmed

the hypothesis formulated by Strachan more than 30 years ago (Ege, 2011-2012).

Connections between asthma and allergy have been recognized for many years, but recently they have been re-emphasized. In fact, today estimates show that 60-78% of people who suffer from asthma also suffer from allergic rhinitis, which is implicated as a common trigger for asthma attacks among adults and children. Controlling allergic rhinitis could help to control the symptoms of asthma (Nayak 2003). Furthermore, studies focused on the connection between these pathologies have identified some chromosomal linkage between atopic dermatitis (AD) and asthma. At this point, it is evident that there is a connection between the development of asthma and a deregulation of the immune system.

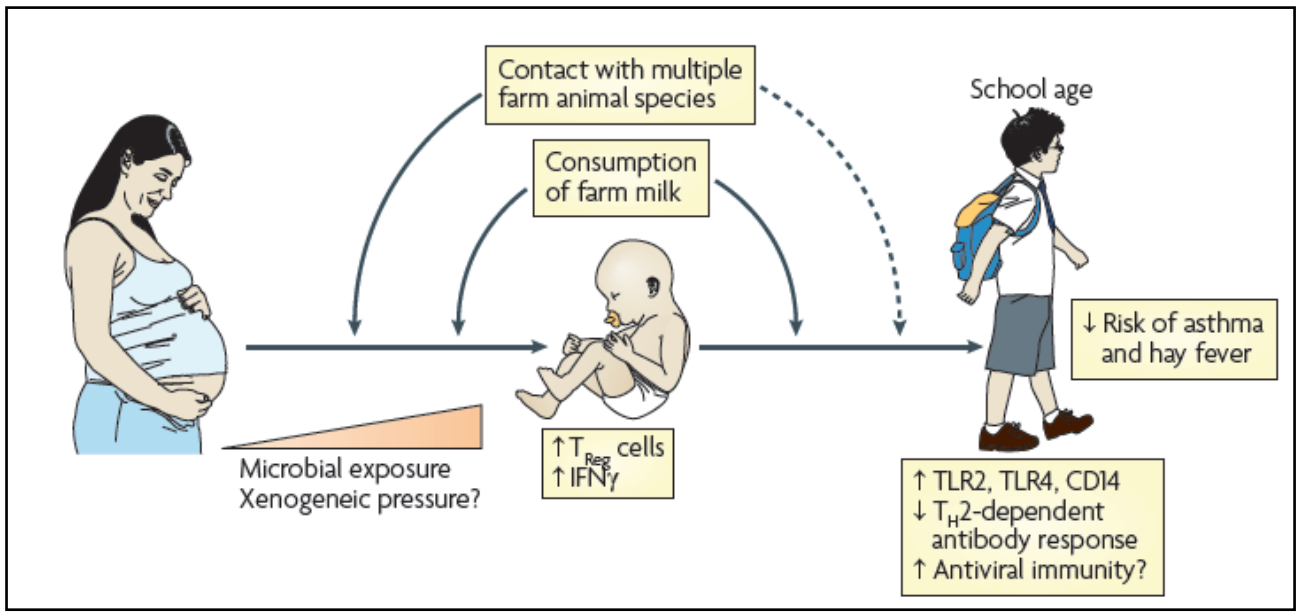

Fig.7:*Hygiene hypothesis.*
Von Mutius, 'Farm living: effect on childhood asthma and allergy', Nature Reviews Immunology 2010

1.3.1.4 The PARSIFAL and GABRIELA projects

Starting from this key notion, at the beginning of the 90s, two different projects were created with the same basic idea: the PARSIFAL and GABRIELA studies. Both compared children living on farms with a reference group, with the first study (PARSIFAL) focusing on the prevention of allergy, and the second study (GABRIELA) focusing on the study of the environmental causes of asthma. Dust samples and milk used by the families involved in the study were analyzed. In

both studies, children who lived on farms had a lower prevalence of asthma and atopy, and were exposed to a greater variety of environmental microorganisms than the children in the reference group. To give an idea of the dimensions of the studies, the PARSIFAL project involved 14893 children, while the GABRIELA study involved 9668 children. The first part of the projects consisted in a questionnaire that included information on environmental and life style factors as well as on clinical symptoms. Special emphasis was given to the assessment of different dietary habits associated with farming or an anthroposophic lifestyle. Another part of the studies was the analysis and characterization of elements that compound the dust collected on the farms (from vacuum cleaner bags, mattresses or floors for a total of 4000 samples). In a subsequent part of the studies the dust samples were analyzed. In the PARSIFAL study, the samples were subjected to a single-strand conformation polymorphism (SSCP) analysis to reveal the various bacteria species present in the dust (Korthals, 2008). In the GABRIELA project, the colonies were isolated from the dust samples and analyzed to identify the different species of bacteria and fungi.

Both studies evidenced differences between the two groups of children, in particular in relation to the prevalence of atopy. In both subpopulations for which dust samples were available, similar correlations between the living environment (farm vs urban) and the prevalence of asthma and atopy were found. In the PARSIFAL study, as expected, the percentage of samples of mattress dust positive for different species of bacteria was higher among the samples collected from the farms than among those collected from the homes of the reference group.

In GABRIELA, all bacterial and fungal taxa cultured from the mattress dust were more prevalent among samples collected from the farms than among those collected from the homes of the reference group.

The conclusions drawn up from the results of both studies indicated that children growing up in a rural environment were protected from asthma and atopy. They were exposed to a wide variety of bacteria and fungi, especially in comparison with the reference group who lived in an urban environment in the same region. This variety of environmental microorganisms was inversely correlated with asthma. These data concur with the "hygiene hypothesis" that kicked off the studies. Microorganisms trigger the innate immune system through pattern-

recognition receptors, such as the toll-like receptors. Activation of several toll-like receptors has been found in children exposed to farming environments.

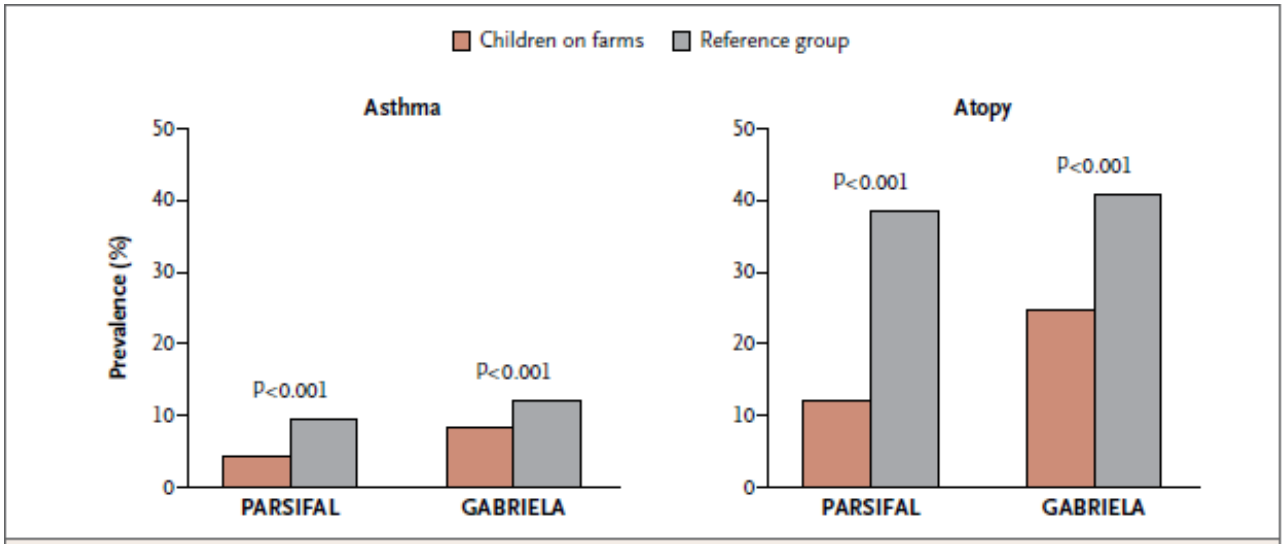

Fig.8: *Prevalence of asthma and atopy in children living on farms, compared with reference groups.*
Exposure to Environmental Microorganisms and Childhood Asthma (The New England Journal of Medicine, 2011, 364; 8)

A more specific example is a study conducted on *Staphylococcus sciuri,* one of the species founded in the dust samples collected for the PARSIFAL project (Hagner, 2013). This preliminary study, carried out on a murine model, assessed the protective capacities of the bacteria to prevent the airway inflammation. In this study, two protocols of acute airway inflammation in mice were employed by administering either ovalbumin (OVA) or house dust mite extract (HDM) for sensitization. Mechanistic studies were conducted on the activation of innate immune responses to *S. sciuri* W620 using human primary monocytic dendritic cells (moDC) and co-culture with autologous T cells. The study evidenced protective properties on the HDM model generated by the abrogation of eosinophils and neutrophils in the airways, together with a parallel decrease in the cytokine levels.

1.4 The Oral Mucosa

The mucosa of the oral cavity is constituted by:

- An outer layer of epithelial cells;

- A basement membrane, called "lamina propria";

- An inner layer of submucosa.

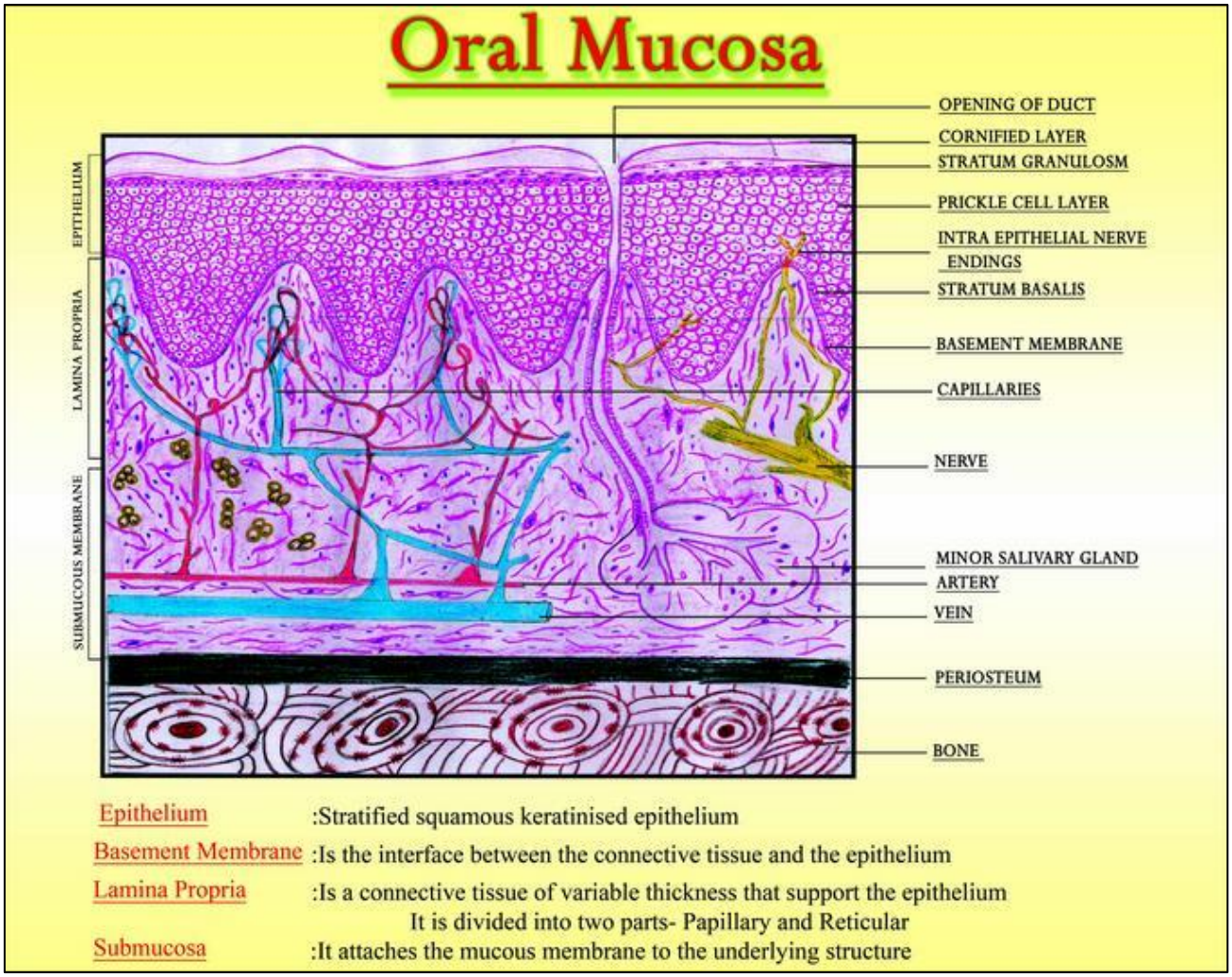

Fig.9: *Sketch of the oral mucosa* (Wikimedia.org)

Most of the oral mucosal surface is lined by non-keratinized stratified squamous epithelium except gingiva, hard palate and dorsal surface of the tongue, where the epithelium is keratinized. The oral epithelium is divided into four different layers: Stratum *Basale, Stratum Spinosum, Stratum Granulosum* and *Stratum Corneum*. In its basal layer there is a population of mitotically active cells, in various stages of differentiation, which have a turnover of 5-6 days. These cells

are cuboidal or low columnar and form a single layer resting on the basal lamina, which is at the interface of the epithelium and lamina propria. The *stratum spinosum* is usually several cells thick, shaped like polyhedrons with short cytoplasmic processes and its first layers with the *stratum basale* are also referred to as *stratum germinativum* because these cells give rise to new epithelial cells. Cells of the *stratum granulosum* are flat and are found in layers of three to five cells thick; this layer is prominent in keratinized epithelium and absent in non-keratinized epithelium. Cells of the *stratum corneum* are flat, devoid of nuclei and full of keratin filaments surrounded by a matrix; these cells are continuously being shed and replaced by epithelial cells that migrate from the underlying layers. This layer is exclusive of keratinized epithelium too. Non-keratinized epithelial cells in the superficial layers do not have keratin filaments in the cytoplasm but present nuclei. The *stratum corneum* and *stratum granulosum* layers are absent. Epithelial cells are immersed in an intercellular base substance, the mucus, which consists mainly of complex carbohydrates and proteins (mucopolysaccharides and mucoproteins). This glycoprotein matrix plays an important role in cell-cell adhesion and as a lubricating agent. The *lamina propria* is composed of connective tissue and exercises trophic functions for the epithelial layer. It can be divided into a papillary layer and a reticular layer. The papillary layer is prominent in the masticatory mucosa whereas the reticular layer is more present in the lining mucosa. The *lamina propria* consists of blood vessels and cells such as fibroblasts and endothelial cells, and nerves.

1.5 Environmental stress

The principal sources of environmental stress to the human mucosae that are naturally exposed to inhaled stimuli, are represented by cigarette smoke, environmental pollution, local inflammation and microorganism infections. Pseudomonas aeruginosa is one of the most commonly found bacterium in the lungs of subjects with chronic inflammatory lung diseases whereas exposure to cigarette smoke (CS) is certainly one of the primary stimuli of airway inflammation.

1.5.1 Pseudomonas Aeruginosa

Pseudomonas Aeruginosa is a bacterium that can cause disease in humans. It is found in water, skin flora, soil and many other natural and artificial environments. The versatility of this bacterium enables it to infect various organisms, but only if the target organism suffers from tissue damage or compromised immunity. Normally a P. Aeruginosa infection does not have fatal consequences, unless it interests critical organs (lungs, urinary tract or kidneys) affected by other concomitant diseases.

It can be defined as an opportunistic, nosocomial pathogen typically found in immunocompromised individuals.

Pseudomonas Aeruginosa has the ability to induce damage in the apical and basolateral membranes of airway epithelial cells. Past experiments conducted by immunofluorescence have shown direct evidence of damage. In particular, transepithelial resistance (Rt) is an important parameter to consider in order to evaluate the integrity of an epithelial layer. An elevated Rt value (>1,000 Ωcm^2) is an expression of epithelial continuity, while it has been shown that for low Rt values (100-200), the susceptibility of the cells to damage by P. Aeruginosa is increased by 25 times. In fact, the bacteria attack the epithelial cells near the "free edges" of holes, wounds and peripheral sides. In particular, P. Aeruginosa binds three times more frequently to regions between cells than to cell membranes, emphasizing the importance of tight junctions as protective structures. At the same time, these structures are the target of the bacteria itself, that decreases the function of the epithelial barrier by disrupting the proteins that constitute them. Moreover, P. Aeruginosa can cause stress to the endoplasmic reticulum. This condition can have severe consequences in patients with ER stress-associated lung disease, like cystic fibrosis and COPD. The results of a recent study have shown that the use of a culture medium conditioned with P. Aeruginosa strain PAO1 can produce a reduction in the synthesis of *zonula occludens*-1 protein, leading to a gradual decline in epithelial resistance (Van 't Wout, 2012)

1.5.2 Cigarette Smoke

Exposure to cigarette smoke (CS) represents a considerable oxidant burden on the respiratory epithelium, which is the first line of defense to inhaled substances. CS, which is one of the most important indoor air pollutants, is a complex mixture of over 4,000 different compounds, and high levels of oxidants and ROS have been detected in both mainstream and sidestream smoke (Faux, 2009). A high toxicity has been observed for at least 52 components of CS: 18 phenols, 14 aldehydes, eight N-heterocyclics, seven alcohols, and five hydrocarbons. Most of these compounds are capable of generating ROS during their metabolism. Thus, the mechanism of cigarette smoke toxicity is thought to incorporate oxidative stress, which mediates cell death via necrosis and apoptosis, due to the fact that cigarette smoke has been shown to cause oxidative DNA damage and cell death. The oxidative damage to cellular components occurs when the increase in ROS production causes oxidative damage in cellular components by overwhelming their antioxidant defense mechanisms; the presence of apoptosis confirms that this causes damage to DNA, nuclear DNA being one of the targets of ROS (Howard, 1998). CS also facilitates allergen penetration across respiratory epithelium and is a potent source of oxidative stress, DNA damage and apoptosis in alveolar epithelial cells. Moreover, CS is considered an important player in the pathogenesis of asthma as a trigger for acute symptoms, modifying inflammation that is associated with this pathology and it is also considered a major risk factor for COPD development as demonstrated in animal models. Furthermore, smoking is common in asthmatic patients and it has been found to contribute to poor symptom control.

1.6 Tissue Engineering: Development of Complex Culture Methods

1.6.1 Primary cultures

Since the beginning of the last century, it has been noted that fibroblasts cultured on a blood clot (three-dimensional structure) possess complex shapes, following the orientation of the fibers of the clot, showing considerable and dynamic interaction between the cells and the surrounding environment. Similar characteristics have also been observed mesenchymal cells, placed on glass coverslips, but in this case, "tension lines" emerged. These stress fibers are rarely observable in fibroblasts *in situ,* except under conditions of tissue activation such as the regeneration of a wound or a fibrous state.

Currently, various types of cell culture models are available for the study of diseases that affect the respiratory tree, from the simple immortalized monolayer culture, to the three-dimensional primary cultures (Fulcher, 2005). Each of the available models has advantages and disadvantages. Clearly, the use of more complex culture models increases the likelihood to obtain structures more similar to that of the actual architecture of the respiratory mucosa, but, at the same time, it also increases the amount of potential complications (cost, time, reproducibility, etc.).

It is essential to consider the first important variation: the use of primary cell cultures vs the use of immortalized cell lines (Yamaya, 1992). The primary cultures are obtained directly from the tissue of interest, transferred and successively amplified *in vitro* (Widdicombe, 2005). Unfortunately, these cells can only go through a limited number of divisions, or passages, *in vitro*. Once this limit is reached, they succumb to apoptosis. To avoid the "apoptosis limitation" it is possible to use specifically created cell lines. They are cells that have undergone a mutation and will not undergo apoptosis after the limited number of passages. They will grow indefinitely thanks to a transformation induced by a virus or by a chemical procedure. At the same time, the immortalized cultures present characteristics that are absolutely unlike to those of *in vivo* cells, and with the increasing passages in culture, they show a lesser

level of differentiation. In addition to the choice between primary and immortalized cells, another important aspect to consider is the spatiality.

1.6.2 Three-dimensional cultures

From a technical point of view, two-dimensional cell cultures (2D) reflect only partially the morpho-molecular pattern of human cells, and they are also unable to reflect the complexity of the *in vivo* microenvironment. In *in vivo* systems, in addition, the development differs significantly from 2D cell culture models, especially with regard to the morphology, growth kinetics, gene expression and the degree of differentiation. In this scenario, the three-dimensional cell culture models (3D) constitute an alternative and/or parallel approach to the 2D cell culture model, since they represent a halfway link between the traditional cell culture and *in vivo* models. In particular, for the respiratory mucosa, the culturing of primary human bronchial (or tracheal epithelial) cells three-dimensionally and at an air-liquid interface mimics the relevant *in vivo* environment and drives differentiation towards a mucociliary phenotype, while these results cannot be achieved with traditional methods like monolayer and submerged culture models. This model is also superior to other *in vitro* models for many research applications, since it results in the generation of a more physiologically relevant model. Submerged cultures of primary human bronchial epithelial cells or tracheal epithelial cells are possible; however, the cells cultured with this method fail to undergo mucociliary differentiation. Air-liquid interface cultures of human bronchial epithelial cells, however, exhibit many of the characteristic properties of the human airways, including mucus secretion, ciliary motility and formation of cellular junctions (Lee, 2005). Despite the presence of these characteristics, the ALI cultures still present some deficits. In particular, the most obvious is the absence of fibroblastic cells. They can only be added to the basal level of the well or to the other side of the insert membrane. In both cases, the co-culture does not respect the real distances and interactions between the two cell populations. Moreover, the ALI model appears to be too sensitive to external insults, affecting long-term treatments *in vitro*. The absence of a realistic ECM is another major flaw.

1.6.3 The role of ECM in cell-cell interaction and development

Various cell-secreted macromolecular components make up the intricate, highly hydrated polymer gel that constitutes the three-dimensional extracellular microenvironment.

One of these components is a fibrillar complex that has the task of diffusing nutrients and metabolites to and from cells; this complex, termed "ECM", is composed of cross-linked, physically immobilized sugar and protein elements.

Further components include growth factors, chemokines, cytokines and other soluble effectors with important signaling functions, as well as membrane-anchored molecules, donated by neighboring cells, that have the crucial task of enabling cell-cell communication in tissue morphogenesis.

Fibrous proteins, such as elastin, fibronectin, laminins and collagens, together with hydrophilic proteoglycans containing large glycosaminoglycan side chains, such as hyaluronic acid, are two of the principal ECM macromolecules.

While these components are present in the majority of ECMs, their form and organization, as well as their biochemical and mechanical properties diverge considerably between different types of tissues. In addition to its basic functions as a solid support structure upon which cells are organized into 3D tissues, or simply as a physical boundary between neighboring tissues, ECM also regulates multiple morphogenesis-driving cellular processes, such as cell adhesion, migration, proliferation and division, via distinct receptor-ligand interactions (Giancotti and Ruoslahti, 1999; Kleinman et al., 2003).

Furthermore, tissue dynamics are modulated by the ECM's binding, storing and sequestering capabilities on soluble growth factor proteins. For the most part, the ECM binding process involves heparan sulphate proteoglygan-related electrostatic interactions. Morphogens can be protected from enzymatic degradation-induced inactivation through binding, and the latter has also been reported to induce conformational changes that optimize receptor-ligand interaction, thus increasing biological activity in some cases. On the other hand, dynamic, bi-directional cell-matrix interaction can be established thanks to the extracellular microenvironments' ability to respond to cell-secreted signals, this ability being most apparent in situations where a protelytic degradation-related

degradation of the ECM is taking place. Proteolytic enzyme secretions can selectively cleave peptide bonds of nearby macromolecular ECM component domains. This matrix responsiveness is a key feature in 3D migration and matrix remodeling occurring during tissue formation, regeneration and several pathological processes, due to the fact that ECMs frequently serve as biophysical barriers for the cells located within. It is worth to note that non-proteolytic strategies can also induce 3D migration, with the cell type and microenvironmental situation determining the type of strategy (Friedl, 2004).

Essentially, proteolytic migration is induced through integrin binding to the ECM, occurring in concomitance with a highly localized degradation of pericellular ECM proteins, activated by cell-secreted and -activated proteolytic enzymes; these include the matrix metalloproteinase family (MMPs) (Page-McCaw et al., 2007), in addition to other enzyme families (e.g. serine proteases) (Lijnen, 2001).

Good progress has been made in the last decade or so in devising artificial ECMs. Suitable materials for productive use in three-dimensional cell cultures and *in vivo* tissue regeneration have become a reality thanks to the application of biological recognition principles. Nonetheless, these artificial systems can still only reiterate a small portion of the key signaling and cell response functions of natural ECMs, with at least five characteristic functions remaining beyond the grasp of the synthetic versions at the moment.

These include the near-physiological multifunctionality capabilities of the ECM; while most artificial ECMs utilize two classes of biomolecules, the natural ones are comprised of various different biochemical cues. Additionally, artificial ECMs lack in the temporal complexity in signal presentation, with the time frames and dynamics being fairly restricted in terms of longevity and complexity. Spatial complexity represents a further shortcoming of artificial ECMs. Matrix-immobilized 3D morphogen gradients are an essential factor in tissue development and regeneration, enabling several cell types and patterns to be spatially generated in relation to the original signal source, as well as controlling the migration of specific cells to specific locations. Although biomolecule gradients have been created using hydrogel surfaces (Burdick et al., 2004; DeLong et al., 2005), to date no one has succeeded in recreating them in artificial cell-responsive 3D ECMs. The versatility of artificial ECMs is also hindered by the absence of a suitable feedback system to control cell-matrix

interactions. Characteristic of natural ECMs, these include, for example, features such as proteases capable of cleaving ECM components, generating cleavage products that can have important signaling functions (Hamano et al., 2003). Moreover, most artificial ECMs presently available have some cell-specificity issues, since protease substrates of cell-responsive matrices consist of short, linear peptides with limited specificity for particular proteases; this is not the case in matrices composed of natural proteins. Therefore, most artificial ECMs are not specific to particular cells or their protease secretions, respectively.

1.6.4 Novel alternative cell culture models

Regarding the current culture models for the reproduction of oral mucosa, some equivalents have been developed for *in vitro* biocompatibility studies, as well as for mucosal irritation and oral disease studies with the aim to better understand disease processes and discover new treatments (Moharamzadeh, 2007; Kinikoglu, 2011). In the last decade, research has concentrated on the characterization of a human mucosal equivalent by introducing new dermal scaffold and epithelial cell culture methods. However, many models use cells derived from oral squamous carcinoma, and this leads again to the use of immortalized cells. Moreover, the scaffold that supports the cells is an important factor in oral mucosa reconstruction, and the elements that constitute the ECM of the model should be as similar as possible to those of the "real" ECM.

Another alternative would be the use of animal models (Cunningham, 2009), but even if excluding the ethical problems associated with any research using animals, they present a lot of defects. Although they can be used to learn more about basic functionality, the porting rates from an animal model to the human model are extremely reduced (it is estimated that 92% of clinical trials of drugs tested on animals fail when ported on humans, FDA, 2007). In particular, although the mouse provides the most common model used for many aspects of the human immune system, the 65 million years of divergence has introduced significant differences between the two species, which can and has impeded the reliable transition of pre-clinical mouse data to clinical studies.

"Replacing animal procedures with methods such as in vitro cells and tissues, volunteer studies, physicochemical techniques and computer modeling, is driven by legislative, scientific and moral imperatives. Non-animal approaches are now

considered as advanced methods that can overcome many of the limitations of animal experiments."

Hence the need to find a new culture model that allows the simultaneous presence of the air-liquid interface, differentiated epithelial cells and fibroblast population. These two populations must interact in the most natural way possible, granting a more realistic response to external stimuli and permitting long-term treatments. It is important to obtain the presence of a natural ECM synthetized by connective tissue cells to improve the faithfulness of assay results. A model that permits long-term monitoring makes regeneration studies possible after a fracture on the epithelium layer, and it should be possible to study the regenerative process with the concomitant presence of epithelial cells and connective tissue cells, all surrounded by a natural ECM.

AIMS

Over the years, the number of annual deaths caused by chronic diseases have increased globally in comparison with the deaths caused by injuries and other disorders. The number of annual deaths caused by all chronic diseases has steadily increased worldwide during the last two decades, with the numbers appearing even more alarming when viewed in perspective. The costs to treat individuals suffering from chronic diseases burden the budgets of individual nations more and more, and this, in conjunction with the increase in the average life span, leads to an increasingly significant expenditure for the public health systems worldwide.

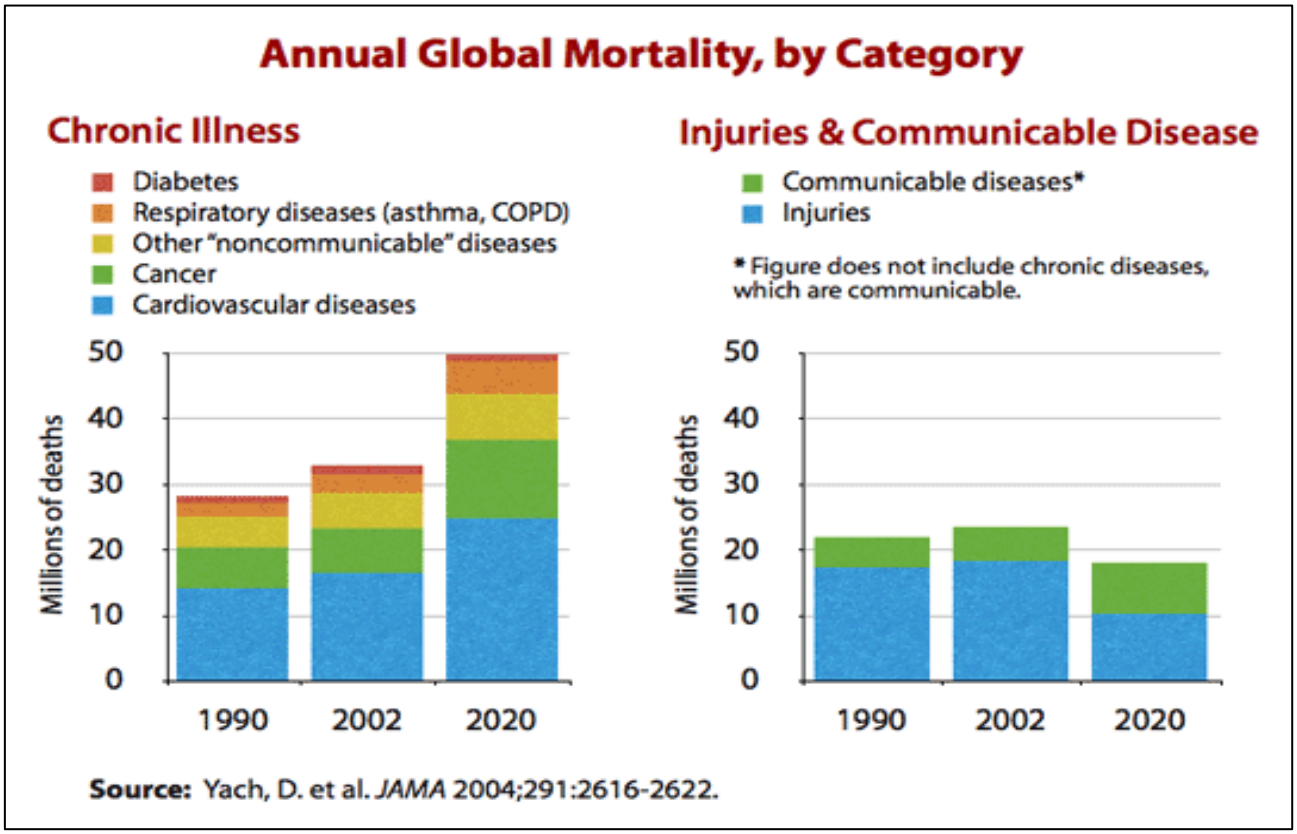

Fig.10: *Predictive view of Annual Global Mortality.*

Often, a chronic disease does not just affect the target organ, for example in COPD, cigarette smoke effects are not restricted to an inflammation of the airways, but exposure leads to systemic inflammation, oxidative stress throughout the body and a general dysfunction of the vascular endothelia. It is not uncommon, but indeed quite frequent, for an individual to suffer simultaneously from multiple chronic conditions. In fact, in recent years it has

been discovered that the individual pathologies "promote" each other, thus facilitating the onset of other chronic disorders alongside the persisting initial pathology. In particular, at least half of the individuals aged over 65 have at least three chronic conditions, and a fifth of them is affected by five or more pathologies, with costs to the health care system that escalate exponentially as the number of diseases presenting simultaneously increases.

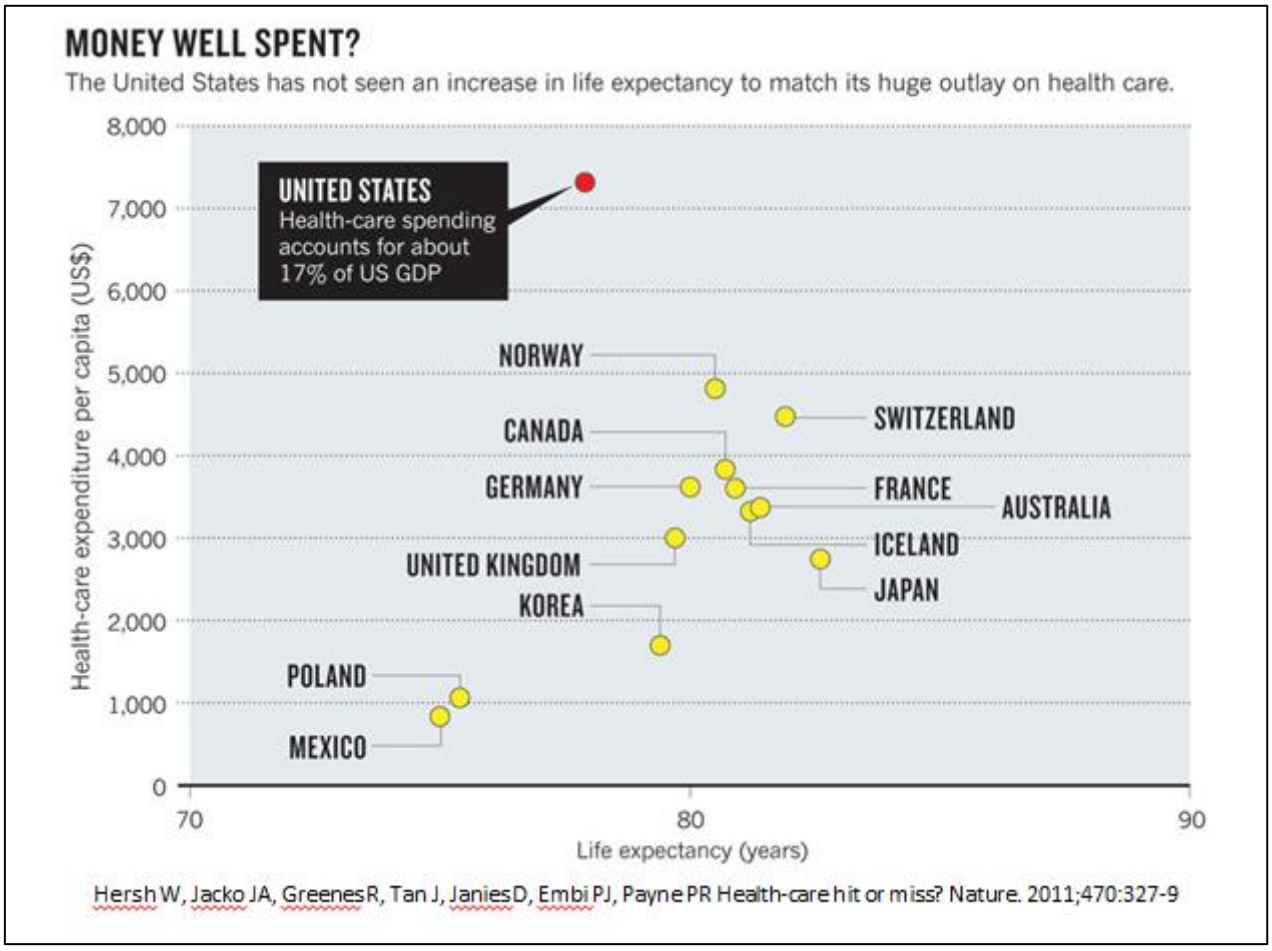

Fig.11: *Health care expenditure per capita of different US States in 2011.*

Several chronic pathologies are inflammatory diseases that affect the mucosae, and given what discussed above, there is an urgent need for a culture model that allows us to study them more accurately.

The main objectives of my PhD studies were therefore aimed at evaluating the use of novel three-dimensional culture models to study non-communicable diseases, offering the opportunity to achieve more accurate and comprehensive results compared to those obtained through the use of classical culture models.

In order to achieve these aims, I decided to use three different approaches:

- studying the potential protective effects of farm dust on the pathogenesis of asthma using ALI cultures;

- investigating the morphological changes that cilia undergo after long-term exposure to cigarette smoke utilizing 3d bronchial outgrowths;

- developing and characterizing a novel tissue-engineered oral mucosal equivalent, the 3d oral outgrowth.

2.METHODS

2.1 Cell Cultures

2.1.1 16HBE Culture

16HBE cells were cultured in T75 flasks. Flasks were coated using a solution of Fibronectin, BSA and Vitrogen in PBS. The cells were stored on liquid nitrogen in vials, and subsequently 10ml of culture medium was added and the cells were transferred to the T75 culture flasks coated beforehand. The medium (Dulbecco's modified Minimum Essential Medium (DMEM) supplemented with 10% v/v heat inactivated fetal bovine serum (FBS), 50 IU/ml penicillin, 50 g/ml streptomycin, and 2mM glutamine) was changed every two to three days. Cells were incubated in a humidified incubator at 37°C, 5% CO2, for approximately one week until they reached the ideal concentration for the subsequent assays.

2.1.2 Trypsinisation of the confluent cell layer

Trypsin-EDTA concentrate (10x) was diluted to a 1x solution with Hank's balanced salt solution (HBSS) without Ca2+ and Mg2+. Prior to use, all media and trypsin were pre-warmed at room temperature. The cell monolayer was washed twice with HBSS to remove traces of serum. Approximately 1-2 ml 1x trypsin-EDTA was added to a T75 flask, enough to cover the bottom surface. Primary fibroblasts were removed by incubation at room temperature for approximately 60 seconds, followed by tapping the flask. For PBEC this period was extended to around 2 minutes. The action of the trypsin was halted by the addition of growth medium supplemented with 10% FBS. The cells were then spun at 150g for 5 minutes to remove the trypsin and the cell pellet was then re-suspended in the relevant growth medium.

2.1.3 ALI Culture

Bronchial segments with a length of approximately 0.5-2 cms long and about 1 cm in diameter were rinsed with cold PBS and the excess parenchymal tissue was s removed. Segments were cut open and minced into 2-3mm^3 pieces of tissue.

The pieces were used as a source of primary cells. After coating 100mm culture plates for 1 hr with a mixture of collagen (30 µg/ml), fibronectin (10 µg/ml), and BSA (10 µg/ml), the tissue pieces were placed in the plates, a mix of Bronchial Epithelial Basal Medium (BEBM) + Dulbecco's Modified Eagle Medium (DMEM) + supplemental hormones (BEGM Kit) + penicillin/streptavidin was added and the plates were placed inside an incubator at 37°C in 5% CO2 humidified air. The culture medium was changed every 2-3 days. The epithelial cells grew from the pieces forming rings with a diameter of about 1.5 cm in two weeks. Cells were lifted using trypsin/EDTA, pooled, counted, and re-plated in T75 Cell Bind flasks to increase their numbers.

Explants were plated in 100mm culture plates. Culture plates were coated using a coating solution. This was done in a Biological Security Cabinet (BSC) in order to keep the culture sterile.

Coating stock solution: fibronectin (10 µg/ml), BSA (10 µg/ml) and collagen (30 µg/ml) in Phosphate Buffered Saline (PBS, sterile).

The media was changed every 2-3 days.

Growing Ciliated PBEC cells in Transwells.

Primary epithelial cells grown from tissue explants/transplants can be expanded up to three times, and then used. A seeding density of 50,000 to 100,000 cells per cm2 is recommended. Higher density promotes faster differentiation.

First, a pretreatment was carried out on the permeable membranes of the transwells by pre-incubating the cell culture inserts with medium. This step was essential for these sensitive cells, and helped cell attachment.

The 6.5 mm inserts that fit into the 24 well plates were used.Medium was added to both sides of the membrane (for the 6.5 mm inserts, 0.5ml was used on the bottom, and 0.1ml was used on the top). The inserts were incubated for 1 hour in a cell culture incubator.
Subsequently, the medium was removed from both sides of the membrane, starting with the basal volume.

The cell suspension was carefully pipetted into the apical side of the membrane: for the 6.5 mm wells, 0.1 ml of cell suspension (i.e. 50,000 cells) was added to the apical side of the membrane.

The cells were nourished from both the apical and basal sides for seven days to establish a well differentiated culture, and the medium was changed three times a week. For cell differentiation, retinoic acid was added to the culture mix (final concentration of RA = 0,1 ng/ml).

On day 7 (approximately) an Air-Liquid interface (ALI) was created by removing the apical medium, and the volume of medium on the basal side of the membrane was reduced to 0.33 ml.

ALI cells were maintained in culture for three weeks, changing the media twice a week. Ciliated cells started appearing two weeks after the creation of the ALI. Cells achieved a uniform differentiation into ciliated cells three weeks after the creation of the ALI.

Primary human bronchial epithelial cells grow well on surfaces coated with fibronectin/BSA/collagen 3. The coating stock solution was used for 100 mm tissue culture plates for explant and transplant cultures as described above;

- Fibronectin (1mg/ml stock solution): Use F2006-2 mg from Sigma. Dissolve 2 mg in 2 ml of sterile Phosphate Buffered Saline (PBS, P3813 SIGMA), filter with 0.2 µm syringe filter in the Biological Safety Cabinet (BSC). Store 1 ml in the -20°C freezer for later use, and use 1 ml for preparing 100 ml of coating solution.
- BSA (1mg/ml stock solution): Use Sigma A4919-1g. Weigh 20 mg BSA and dissolve in 20 ml of sterile PBS, filter with 0.2 µm syringe filter in the BSC. Aliquot into 1 ml vials and store in the -20°C freezer until needed. Use 1 ml of stock to make 100 ml of coating solution.
- Collagen stock solution (provided as 0.1% or 1mg/ml from Sigma C8919). Note: open only in the BSC and seal tightly before returning to fridge. Use 3 ml of stock to make 100 ml of coating solution.
- Coating stock solution: In the BSC: add 3 ml collagen (1mg/ml) to 1 ml Fibronectin (1mg/ml) and 1 ml BSA (1mg/ml), plus 95 ml of PBS (sterile). Mix well and aliquot into 2 ml vials and store in the -20°C freezer until needed. Final concentrations of coating stock solution: fibronectin (10 µg/ml), BSA (10 µg/ml) and collagen (30 µg/ml) in EBSS.

2.1.4 Three-dimensional outgrowths

Bronchial biopsies obtained during bronchoscopy procedures (from patients referred to the Unit of Thoracic Medicine of the University of Palermo), were cut into 0.5mm^3 pieces and placed in the most central location possible in 6.5 mm Transwells on a PET membrane (Becton Dickinson, Franklin Lakes, NJ, USA), embedded in 50µl of Matrigel^{TM} (Becton Dickinson) and then placed in a 24 well culture plate (Corning Life Sciences). Matrigel is a gelatinous protein mixture secreted by the Engelbreth-Holm-Swarm (EHS) mouse sarcoma cells. This gelatin mixture resembles the complex extracellular environment that can be found in many tissues, and is considered to be an excellent substrate for cell culture due to its heterogeneous composition. Laminin, entactin and collagen IV, the major components of Matrigel, are basement membrane proteins in which cultured cells can find the adhesive peptide sequences that they would encounter

in their natural environment (Hughes, 2010). The cultures were grown in a mix of BEGM/DMEM growth medium that was placed underneath the membrane.

This mix was constituted of 1:1 BEGM/DMEM (Bronchial Epithelium Growth Medium/ Dulbecco's modified Minimum Essential Medium with 10% FBS) . The growth medium was replaced every 48 hours. The outgrowths were cultured at 37°C in a 5% CO2 atmosphere.

The expansion of the outgrowths was monitored with a contrast phase microscope. When the cultures reached the required grade of development (or at the end of a treatment) the PET membrane was detached from the transwell and split into four pieces for characterization.

Human oral mucosal biopsies were obtained from patients referred to the Unit of Oral Medicine of the University of Palermo. The following procedures were carried out conforming to the relevant ethical guidelines for human research and in agreement with the Helsinki Declaration of 1975, as revised in 1983, and approved by the Ethic Council of the Polyclinic of the University of Palermo, Italy. All patients gave a written informed consent. A topical antifungal therapy (miconazole 2% oral gel, Daktarin, Janssen-Cilag) was administered three times/day for seven days prior to the biopsy. After a 1 minute oral rinse with 0.2% chlorhexidine, oral mucosa samples were obtained by a 6 mm biopsy punch from the margin of the lesion with clinically healthy tissue.

Each biopsy was divided into two parts. The outer part of the sample was fixed in formalin and sent for a histocytopathological examination, while the inner part was immediately placed in fresh culture medium and processed for the 3D oral outgrowths. The histocytopathological examination of the six subjects recruited for this study resulted negative for dysplastic/cancerous lesions of the oral cavity. Biopsies destined for outgrowth development were washed several times in PBS, subsequently cut into 0.5 mm^3 pieces using a sterile scalpel, and placed in the middle of 6.5 mm Transwells on a PET membrane (Becton Dickinson, Franklin Lakes, NJ, USA) and embedded in 60 µl of Matrigel™ (Becton Dickinson). The Transwells were placed in 24 well culture plates (Corning Life Sciences), and these were then kept at 37°C for 5 minutes to facilitate Matrigel™ jellification. 330 µl of growth medium mix was added to each well.

The composition of the mix was: Keratinocyte-SFM supplemented with 5ng/ml of h-EGF and DMEM supplemented with 10% FBS (1:1), which was placed under the PET membrane of the Transwells. The outgrowths were cultured at 37°C in a 5% CO_2 atmosphere and the medium was changed every 48 hours.

An inverted light microscope equipped with phase contrast rings (LEICA DM-IRB, Leica Microsystems Srl, Milan, Italy) was used to monitor the outgrowths. At specific time points, the membranes with the outgrowths were prepared for Transmission Electron Microscopy (TEM).

2.2 Treatments

2.2.1 Pseudomonas Aeruginosa-conditioned medium

To prepare the medium conditioned with P. Aeruginosa extracts (PAOM), 10ml of bacterial culture medium was inoculated with a single PAO1 colony from an agar plate (stock bacterial plates were stored at 4° C.), and then placed in an incubator overnight at 37°C with continuous shaking. Next, 5ml of the grown culture was added to 100 ml of DMEM, and incubated at 37°C with continuous shaking for three days. Subsequently, the bacteria were removed from the culture by centrifuging at 100,000g for 30 minutes and the supernatant was filtered through a 0.2um filter. The aliquots of the conditioned media were stored at -4°C.

Treatments were carried on the individual cell cultures using different mixtures of PAOM and DMEM.

2.2.2 Preparation of Cigarette Smoke Extracts

The use of Cigarette Smoke Extracts (CSE) to study the effects of cigarette smoke *in vitro* is a commonly used approach. It has been demonstrated that CSE can cause damage to various types of tissues (including endothelial, mesenchymal and epithelial cells) (Di Cello, 2013; Zhang, 2012; Su, 1998). CSE

cause an increase in the formation of free radicals both in a direct and an indirect way (Iwahashi, 2006; Yamamoto 2013). Other examples of CSE properties are its potential to cause epithelial-mesenchymal transition and subsequently induce tumorigenic transformation; CSE also induce stress to the endoplasmic reticulum, and interact with and modulate the efficacy of immune cells (Mortaz, 2009). The most important feature that I would like to emphasize is its widely ascertained ability to produce cytotoxic effects (Hosnino 2001; Park 2013), although the mechanism by which this occurs is not entirely clear.

CSE were prepared by gurgling the smoke from two Kentucky 1R4F research cigarettes (University of Kentucky, Lexington, KY), whose filters were removed, through 50 mL of BEBM for 60-70 s. The resulting suspension was adjusted to a pH of 7.4 with concentrated NaOH, filtered through a 0.22-μM Millex-GS filter (Millipore, Watford, UK) and used instantly on the 3D outgrowths at a concentration range of 10, 15 and 20%.

2.3 TEER Measurements

Transepithelial electrical resistance (TEER) is used to measure the ion movement across the paracellular pathway. Indirect assessment of tight junction establishment and stability of cells grown on permeable membranes is assessed by the measurement of TEER.

The electrical resistance is measured in Ohm (Ω); the unit can be defined as the resistance offered by an element when a voltage of 1 volts applied to the element produces a current of 1 ampere in the element. In the field of cell culture, the TEER depends mainly on the characteristics of the cell line, and to a lesser extent, on the culture medium used.

A good TEER value is important when working with primary cell models. In particular, primary human bronchial epithelial cells may be seeded at the air-liquid interface and forced to differentiate into a more natural phenotype. In this model, the cells organize themselves in a manner similar to cells *in vivo*, to display a pseudostratified, polarized phenotype that includes ciliated and goblet cells and developing a high TEER (Karp, 2002). There has been some debate regarding the reported differences between normal and asthmatic cells. For instance, some studies have reported no difference in the TEER between normal

and asthmatic cultures, while others claim that cells from asthmatic subjects show decreased TEER and disrupted tight junctions. These discrepancies may reflect differences in donor profiles, cell sources (post-mortem donor lungs versus bronchial brushings), or variations in the number of subjects included in the study (Stewart, 2011). The measurement of TEER provides an indirect way to assess the complete formation of tight junctions, and can be used as a marker of disruption of the epithelial layer. Some studies suggest that cells from asthmatic subjects show decreased TEER values, and, as a consequence, disrupted tight junctions (Xiao, 2011). It is necessary consider these details when starting a new primary human bronchial epithelial cell (HBEC) culture, because during the culture period, following the ALI transition, the cells will be more sensitive to TEER disruption caused by external agents (for example, CSE).

The TEER measurements were obtained during the culture period and at the end of specific experiments to acquire specific informations about the condition of the epithelial layer. An EVOM - Epithelial Voltohmmeter was used to measure the TEER. The cells were cultured in the 6.5 mm inserts that fit into the 24 well plates. The procedure required a pre-incubation step with 100 µl of PBS added on the apical side of every Transwell, followed by a 15-minute incubation period to guarantee a correct distribution of ions. The plates were subsequently placed under BSC and the TEER was measured using the EVOM.

2.4 ELISA assay

The ELISA assay was conducted using the standard protocol of the SANQUIN ELISA KIT.

After the preparation of a coating buffer, as described in the standard protocol, the plates used for the experiment were treated by adding 100 µl of coating solution to all wells. The plate was incubated overnight at room temperature (18-25°C). Next day, the wells were washed four times with the PBS working solution (prepared the day before following the instructions in the information leaflet). At the end of the procedure, the wells were totally dried. It was necessary to block the non-specific sites by using a blocking buffer (for 1 hour at room temperature, 200 µl x well).

To prepare the standard curve of reference, the subsequent procedure was followed:

> "Pipette 610 ml of working-strength dilution buffer into the tube labelled 240 pg/ml and 300 ml of working-strength dilution buffer into the other tubes.
>
> Transfer 15 ml of the IL-8 standard (10 ng/ml) into the first tube labelled 240 pg/ml, mix well and transfer 200 ml of this dilution into the second tube labelled 96 pg/ml.
>
> Repeat the serial dilutions six more times by adding 200 ml of the previous tube of diluted standard to the 300 ml of dilution buffer.
>
> The standard curve will contain 240, 96, 38.4, 15.4, 6.1, 2.5, 1 and 0 pg/ml (dilution buffer)." (from the Sanquin protocol)

The samples were analyzed using the *Thermo Fischer Scientific 1000 NanoDrop Spectrophotometer* to evaluate the initial concentration of proteins and diluted if necessary.

For the first incubation step, the samples were added in duplicate for every well, incubated for 1 hour at room temperature (18-25°C), and washed at the end of the procedure.

For the second incubation step, 120 µl of biotinylated antibody was added and the plates were incubated for 1 hour at room temperature with gentle shacking, followed by a final washing to remove the excess antibody.

In the two subsequent steps, spaced out by a washing step, streptavidin and Horseradish peroxidase (HRP) conjugate was added to the substrate solution that contained H_2O_2. After 30 minutes, the reaction was stopped by adding a stopping solution to each well and the plates were analyzed with an ELISA reader.

2.5 Western Blot

Following the treatments, the cells were lysated using a lysis buffer to evaluate protein expression; the entire procedure was carried out on ice to prevent protein degradation. The culture medium was removed and the cells were washed with the wash buffer at 4°C. The wash buffer was then replaced by a lysis buffer, and the cells were incubated for 10 minutes on ice (50 µl lysis buffer/well x 24 well plate). At the end of the 10 minutes, the cells were scraped and the lysate was transferred into a tube and centrifuged at 10.000rpm for 5 minutes at 4°C. The supernatant was collected and stored in new tubes at -20°C.

Solutions:

- Wash buffer:

• Dist.Water	1 L
• Tris pH 7.4	5 mM (605,7 mg)
• NaCl	100 mM (584,4 mg)
• CaCl2	1 mM (147,0 mg)
• MgCl2	1 mM (203,3 mg)

- Lysis buffer:

• Wash buffer (See above)	10 ml
• Triton X-100(0,5% v/v)	50 µl
• Protease inhibitor cocktail	1 tablet

A standard Western Blot technique was followed to separate protein using a concentration of 7.5% of BisAcrylamide as reported in the following chart:

Running gel:

For 2 gels				
	7,5%	**10%**	**12,5%**	**15%**
Tris-buffer A	2,5 ml	2,5 ml	2,5 ml	2,5 ml
Acryl-bis	2500 µl	3300 µl	4100 µl	5000 µl
H_2O	5 ml	4,2 ml	3,4 ml	2,5 ml
APS	50 µl	50 µl	50 µl	50 µl
TEMED	10 µl	10 µl	10 µl	10 µl

Stacking gel:

For 2 gels	
Tris–buffer B	500 µl
Acryl-Bis	650 µl
H_2O	3,8 ml
APS	25 µl
TEMED	10 µl

Solutions:

- TRIS-buffer A (4x):

• Tris	45,4 g
• SDS 10%	10 ml
• Dist. water	250 ml
	pH 8,8

- TRIS-buffer B (10x):

• Tris	37.6 g
• SDS 10%	25 ml
• Dist. Water	250 ml
	pH 6,8

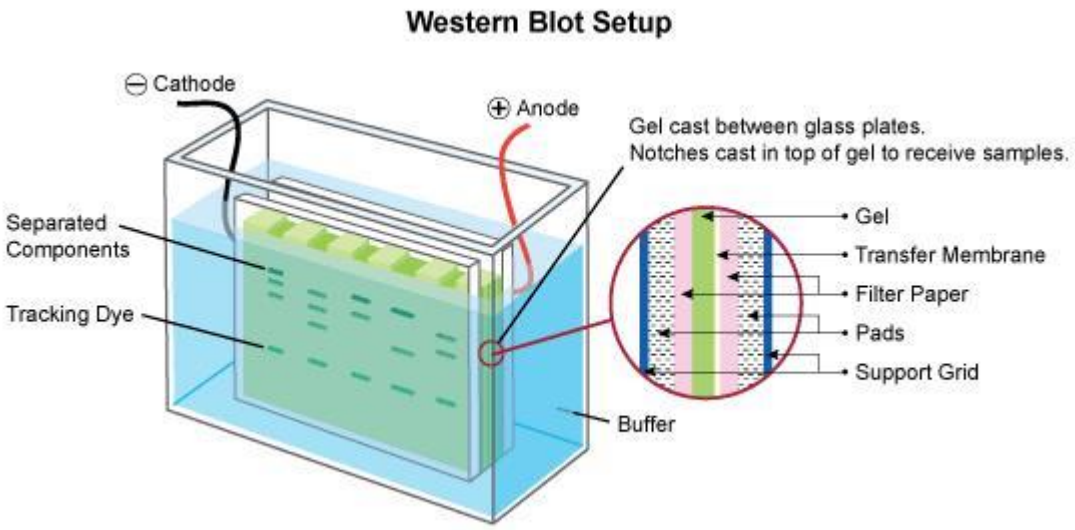

Fig. 9: *Western Blot Scheme (nacalai.jp)*

At the end of the procedure, the membrane, with the spotted protein was analyzed to measure the ZO-1 protein levels using procedure and antibody concentration perfected by others.

2.6 PCR, Primers and Antibodies

The protocol used to carry out the PCR, the preliminary testing to find the best work conditions for gene primers and antibodies used in treatments was perfected by the work group of the Pulmonology Department of the Leiden University Medical Center.

2.7 Indirect Immunofluorescence

3D outgrowths were stained *in situ* at the appropriate time points. Briefly, outgrowths were washed once with 1ml/well of HBSS and fixed *in situ* in 500µl/well of ice-cold absolute methanol for 20 minutes at –20°C. Outgrowths, inside their plastic supports, were then left to dry in a laminar flow cabinet for 30 minutes and stored at –20°C. Trays were defrosted at room temperature, and washed twice with 1ml/well of phosphate buffered saline (PBS), permeabilized with 500µl/well of Triton X-100 (Sigma, UK) 0.1% in PBS for 3 minutes on ice, and washed once with 1ml/well of PBS. Unspecific binding sites were blocked with 250µl/well of DMEM 10% FBS for 15 minutes. During this period, the primary antibodies were diluted in incubation buffer (DMEM 10%, Tween-20

0.1% and Sodium Azide 0.1% in PBS). The blocking buffer was then removed, and without washing, the diluted antibodies were added to the wells for 45 minutes. Wells were then washed twice with 1ml/well of incubation buffer and, when needed, secondary antibodies were diluted in incubation buffer and applied to the wells for 45 minutes. Secondary antibodies were conjugated with different fluorochromes.

Table 1 shows a list of all the primary antibodies employed and their working dilutions.

	Supplier	Clone	Source	Dilution
CK1	Santa Cruz, UK	4d12b3	Mouse IgG1	1:100
CK5	"	H-40	Rabbit IgG	1:600
CK10	"	AE20	Mouse IgG1	1:50
CK13	Abnova, USA	1C7	Mouse IgG2a	1:200
CK19	Santa Cruz, UK	BA17	Mouse IgG1	1:200
CK20	"	E-9	Mouse IgG1	1:100
Collagen type I	Millipore, UK	5D8-G9	Mouse IgG1	1:50
Collagen type IV	Santa Cruz, UK	Col-94	Mouse IgG1	1:200
Laminin	Millipore, UK	2G6/A2	Mouse IgG1	1:200
E-cadherin	Santa Cruz, UK	G-10	Mouse IgG1	1:50
Fibronectin	Abnova, USA	568	Mouse IgG1	1:30
Involucrin	"	m-116	Rabbit IgG	1:400
MITF	"	H-50	Rabbit IgG	1:500
CD3	R&D Systems, USA	UCHT1	Mouse IgG1	1:100
CD4	"	34930	Mouse IgG1	1:50
CD8	"	37006	Mouse IgG2b	1:50
CD45	"	2D1	Mouse IgG1	1:100
CD68	"	298807	Mouse IgG2b	1:100
MPO	"	392105	Mouse IgG2b	1:50

Table 1: *List of primary antibodies used on oral human outgrowths.*

The secondary antibodies were: a secondary Alexa Fluor647–conjugated goat anti-rabbit Ab (1:500; Molecular Probes, USA); a secondary FITC-conjugated goat anti-mouse IgG Ab (working dilution 1:400, purchased from Sigma, UK); and a secondary TRITC-conjugated goat anti-mouse IgG Ab (working dilution 1:500, purchased from Sigma, UK). At the end of the 45 minutes incubation with the secondary antibodies, wells were washed twice with 1 ml of PBS and coverslips were mounted with MOVIOL (DABCO) mounting medium. Appropriate negative controls were prepared by replacing primary antibodies with the appropriate isotype control sera.

The trays were then ready to be observed with a LEICA SP5 inverted confocal microscope (Leica, Heidelberg, Germany) with filters for FITC (excitation 488 nm, emission 500–535 nm), TRITC (excitation 557 nm, emission 560–600 nm), and Alexa Fluor647 (excitation 633 nm, emission 640–680 nm). Each image was averaged from 14 scans within a thickness of 5 to 7 μm.

Immunofluorescent staining was semi-quantified by scoring the percentage of positive cells or area (depending on the antigen of interest), evaluated by three different operators (AMG, AF and AP) in five different mid-magnification (400x) microscopic fields (score: - absence of immunostaining, -/+ less than 10% of the total number of cells/area scored positively; + between 10% and 50% scored positively; ++ 50-100% of the total number of cells/area were positive).

2.8 Transmission Electron Microscopy

Immediately after excision of the PET membrane from the Transwells using a scalpel, the outgrowths were fixed in a 2.5% glutaraldehyde solution in phosphate buffer, pH 7.4, for 20 minutes at room temperature. The glutaraldehyde was removed and the outgrowths were stored in Millonig's Buffer at 4°C until the next steps. Two different solutions were prepared to produce Millonig's Buffer:

A Solution: 25,6g of NaH_2PO_4 x $2H_2O$ was added to 1 liter of distilled water; B Solution: 25,2g of NaOH was added to 1 liter of distilled water.

The final step was to mix 83 ml of the A solution with 17ml of the B solution to make 100ml of Buffer; the pH was adjusted to 7.4.

After washes with Millonig's Buffer, the pieces were post-fixed in 1% OsO_4 for 2 h, dehydrated in an ascending ethanol series, treated with propylene oxide for 30', infiltrated with epoxy resin (Epon812, Electron Microscopy Science, Hatfield, PA, USA) in propylene oxide (1:3, 1:2, and 1:1 for 30 minutes at room temperature, respectively), and finally embedded in Epon812 with DMP30. The resin was then polymerized in an oven at 60°C for 48 hours. Ultra- and semithin sections were cut with an ultramicrotome (Ultracut E, Reichert-Jung, Depew, NY, USA) at different thicknesses and mounted on copper and gold grids or on glass slides for further use. Contrast solution for the grids to be used for electron microscopy was prepared by:

dissolving 0,7g of uranyl acetate in 10ml of methanol; Reynolds' solution was prepared by dissolving 1,33g of $Pb(NO_3)_2$ and 1,76g $NaC_6H_5O_7$ x H_2O and 8ml of NaOH 1N in 50 ml of distilled water at pH 12.

Ultrathin (50nm) sections of the embedded samples were cut with an ultramicrotome and placed on Cu/Rh grids. Before observation with the transmission electron microscope (JEM-1220; JEOL, Japan) the specimens were contrasted with uranyl-acetate 7% in methanol and Reynold's lead citrate.

2.9 Immunogold

Ultrathin sections were mounted on gold grids to prepare them for the immunogold assay. The outgrowths were included in epoxy resin that notoriously covers antigenic sites, making the execution of immunological investigation techniques considerably more difficult. A pre-treatment to unmask the sites with sodium citrate was performed to ensure better results. Gold grids were placed in a baker filled with a sodium citrate solution and subsequently microwaved for 4 minutes at 850W.

The grids were then washed twice in PBS, and subsequently incubated in a serum blocking solution for 30 minutes and, without washing, the incubation proceeded with primary antibodies diluted in dilution buffer for 1 hour and a half at room temperature. Primary antibodies used were against laminin, fibronectin and collagen type IV, and their dilutions can be found in Table 1. Grids were rinsed five times with PBS for 3 min and incubated with the secondary antibody conjugated with 10nm colloidal gold particles for 30 minutes at room temperature, and washed again for five times with PBS for 3 min. Subsequently, the grids were fixed in a 2.5% glutaraldehyde solution in PBS for 15 minutes, and washed five times in distilled water for 3 minutes. The grids were then prepared for contrast staining by treating them with uranyl acetate for 5 minutes, followed by eight washes with methanol for 2 minutes, treated with Reynolds' solution for 5 minutes and finally rinsed eight times in distilled water for 2 minutes. After this procedure, the grids were ready for electron microscopy.

3.RESULTS

3.1 Use of the ALI culture model to study farm dust properties

Aims: Firstly, it was deemed necessary to test the properties of the new conditioned media prepared from Pseudomonas Aeruginosa extracts. The previously used conditioned media, prepared following the old protocol, caused stress and cell death, depending on the concentration. At the same time, it was necessary to not only test if the "new" medium would cause the same effects (the stock of bacteria was different) but it was also essential to ascertain which concentration was ideal for our purpose (effects on tight junctions). From existing literature and previous studies it was clear that dust collected from the rooms of children living in a farm has the potential to prevent allergy and atopy in adults. At the same time, a good number of experiments conducted on mice to test the effects of farm dust (Hylkema, 2011; Robbe, 2012) had shown similar results. For my PhD studies, in order to test the properties of the dust, various samples taken from bedrooms of children living in rural environments were mixed together to obtain a uniform "farm dust" to use for the experiments. Initially I wanted to see if farm dust has some direct effects on tight junction proteins. As noted before, other studies conducted on mice had shown the protective properties of farm dust, but, at the same time, it was discovered that the dust does not prevent the onset of an inflammatory response. In fact, in mice, the administration of dust causes the release of IL-17, an interleukin found in many chronic inflammation diseases. For these reasons, I wanted to see whether the release of pro-inflammatory interleukins would take place in the ALI culture model too, or furthermore, if the exposition to dust would prevent the release of inflammatory cytokines from cells exposed to dust and PAOM, or both. In order to answer these questions, I monitored the levels of IL-8. IL-8 was chosen since it is another interleukin linked with inflammation status and produced *in vivo* by airway epithelial cells and its release is a known marker in many pathologies (such as asthma, cystic fibrosis and tumors). Finally, I tested if farm dust can increase levels of TEER in the ALI culture model. Therefore, Primary Epithelial Bronchial Cells were cultured at air-liquid interface to promote

cell differentiation and obtain a polarized epithelium with a cell composition and organization that mimics the *in vivo* state. In addition to the TEER assay, I also evaluated whether farm dust presented some regenerative properties or if a "chronic" exposition had some specific effects.

3.1.1 Testing the disruptive effects of PAOM

Preliminary experiment on 16 HBE: To verify the potential of the new PAOM prepared as explained in the "Methods" chapter, the best choice to reduce inconsistencies in the results was the 16 HBE cell line. These cells are characterized by uniform growth properties (especially in the early passages), compared to primary cells, mainly due to the exclusion of "donor" variability. Once the conditioned culture medium was ready, four flasks of 16 HBE were treated with different concentrations of PAOM. The cell confluence was about 80-90% to avoid cell detachment due to overcrowding. The three concentrations used were 1:5, 1:10 and 1:20, with one part of PAOM for 5, 10 and 20 total parts of media, respectively; the latter consisted of normal growth medium (DMEM integrated with 10% FCS, for further details refer to methods). Flasks were observed by optical microscopy at 1, 3 and 6 hours for monitoring.

Results: The most concentrated mix showed excessive disruptive effects immediately. After only one hour of exposition to PAOM mix, the result was that shown in Figure 13. The 16 HBE layer was totally destroyed, it was impossible to discern any cells, and the only observable structure was a shapeless lipid mass.

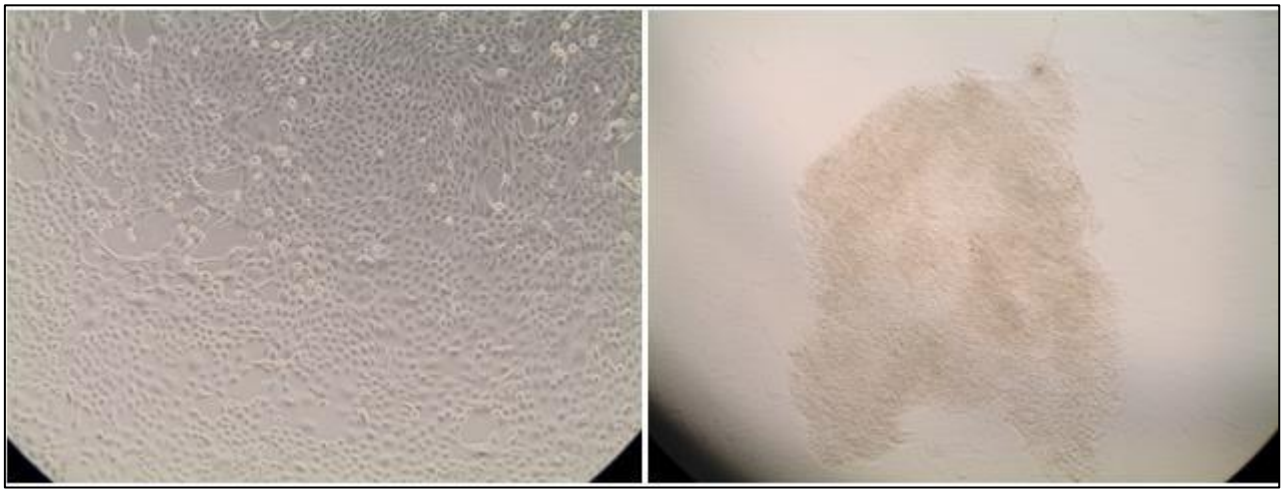

Fig.13: *16HBE treated with PAOM mix. Control on the left side. Sample treated with 1:5 PAOM mix on the right side. Both flasks of cells were treated for 1 hour.*

Better results were obtained with the second concentration, 1:10 PAOM mix, but after 6 hours of treatment the fate of the cells was the same. The dilution of the mix gave the expected result but for our purpose the damaging effects were still too elevated. The results are displayed in Figure 14.

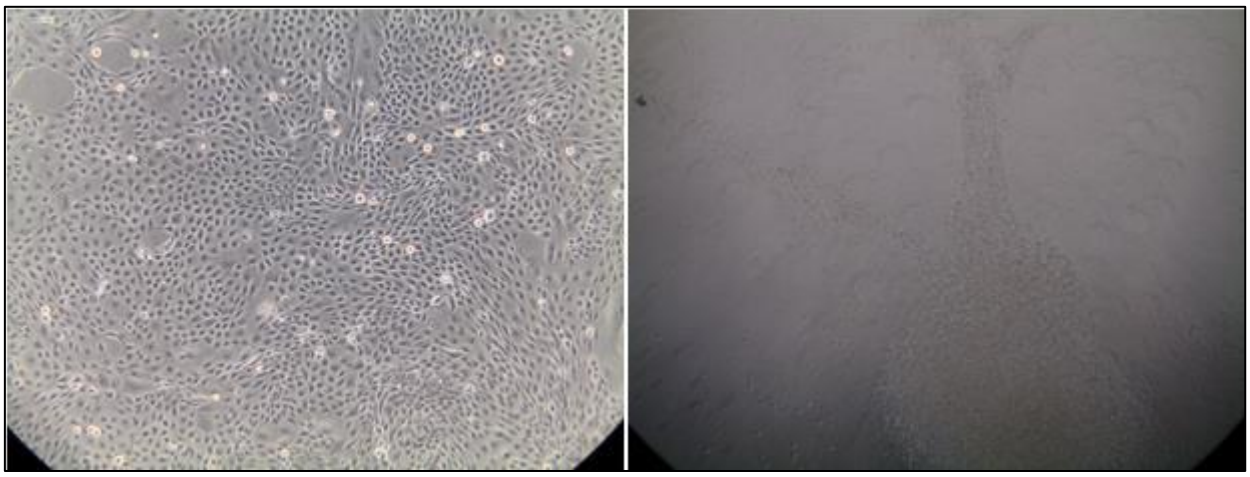

Fig.14: *16HBE treated with PAOM mix. Control on the left side. Sample treated with 1:10 PAOM mix on the right side. Both flasks of cells were treated for 6 hours.*

Finally, the last concentration, 1:20 PAOM mix, determined the ideal effects. The mix damaged the epithelial layer but not in an excessive manner like the previous concentrations. After 6 hours, the number and dimensions of the "holes" in the epithelial layer were increased in an appreciable way.

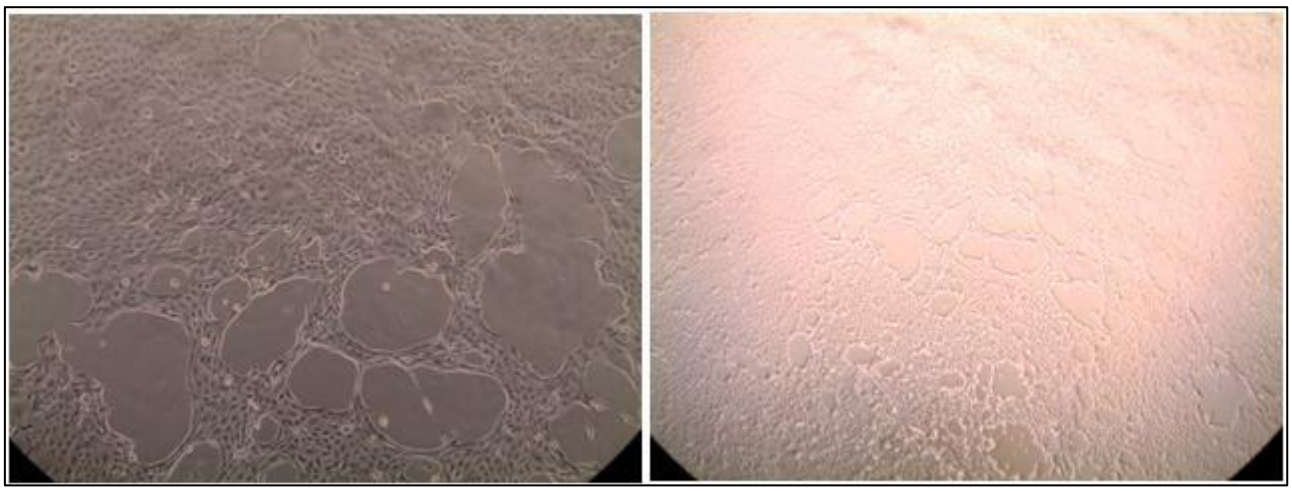

Fig.15: *16HBE treated with PAOM mix. Sample treated with 1:20 PAOM, two different magnifications. Cells were treated for 6 hours.*

Specific effects of PAOM: The three different PAOM mixes were tested to see the specific effect of Pseudomonas to cause disruption of tight junction proteins. In particular, the effect on ZO-1 was assessed. Considering the results of the

previous experiment, the 16 HBE were treated for only 1 hour with the three different mixes; at the end of the treatment, protein isolation and western blot procedure were carried for ZO-1. This protein was chosen in line with the results of previous experiments. As expected, linearity was found between the increased disruption of ZO-1 and a more concentrated mix. Results are shown in Figure 16.

Fig.16: *Western Blot vs ZO-1 using three different dilutions of PAOM. The columns are displayed in the following order: Control, 1:5, 1:10 and 1:20. A partial disruption of the protein was achieved only with the 1:20 mix, while the use of the more concentrated mixes resulted in the destruction of the protein of interest*

3.1.2 Effects of farm dust on 16 HBE.

qReal Time PCR: To execute the initial assay, 16 HBE cells were treated with farm dust at a concentration of 50mg/ml for 2 and 4 hours. The experiment was conducted in parallel with samples without FCS in the culture media to see if the FCS influenced the properties of the dust. At the end points, Maxwell® 16 System RNA Purification Kits were used to isolate RNA from the cell cultures with the automated Maxwell® 16 Instrument using standard protocol. The RNA was retro-transcribed to cDNA using a MyCycler (BioRad) and analyzed with a quantitative RealTime PCR conducted by CFX384 Touch™ Real-Time PCR Detection System and data were collected using the specific software. The two target genes were Occludin and ZO-1, two of the main components of tight junctions. The housekeeping gene used to normalize the data was RPL13A that presented a better efficiency of amplification (102%) in comparison with the other candidate, ATP5B.

Data Discussion: The data were collected using the original software of the instrument and normalized automatically. Figure 17 shows the relative expression of the different samples, paired with the Control Sample, at 2 hours.

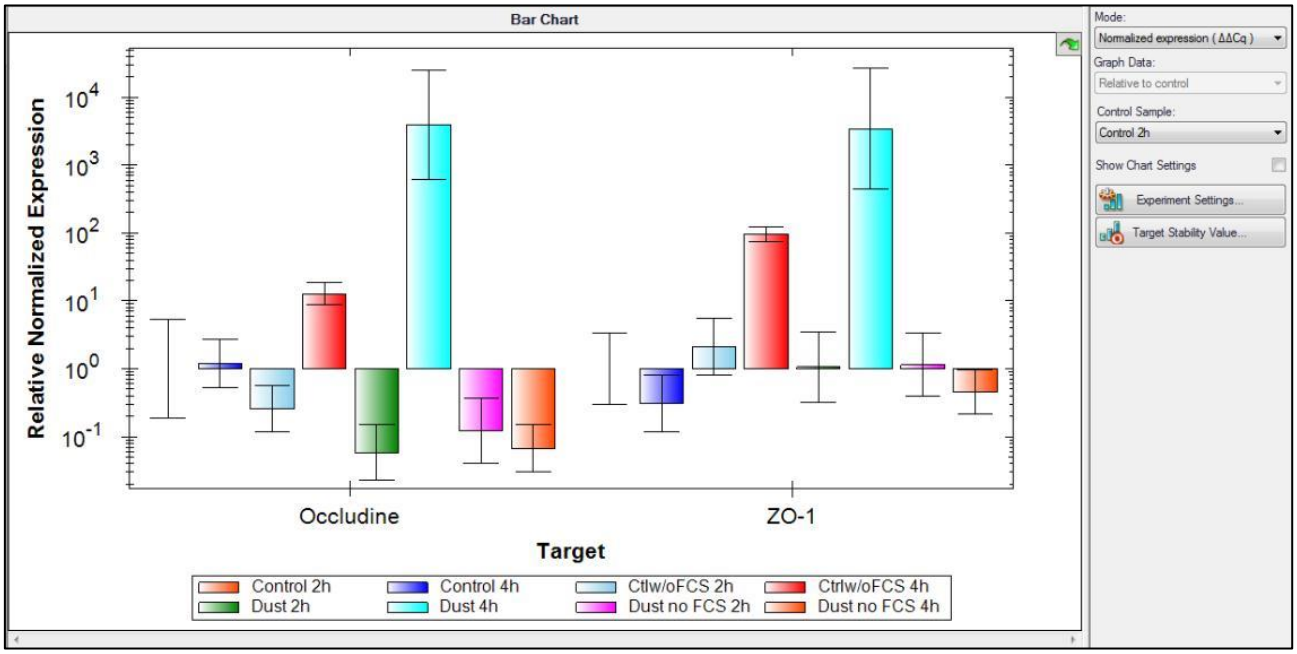

Fig.17: *Results of qRTPCR. Target genes Occludine and ZO-1. Results normalized via RPL13A expression. The relative expression of gene of interest is compared with the expression of control at 2 h.*

The relative expression of both genes was increased in the samples treated with dust after 4 hours from the beginning of the assay. Instead, at 2 hours there was no appreciable increase in the RNA synthesis. Probably more than 2 hours are needed before the pathways activated by exposition to farm dust begin to promote the transcription of tight junction protein RNAs. The parallel experiment (to assess the effects of serum absence) led to a particular result: the samples treated with farm dust but without serum did not present signs of increased transcription, even after 4 hours. Probably, some component present in the serum is necessary to activate or to promote the pathway that leads to the increase in transcription, or, the cells, that are now in a starvation condition, do not have enough energy to synthesize new proteins (and at that point, the transcription machinery is silenced).

3.1.3 Analysis of Farm Dust effects on ALI culture

Procedure: Once the ideal level of differentiation was reached, six ALI inserts were treated with farm dust at a concentration of 50mg/ml. To emulate the normal *in vivo* exposure, the dust was diluted in normal PBS with a final volume of 100µL per insert and put on the apical side of the epithelial layer for 2 hours. After 2 hours, the PBS with the dust was removed and both a control and a sample pre-treated with dust were processed with the PAOM mix 1:20 for further 4-24 hours. At the end of the assay, media were collected and analyzed by ELISA to measure levels of IL-8. The experiment was conducted in triplicates (3x Controls, 3x Treated only with dust, 3x Treated only with PAOM, 3x Treated with both dust and PAOM).

Data: The data collected are shown in Figure 18. A sort of continuity can be observed between the two graphs illustrated in this figure. The release of IL-8 remains similar at both 4 and 24 hours, with samples treated with PAOM (independently from dust presence or absence) that responding to external stimuli with an increased release of IL-8. Samples exposed only to dust do not show appreciable variations compared to controls.

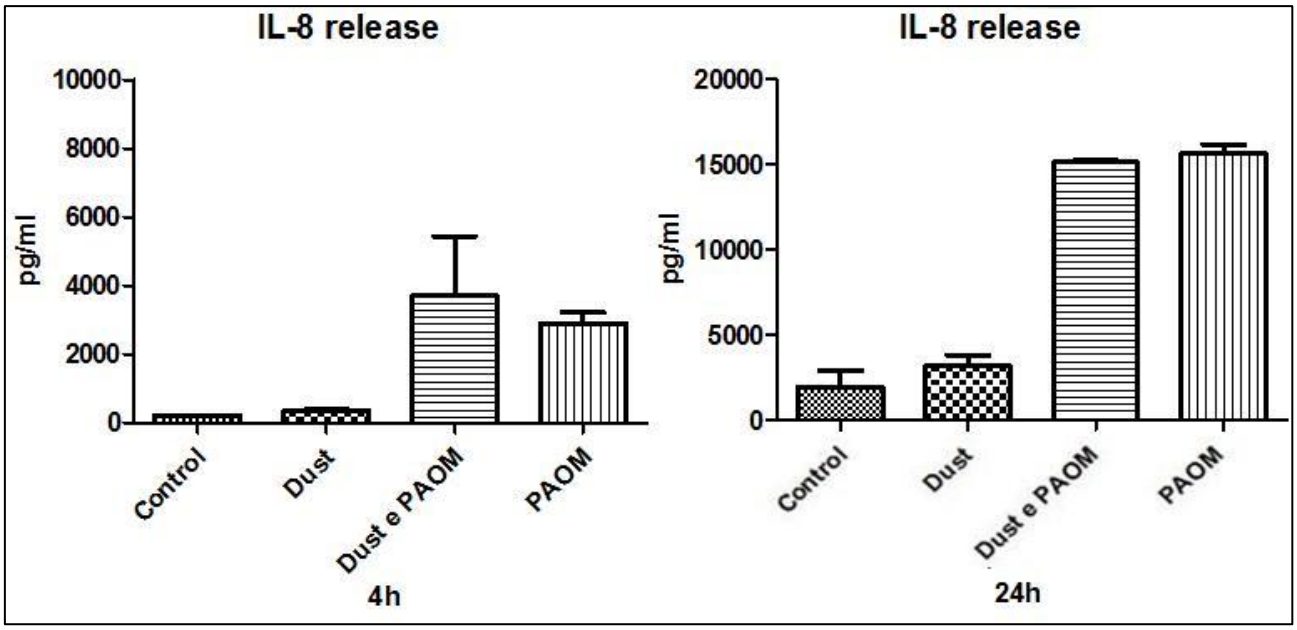

Fig.18: *Elisa assay. IL-8 release levels. Samples were treated for 2 hours with dust and for 4 and 24 hours with PAOM and media were then collected and analyzed. Dust does not prevent release of IL-8 if PAOM is administered concomitantly, but at the same time dust alone does not increase the release of the protein.*

3.1.4 TEER analysis on ALI cultures treated with PAOM and farm dust

Preliminary preparation: 12 inserts were cultured with the ALI method until they reached a good level of differentiation and total confluence on the PET membrane (about 3 weeks). From previous attempts and literature data, I noticed that it is necessary to check the TEER levels for one week before to begin the treatments, to have an idea of the normal intrinsic oscillations of the TEER surveys. Furthermore, I realized that the TEER levels drop every Monday, probably an effect of the slight starvation occurring during the weekends ("Manic Monday" effect, Bangles, 1986); in order to avoid this effect I started the assay on Tuesday thus preventing the starving effect by changing the medium exactly every 48 hours. A preliminary test was conducted to select the best donor to use, with high basal level of TEER (according to literature, > 700 Ω/cm^2 can be considered a good value) and a good level of differentiation.

Dust Exposition: After one week of TEER level monitoring, ALI cells were exposed to farm dust, that was dissolved in PBS, with a final volume of 100µL x insert and put on the apical side of the epithelial layer for 2 hours.

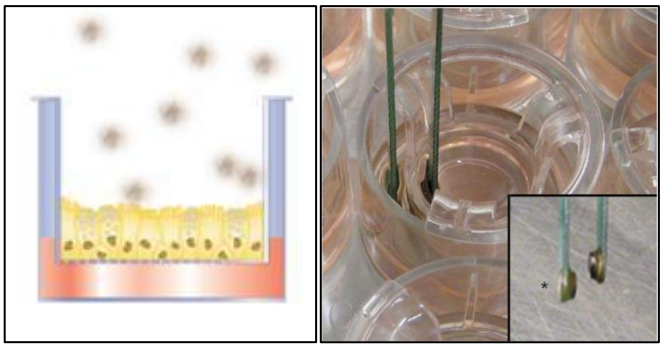

Fig.19: *Left Side: schematic representation of dust exposition of ALI cells. Right Side: TEER measuring.*

After 2 hours, the dust was removed and the relevant samples were treated with 1:20 PAOM mix for further 36 hours. The inserts were divided into four categories: control, exposed to PAOM only, exposed to dust only, and exposed to both dust and PAOM. During this time, every 12 hours, TEER levels were measured and pictures were taken with an optical microscope to monitor the status of the cell cultures. To reproduce a similar chronic exposition to dust, after 12 hours of culture I treated one of the dust + PAOM samples with a second dust exposure followed by a third exposure after 48 hours. I decided to avoid a more frequent exposure to dust to prevent a drop in TEER levels caused by an excessive manipulation of the samples. Another sample belonging to the group treated only with PAOM, was exposed to dust too, but only for 12 and 48 hours to see if the dust could block the damage after the external stimuli was applied. To study the restoration of normal TEER values it was necessary to remove the PAOM mix, when present, and from previous experiments and direct observations, I determined that the ideal time point for PAOM removal was at 36 hours.

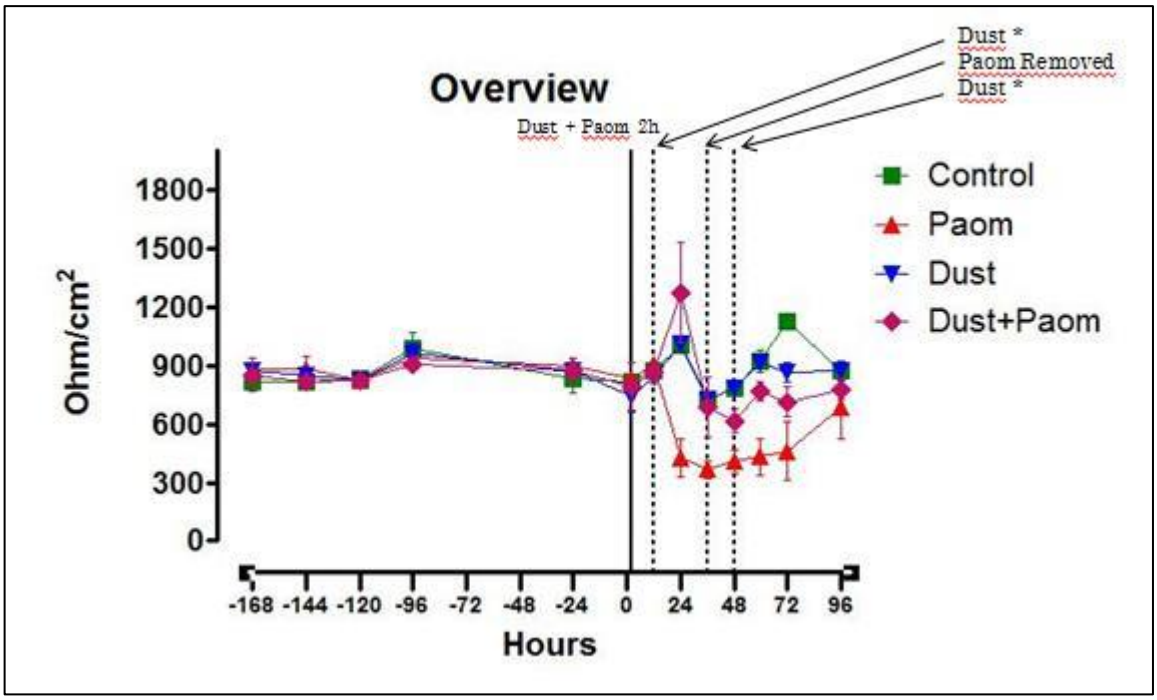

Fig.20: *Schematic representation of TEER levels. 4 categories: Control, Treated with PAOM at 1:20 dilution, Pre-exposed to dust for 2 hours, dust+Paom.*

In the next table, are collected all the data of TEER levels measured during the culture period. Data collection was started one week prior to the beginning of the treatments and during this period the TEER surveys were performed every 24 hours. After the start of treatment, the frequency of the data collection was increased to every 12 hours until the end of days.

	Control			PAOM			Dust			Dust+ Paom		
Tue -168h	825	835	791	845	904	892	842	895	887	778	833	947
Wed -144h	812	802	840	818	879	950	836	853	848	787	821	848
Thu -120h	802	822	870	798	837	840	788	848	845	825	807	855
Fri -96h	901	977	1076	905	973	943	948	1017	936	898	939	893
2 week												
Mon -24h	796	913	789	903	893	905	908	867	840	943	828	863
Tue 2h	810	807	825	832	842	829	795	790	650	747	930	700
Tue 12h	825	921	887	915	928	877	802	876	845	818	859	927
Wed 24h	998	1015	991	315	492	472	1053	1005	981	1095	1160	1568
Wed 36h	701	742	734	312	401	386	771	712	702	582	608	864
Thu 48h	792	796	774	338	432	451	770	794	780	602	564	681
Thu 60h	920	982	868	324	485	486	913	944	895	734	747	825
Fri 72h	1130	1146	1094	289	535	566	823	919	850	660	682	804
Sat 96h	878	880	872	502	780	777	865	925	831	724	828	785

Fig.21: *Table with all the measured TEER levels. Data are divided by sample categories. The underlined data belong to samples treated with dust at 12 and 48 hours. Values are expressed in* Ω/cm^2

Data and figures discussion: For ease of viewing, I have divided the graphic representation of the data into several comparative graphs. Photographs of the samples were taken at 36, 48 and 72 hours. In every graph, the four dotted lines indicate: the starting point at time 0, the first additional dust exposure at 12 hours, the removal of the PAOM mix and the substitution with normal growth medium at 36 hours, and the second dust exposure at 48 hours. The values indicate Ω/cm^2 resistance levels on the y-axis and the hours passed on the x-axis. I decided to not report again the part of the graph antecedent to the beginning of the experiment because that part of the data collection was necessary only as a benchmark to determine the basal level of TEER and to demonstrate that all samples started the experiment with similar TEER values.

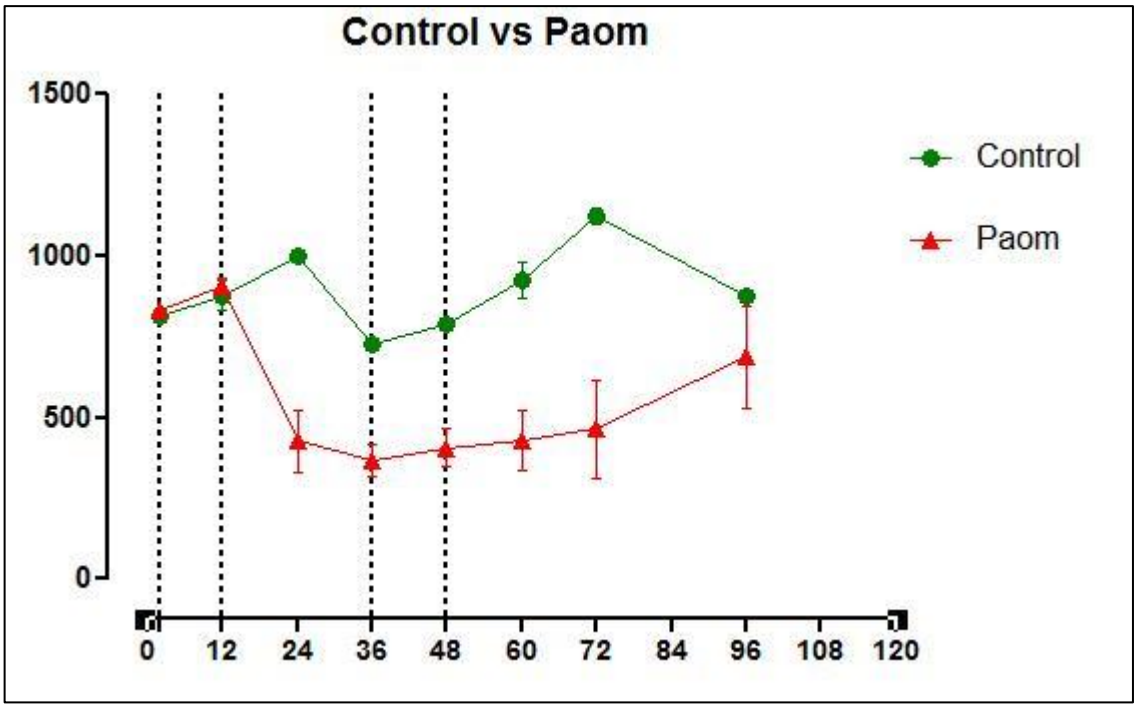

Fig.22: *Teer surveys. Control and PAOM treated comparison.*

Samples treated with PAOM mix at 1:20 dilution started to suffer the effects of P.Aeruginosa extracts after 12 hours, with the lowest point at 36 hours. From that point onwards, it was necessary to remove the conditioned medium and change it with normal cell culture medium to avoid losing the culture and to be able to observe the following regeneration phase. Note: after 36 hours there was a reduction in the TEER levels in the control samples too, probably deriving from manipulation.

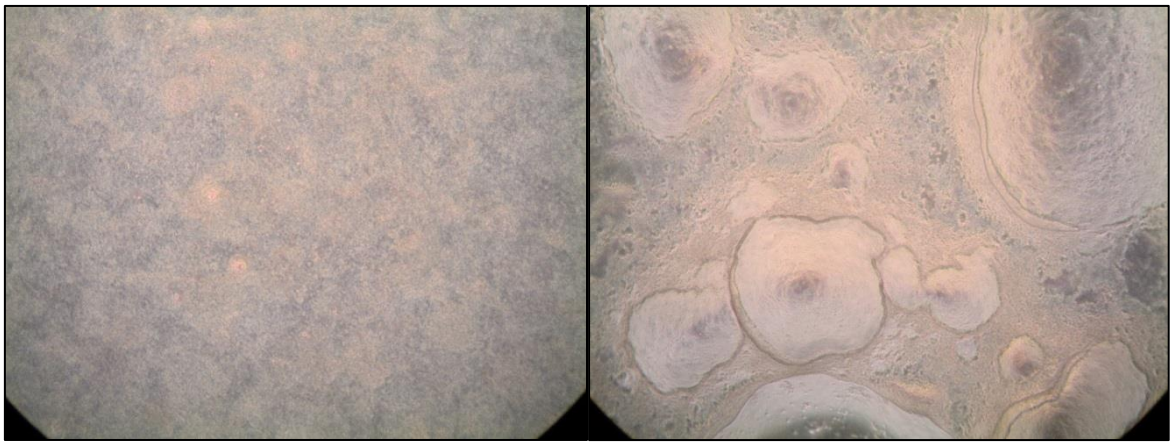

Fig.23: *36 hours. 120x magnification. Control on the left side. PAOM mix 1:20 treated on the right side.*

After 36 hours it was possible to observe that the TEER levels of control samples were acceptable, whereas the levels in samples treated with the PAOM mix displayed a significant drop. It is clear from the photographs that while the epithelial layers of the control inserts were still intact, the same thing cannot be said for the samples treated with PAOM. The latter presented several holes of various dimensions within the epithelial layer, resulting from the exposure to the Pseudomonas extracts. The presence of the holes, with the consequent loss of continuity, the reduction of the number of tight junctions caused by direct damage from bacteria extracts and the decreased cell contact, result in an easier passage of ions from the apical to the basal side and the subsequent reduction in TEER levels revealed by the instrument. The average reduction in TEER levels was approximately half of what measured in the control samples.

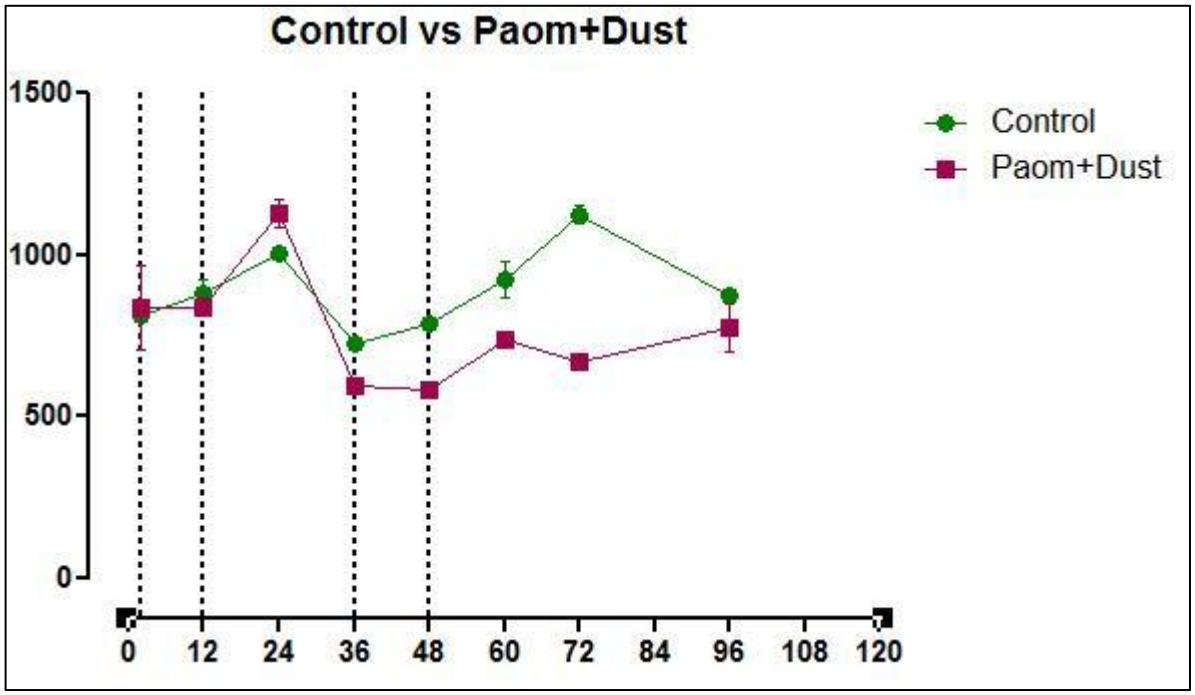

Fig.24: *TEER surveys. Control and PAOM+DUST treated comparison. For a more appropriate analysis the sample treated with subsequent dust doses was omitted from the graph.*

Instead, a comparison of the TEER levels of the control samples and samples treated with PAOM+DUST revealed a loss of TEER of about 150-200 Ω/cm^2 after only 24 hours; the beneficial effects of the dust are probably lost by this time point, and the damaging effects of the PAOM are evident.

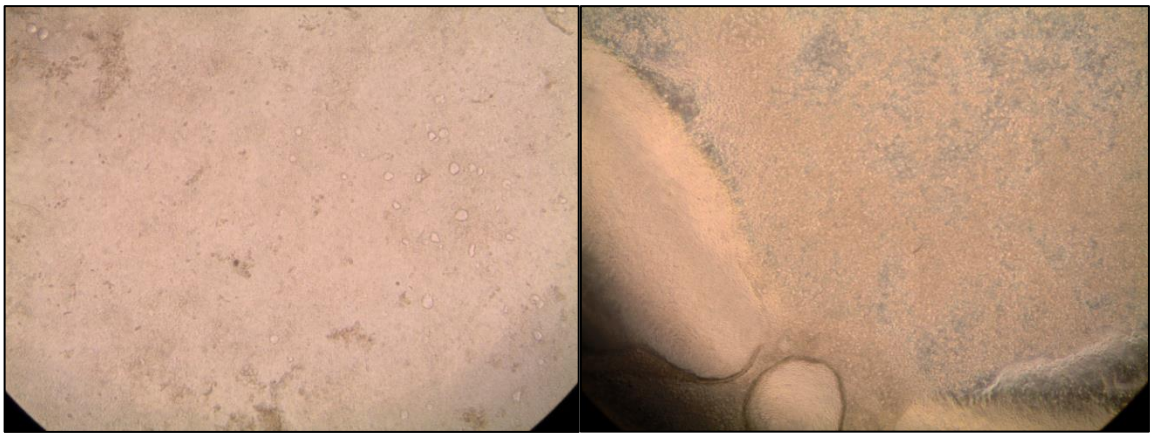

Fig.25: *36 hours. 20x magnification. Two different samples treated with PAOM+DUST.*

At 36 hours, the inserts treated with the PAOM+DUST combination showed some damaged areas within the epithelium. In comparison with control samples, inserts treated with PAOM+DUST (without additional dust exposures) presented more damage after 36 hours of treatment; however, a comparison with the inserts treated with PAOM only revealed remarkable differences. As it is possible to appreciate in the next graph, the pre-treatment with farm dust acted as protection in the first 24 hours, and when the PAOM mix was removed from both sample groups, the TEER levels in samples treated with dust were more elevated permitting a faster recovery period up to the pre-treatment TEER values (about 60 hours for the PAOM+DUST samples, and about 96 hours for PAOM-only samples).

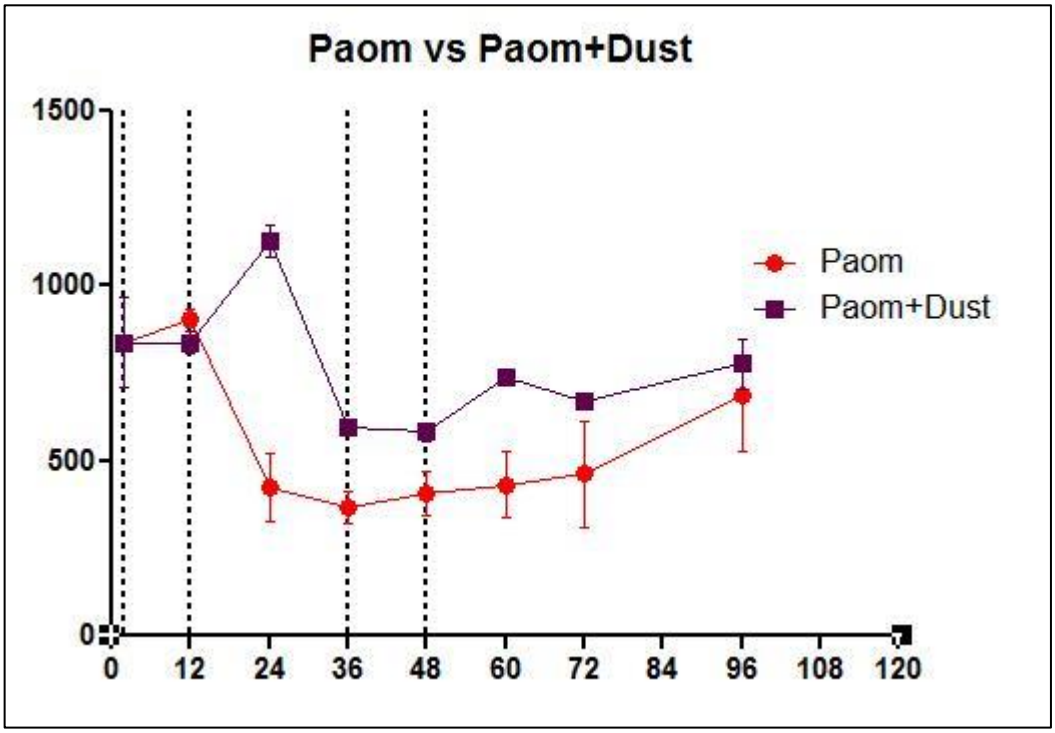

Fig.26: *TEER surveys. Comparison of PAOM and PAOM+DUST treated samples. For ease of viewing, the sample treated with subsequent dust exposures was omitted from the graph.*

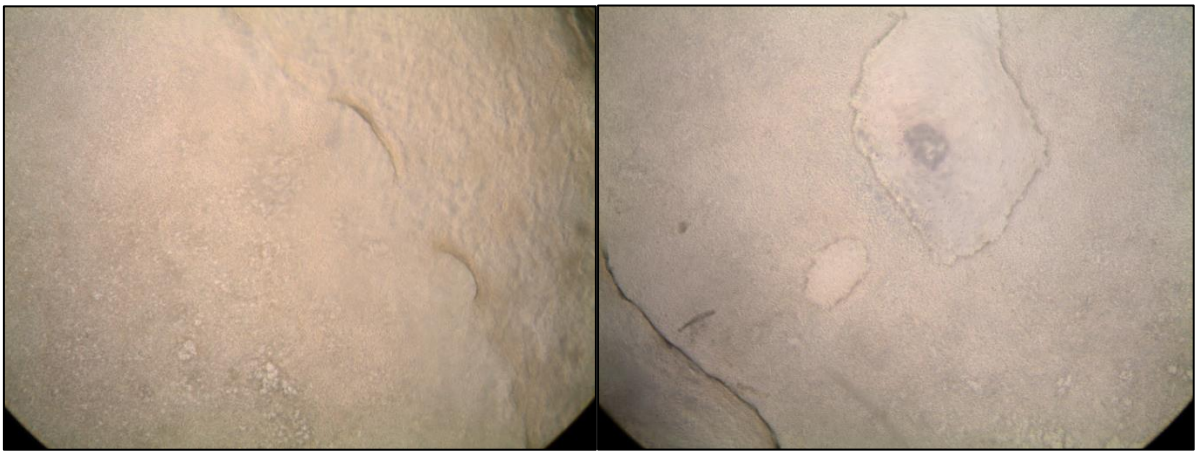

Fig.27: *72 hours. 20x magnification. PAOM+DUST on the left side. PAOM-only on the right side.*

As anticipated above, I selected one insert from the group of samples treated with the PAOM+DUST combination to test whether multiple exposures to DUST would influence the results. In addition to the initial exposure, the selected sample was treated for 2 hours with two further dust exposures (following the same protocol as for the initial exposure) at 12 and 48 hours. The treatment at

12 hours was intended to simulate a continuous exposure to farm dust during the concomitant presence of an external stimulus. The second treatment at 48 hours, following the removal of the PAOM mix, was carried out to assess if the dust would exert any regenerative effects. These additional exposures were performed on a sample treated with the PAOM mix, but not with the initial pre-treatment with farm dust at -2 hours, in order to evaluate whether the dust exposure would still have protective effects after the damage caused by P.A. extracts, and whether the hypothetical regenerative characteristics of dust are effective on damaged tissue.

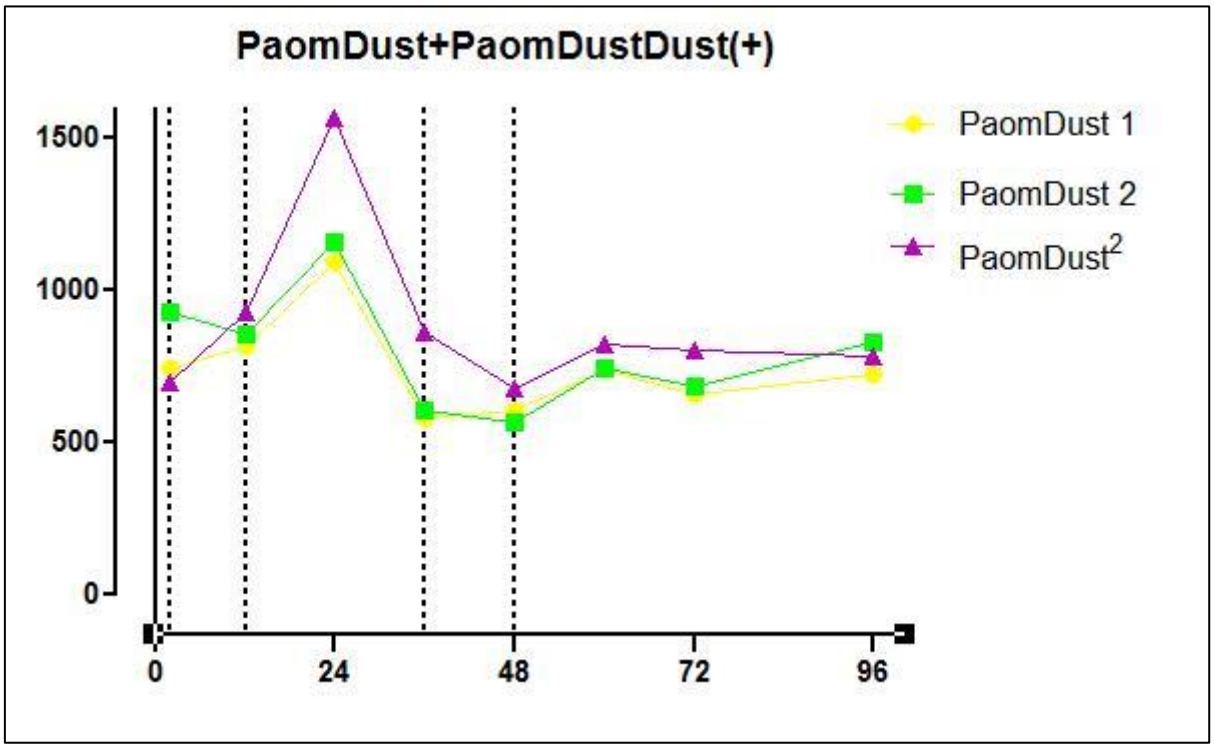

Fig.28: *TEER surveys. Comparison of samples treated with PAOM+DUST. The violet sample was treated with dust multiple times.*

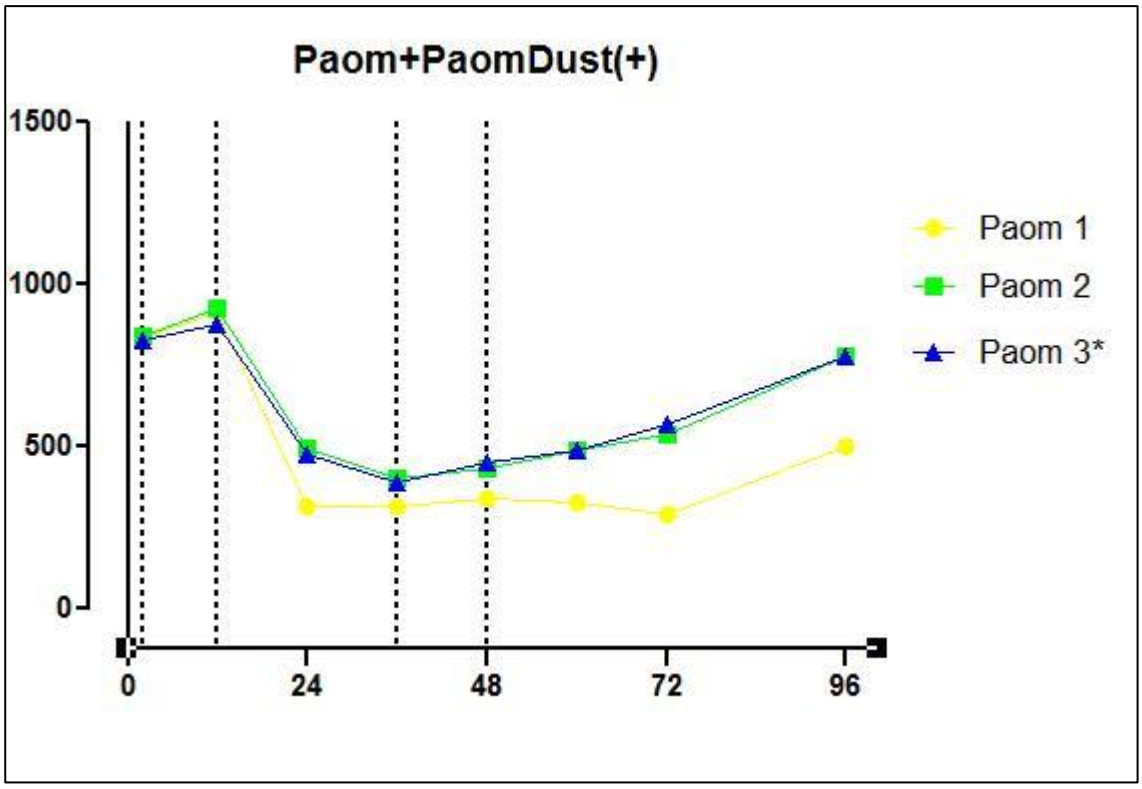

Fig.29: *TEER surveys. Comparison of samples treated with PAOM. The blue sample was treated with dust multiple times without the pretreatment at -2 hours.*

The sample treated with the early double exposure to farm dust showed an increase in TEER levels, with the levels practically doubling at 24 hours compared to the initial values at time point 0. The beneficial effects of farm dust ceased at some point within the 24-48 hour period, so it is probably necessary to provide a continued supply of dust (maybe with exposures every 12 hours) in order to maintain the protective effect. The second additional dust exposure at 48 hours showed (as better evidenced in a subsequent graph) that the dust did not improve the regeneration process, since the other samples in the same category followed the same TEER level recovery trend. At the same time, however, it is worthwhile to note that samples subjected to multiple dust exposures were able to maintain TEER levels higher than the initial value throughout the experiment. On the other hand, the sample treated initially with PAOM mix and exposed to farm dust only after 12 hours from the start of the treatment did not show particular benefits from the exposure. It followed, step by step, the trend of the other samples of the group that were never exposed to dust. In fact, after the PAOM mix was added at time point 0, the absence of the pretreatment with dust left the epithelial cells more vulnerable to damage from P.A. extracts. Once the

damage has been caused, the protective mechanism probably fails. Likewise, the second additional exposure to dust at 48 hours to evaluate the eventual regenerative properties gave negative results. The sample treated with dust followed the same TEER variation trends of untreated samples, and in this particular case, the levels were practically identical.

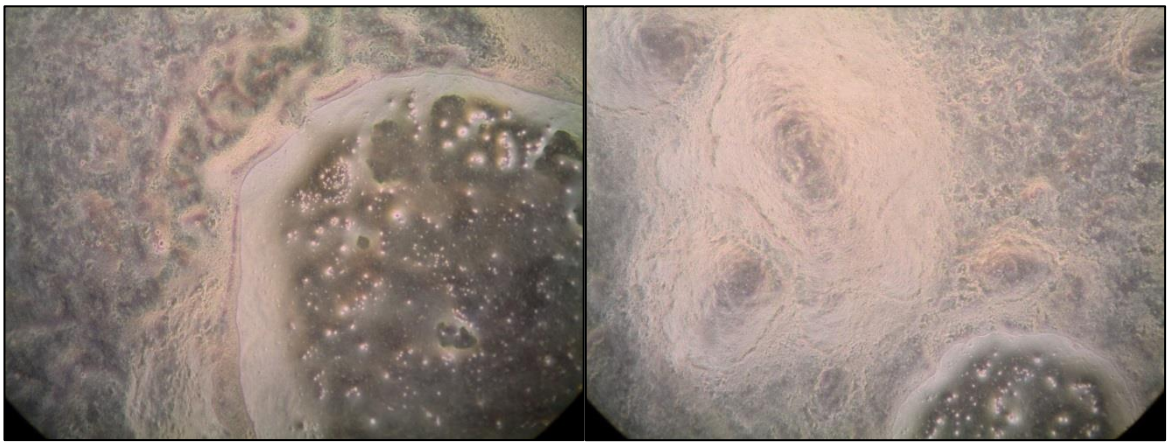

Fig.30: *36 hours. 20x magnification. Two different samples treated with PAOM. The sample on the left was exposed to farm dust after 12 hours but no positive effects were observed.*

3.1.5 Conclusions

The PAOM mix, used to final concentration 1:20, showed the ability to mimic a natural insult in vitro. The exposition of cells to farm dust provided interesting answers:

- Levels of the mRNA transcription of tight junction proteins increased after 4 hours from the exposition,

- The exposure to farm dust has led to an increase in the levels of TEER of ALI cell cultures,

- The release of pro inflammatory cytokine was not reduced by exposure to Farm Dust,

- The Farm Dust reduced the damaging action of PAOM mix but wasn't able to improve the regeneration process.

3.2 Application of Human Bronchial Outgrowths to study Ciliogenesis

Aims: Ciliary shortening and dysfunction are known features of moderate to severe asthma (Thomas, 2010) that are also strongly associated with cigarette smoke (Lam, 2013). To date however, the lack of a proper in vitro model in which to study these phenomena has severely impaired any real progress in our understanding of the underlying mechanisms. My hypothesis was that the human bronchial outgrowth model is well suited for studying ciliogenesis and testing the effects of CSE on the regeneration of ciliated elements. The inherent features of the model (long term culture, high resistance to damage compared to monolayer culture models, three-dimensionality, signaling between the epithelial and connective cell populations) offer the possibility to carry out long-term treatments and assess responses to external stimuli. In order to carry out this study, five non-smoking subjects with no relevant airways pathologies were recruited, and bronchial outgrowths were prepared as explained in the Methods chapter.

3.2.1 Phase Contrast Monitoring

After the 3D outgrowths were prepared and put in culture, they were routinely photographed before and after treatment to record any morphological changes occurring in the cells that constitute the mucosa reproduced *in vitro*. An inverted light microscope equipped with phase contrast rings (LEICA DM-IRB) was used to visualize changes in cell morphology, size and macroscopic modifications; these were recorded by digital photography.

Phase contrast microscopy showed that the "outgrowth" of the cells from the central biopsy was gradual, with the fibroblast initially forming a network of spindly cells and epithelial cells appearing only later on the apical side of this cell network.

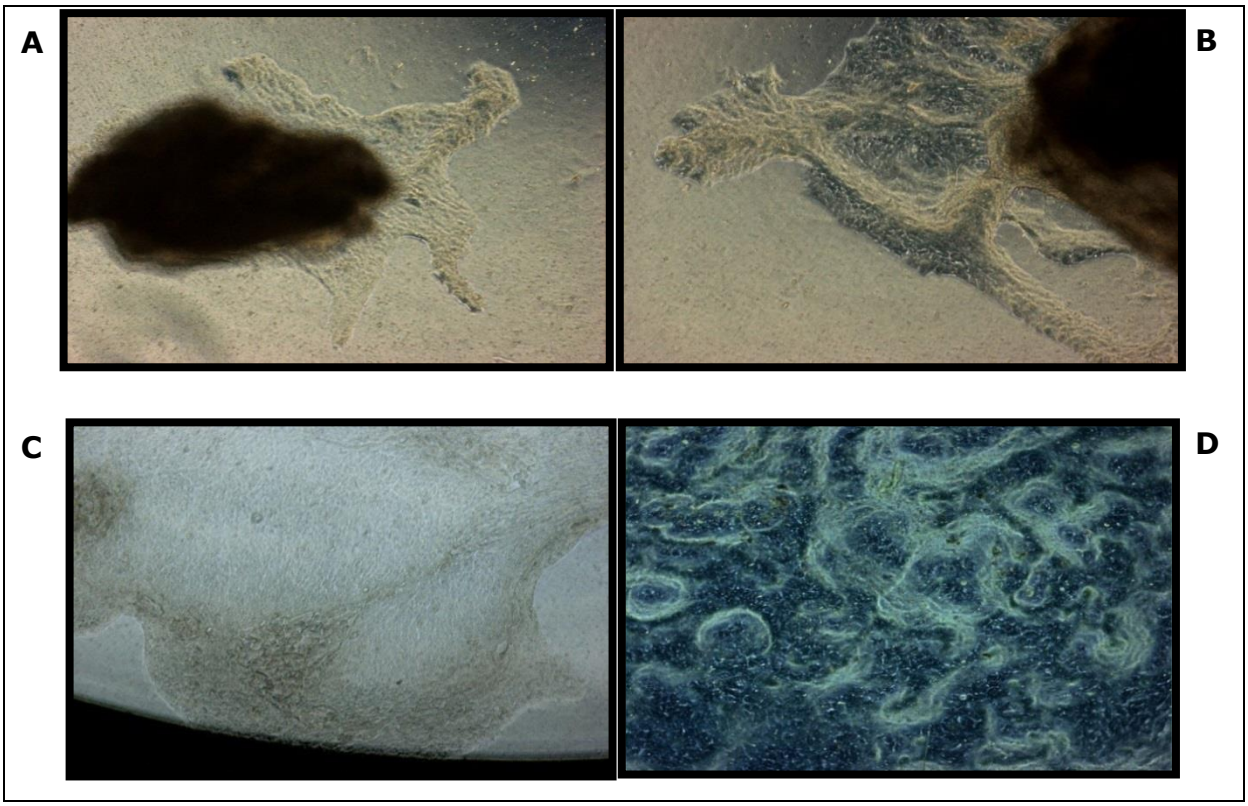

Fig. 31: *Phase-contrast observation of outgrowths in culture, A: for 3 days, B: for 7 days, C: for 10 days, and D: for 28 days.*

After 10-12 days, the PET membrane covering the bottom of the insert was completely covered with the newly grown tissue, and from that time, the culture had a three-dimensional structure. After 30 days of culture the morphological features of the outgrowths presented a complex architecture and it was possible to see the movement of the cilia. In our experience, unless specific damaging events (eg. contamination with infectious organisms), occur during the culture period, and providing that proper culture conditions are maintained, it is possible to grow these 3D outgrowths continuously for more than 4 months.

3.2.2 Use of electron microscopy to monitor the cilia development

Electron microscopy, both SEM and TEM, enabled us to monitor in detail the development of the cilia on the epithelial cells that constituted the apical side of the outgrowths. This model was developed and characterized by Prof. Fabio Bucchieri and Figures 31-33 show some examples of the ultrastructural

characterization that has been carried out by him and his collaborators. For this thesis, I focused my attention on the process of cilia genesis. The outgrowths were cultured for 10-20-30 days and prepared for electron microscopy as explained before in the "Methods" chapter. As shown in Figure 32, the 3D outgrowths show a progressive development and differentiation of their apical surface. After 10 days, this surface is completely covered with microvilli (Fig. 32 A, B and C). The cell borders are also easily defined. At around 20 days, the apical surface starts to present a small percentage of ciliated elements (Fig. 32 C, D and E) that represent around 10-15% of the total surface area. At the end of the 30th day in culture (Fig. 32 F, G and H), the ratio between ciliated cells and cells with microvilli is around 40:60, and does not change significantly after this time point. The cilia measure around 8 µm (Fig. 32 F, orange line) which is comparable with the normal length of cilia of the normal bronchial epithelium *in vivo*.

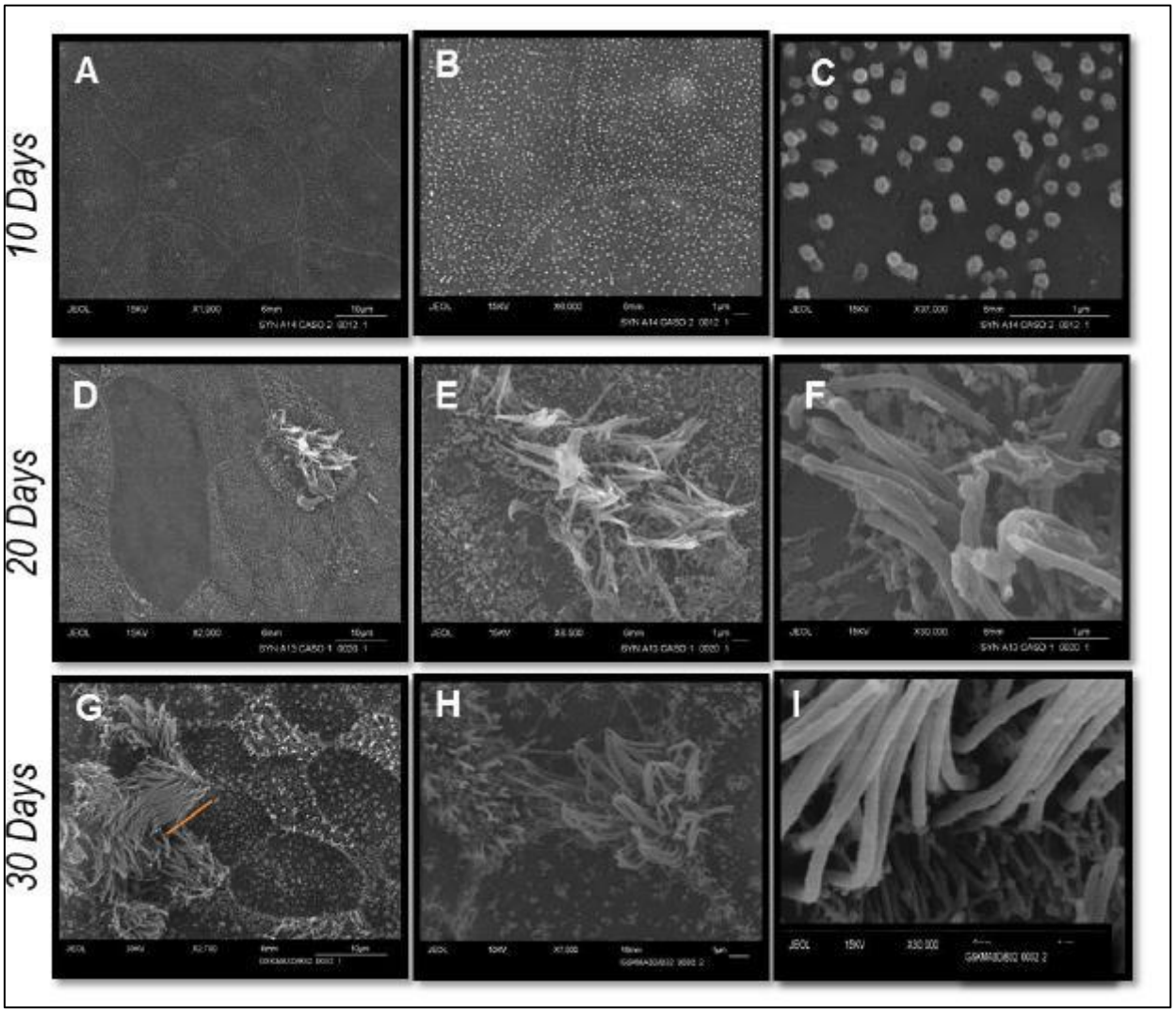

Fig.32: *SEM monitoring during the first 30 days of culture. It was possible to see the new ciliate elements starting to emerge at around 20 days in culture, and the final proportion between cells with cilia and cells with microvilli was achieved after a month in culture.*

Figure 33, taken with TEM, shows a panoramic view of a 30 days old outgrowth: it is very easy to identify two different distinct strata, the top one formed of two layers of epithelial-like cells, a basal and an apical one, and the bottom one where fibroblast-like cells are dispersed in a highly organized ECM that was neo-synthesized. The two layers are separated by a well-developed basement membrane.

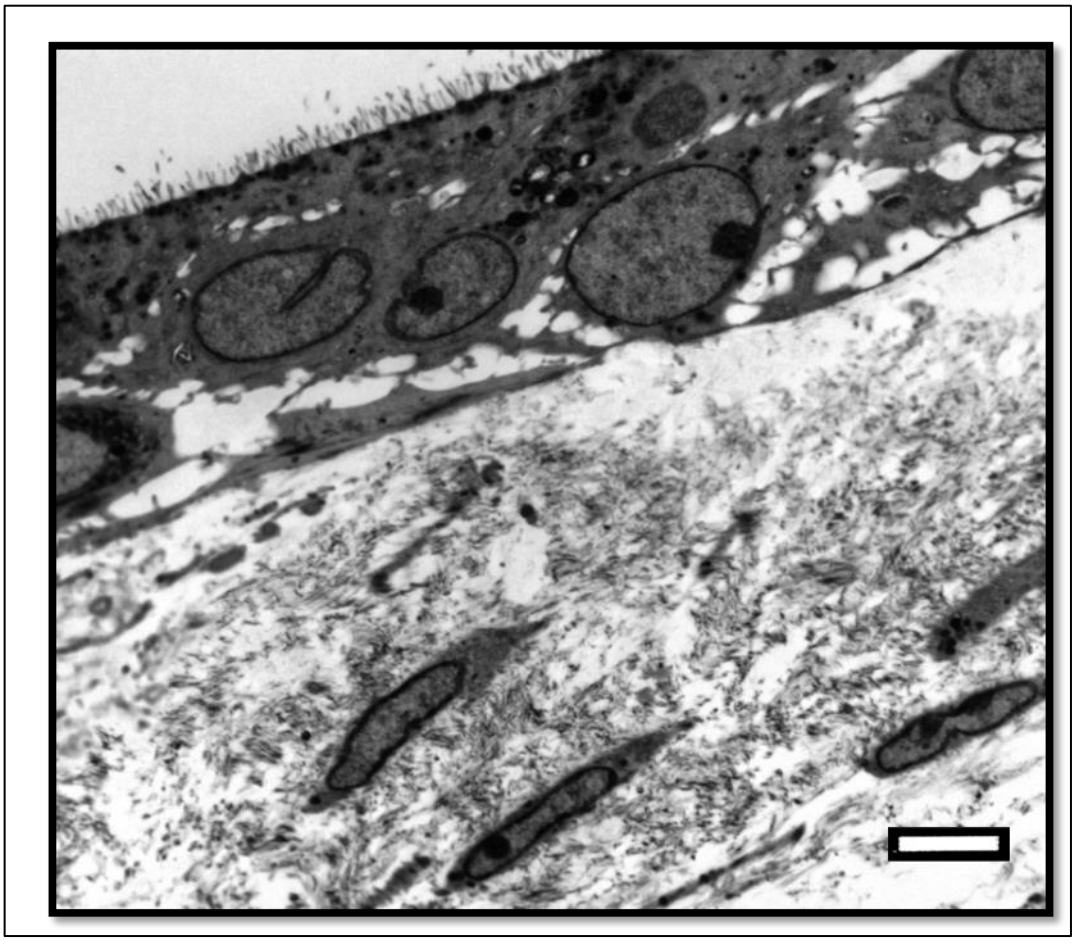

Fig.33: *30 days old outgrowth. Picture taken with TEM. Note the superior (epithelial) part, divided into apical and basal regions, the basement membrane that divides the two cell layers, and the inferior part containing fibroblasts and neo-synthetize ECM. Bar = 1µm*

As mentioned before, the first ciliated elements start to appear after the first three weeks in culture. For this reason, I chose to focus my studies on a time point ranging between 20 and 30 days. Figure 34 shows the typical ultrastructural aspect of the apical portion of a ciliated cell, with basal bodies and the cilia clearly visible. In Figure 35, where the section has encountered the cilia

perpendicularly to their main longitudinal axis, it is possible to observe the presence of the microtubule doublets surrounded by a phospholipid membrane. The basal bodies of cilia are a fundamental structure in order to define the formation of the cilia themselves. Another essential characteristic is a complete internal cytoskeleton with the inner core of microtubules arranged in a 9+2 pattern.

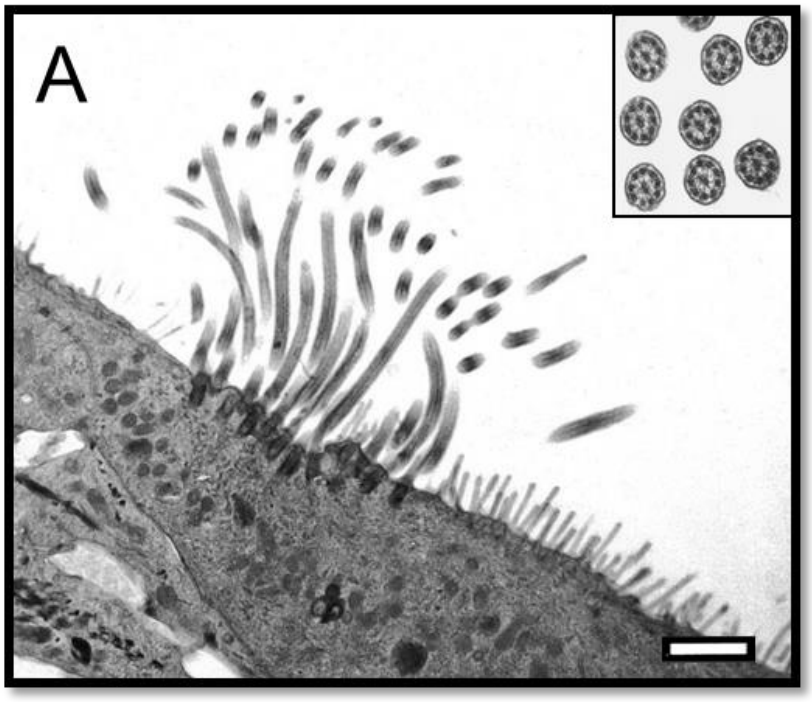

Fig.34: *Ciliated cell and particular of cilia. Photograph taken with TEM. Bar = 1 µm*

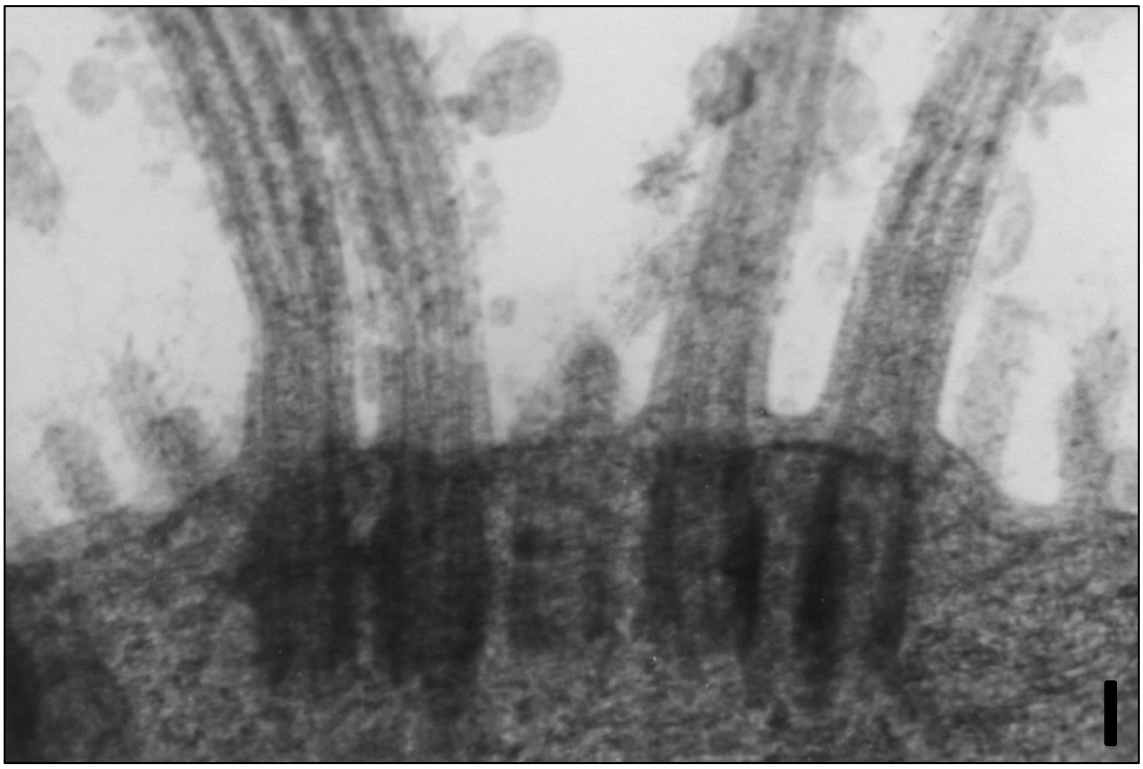

Fig.35: *Particular of a Cilia Basal Body. Photograph taken with TEM. It is possible to observe the "inside" of a cilium that probably was bent during fixation. Bar = 200 nm*

3.2.3 CSE treatments and cilia regeneration

In order to study the alterations that the cilia undergo following long-term CSE exposure, bronchial outgrowths were grown until complete differentiation (approximately 30 days) and then treated (except for the untreated control) with a mix of normal cell culture media mix (BEGM:DMEM 1:1) and a 20% CSE preparation as explained above, up to 21 days.

This dose was chosen because it represents a good approximation of the amount of CSE present in the bronchial mucosa of an average smoker (a subject that smokes 15-20 cigarettes per day).

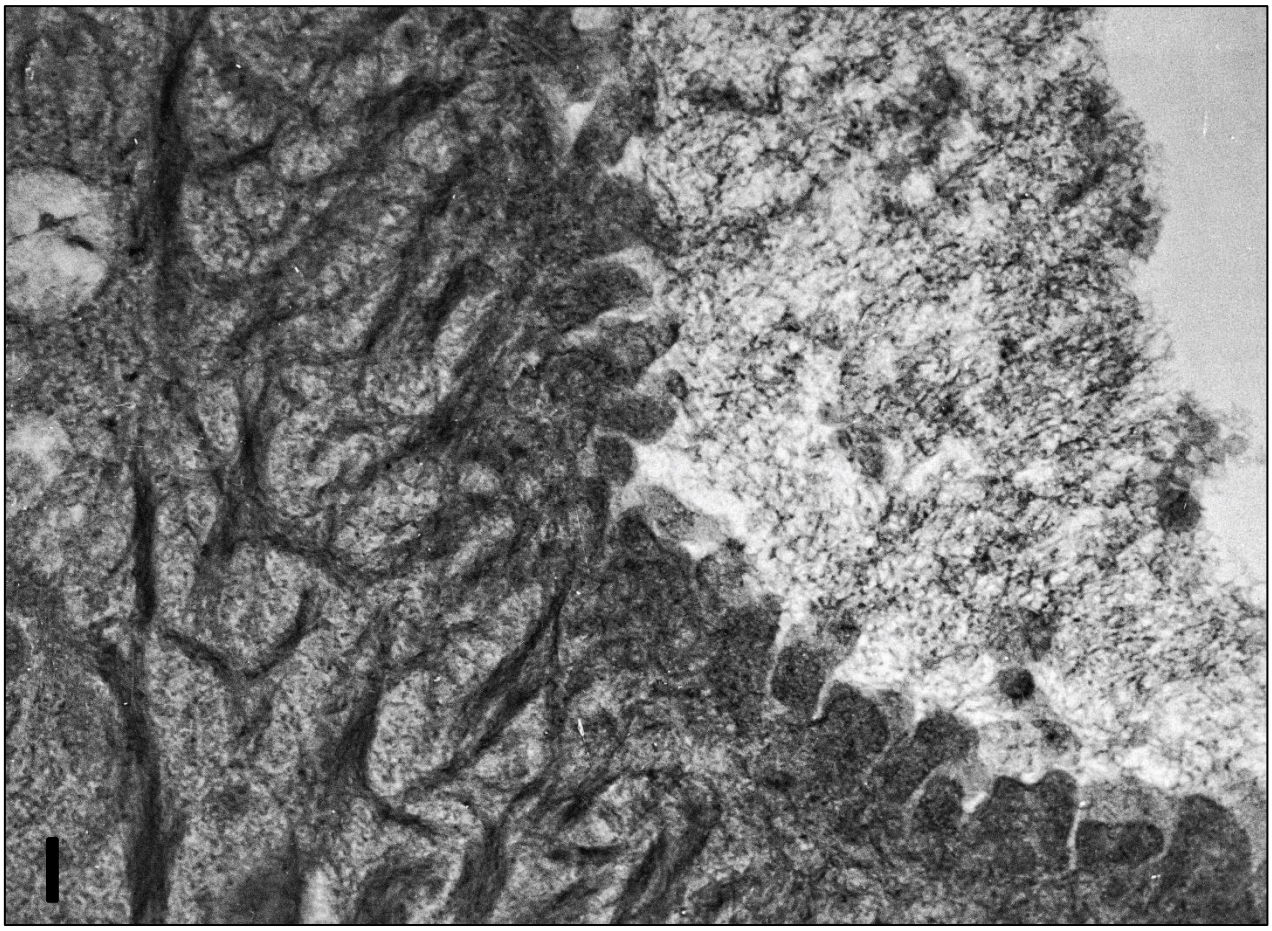

Fig.36: *Human Bronchial Outgrowth.3rd day of treatment with CSE at 20%.*

As shown in Figure 36, after only three days of exposure to CSE at 20%, the entire apical ciliated apparatus has disappeared and the apical surface presented short and thick microvilli covered by what appeared like the debris of the cilia. After being subjected to a stressful and toxic environment, it is likely that the cells stripped of the apical cilia as a first response (probably because the cilia are

a cause of energy expenditure) and immediately increased their membrane surface with strips of microvilli to allow greater mucus secretion to defend themselves from the external injury and to expel the toxic substances penetrating inside.

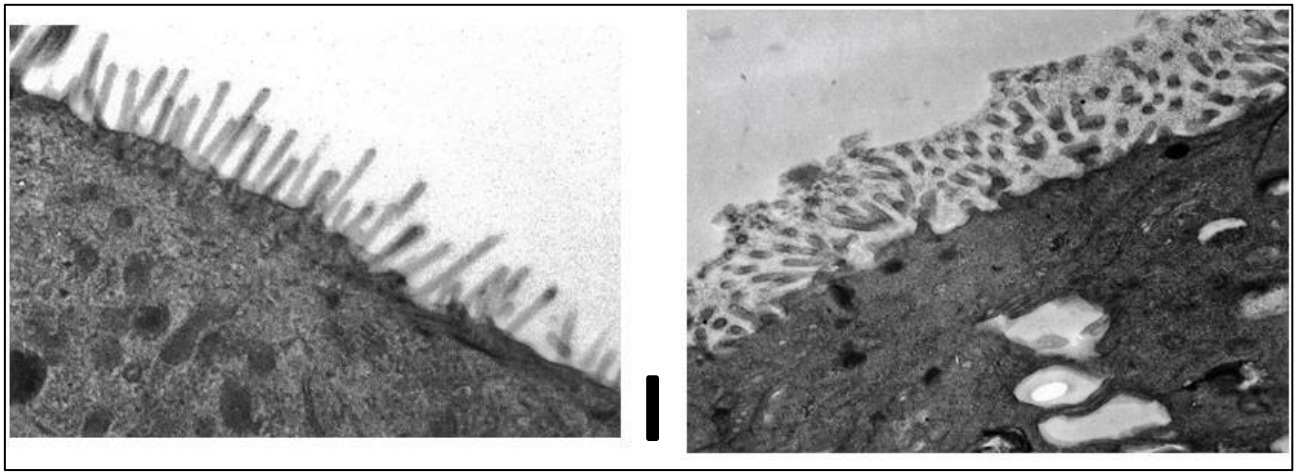

Fig.37: *Human Bronchial Outgrowth. 21th day of treatment with CSE at 20% on the right side vs an untreated control on the left side. Bar = 500nm*

After 21 days of CSE exposure, it is interesting to observe the response of epithelial cells to a stimulus that is no longer desultory or occasional, but now a chronic insult. After determining that the external insult is not temporary, the cells tried to return to their original function of removing the mucus with the cilia. However, the simultaneous necessities to remove the mucus and to produce more mucus probably stress cells, and leads to the development of incomplete cilia. Indeed, it is possible to see in the Figure 37 how the exposed apical side of the cells appear to present structures halfway between microvilli and fully developed cilia after 21 days in culture. These thick elements were surrounded by mucus that is still produced in large quantities. In another area of the outgrowth, shown in Figure 38 B and C, can be observed the simultaneous presence of elongated protein-enriched microvilli and ciliary precursors (a normal control is provided for comparison in A). Structures with a markedly thickened protein at their base can be observed protruding from the apical side; these are probably deuterosomes. Normally, deuterosomes appear as electron-opaque globular bodies without limiting membranes, and serve as the core for centriole formation; they are thought to be generated by aggregation and condensation of fibrous granules, or independently from fibrous granules (according to the differing data in literature); in the human they have a diameter of 100–110nm.

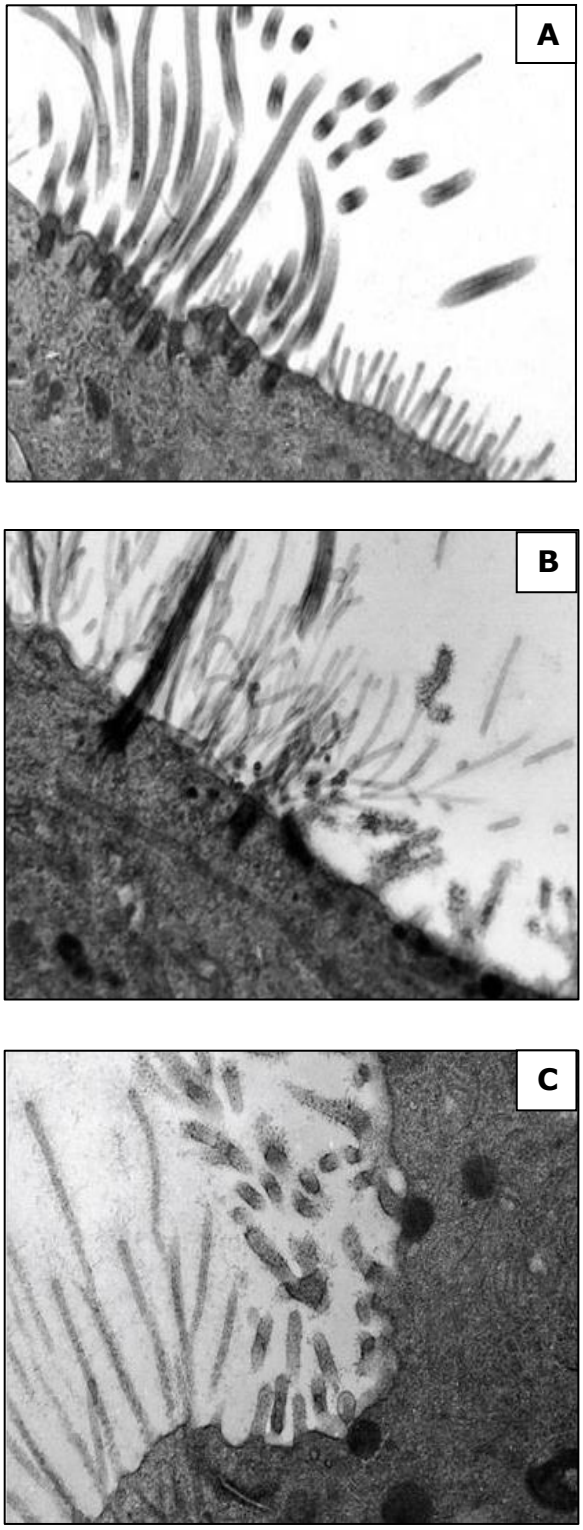

Fig.38: *Human Bronchial Outgrowth. 21th day of CSE exposure at 20%, B and C vs an untreated control, A. Bar = 200nm*

Therefore, the formation of these stubby protrusions may be an attempt to regrow the ciliated elements of the cell while subjected to stress. In Figure 39, it is possible to appreciate how these structures have characteristics halfway between the microvilli and the cilia, with a diameter that is closer to that of the microvilli, but with an internal organization of the cytoskeleton that is reminiscent of the cilia (as indicated by the arrows).

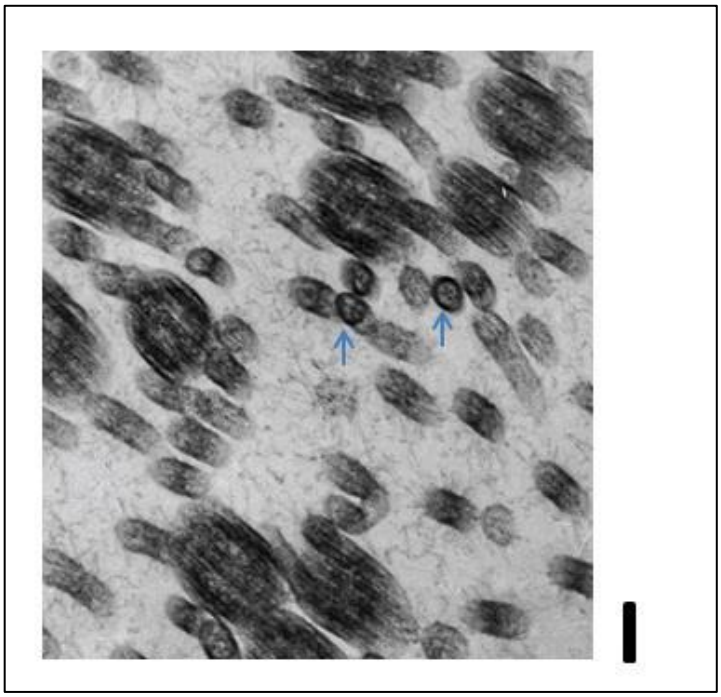

Fig.39: *Human Bronchial Outgrowth treated with CSE for 21 days. Presence of unusual structures. Bar=100nm.*

3.2.4 Conclusions

The results I have presented in this chapter are only preliminary morphological observations that obviously need to be followed up by a more accurate and complete immunophenotypical characterization to study how the expression of the main known modulators of ciliogenesis, such as GNS, ANVIL or the ARp2/3 complex, might change during long-term exposure to CSE.

However, these findings already confirm that the human bronchial outgrowths can be considered a valid tool to study ciliogenesis modulation in vitro.

3.3 Characterization of a novel three-dimensional model of normal human oral mucosa

Aims: Tissue-engineered oral mucosal equivalents have been developed for in vitro studies for a few years now. However, the usefulness of currently available models is still limited by many factors, mainly the lack of a physiological extracellular matrix (ECM) and the use of cell populations that do not reflect the properly differentiated cytotypes of the mucosa of the oral cavity. For this reason, my main aim was to tissue-engineering a novel 3D model of the normal human oral mucosa, to overcome some of the shortcomings of the current in vitro models. Our model includes two cell populations (keratinocytes and fibroblasts) that outgrow from an oral biopsy fragment into a natural extracellular 3D matrix (MatrigelTM) that initially drives the outgrowth of the cells, and is completely replaced during the culture period by a newly deposed matrix produced by the fibroblasts. My hypothesis was that this kind of model could exhibit a proper histological architecture and biochemical composition (two essential features required of an in vitro model that is to be employed to study the responses to exogenous modifications of its microenvironment, such as those that take place during drug administration assays). In order to achieve this goal, I characterized the outgrowth model both at an ultra-structural and immunophenotypic level. This model was also used for other experiments in our laboratories (for example a drug administration assay, Campisi, 2012).

3.3.1 Morphological Analysis

Briefly, like in the bronchial model, the oral mucosal outgrowths initially formed a network of spindly cells (likely fibroblasts) and rounded cells (possibly epithelial cells), growing out into the Matrigel™ from the biopsy which was originally placed in the middle of the transwell system. After 7-8 days, the PET membrane covering the bottom of the insert was completely covered with the newly grown tissue that originated from a biopsy, and the new cell populations started to spread out three-dimensionally, forming ridges and more complex 3D structures. After 13-15 days of culture, the morphological features of the outgrowths did not change consistently. The outgrowths were monitored by phase contrast microscopy and analyzed by electron microscopy showing that the newly formed

mucosa presents all the characteristic hallmarks of a properly differentiated oral mucosa (see Figures 40, 41 and 42 and the respective legends).

Cells from our 3D outgrowths find in the Matrigel all the necessary factors to develop and reconstitute the structures of the original tissue. However, after this initial phase, cells within the outgrowth start to demolish the Matrigel and begin to lay down their own ECM, strengthening the biological and structural characteristics of the model.

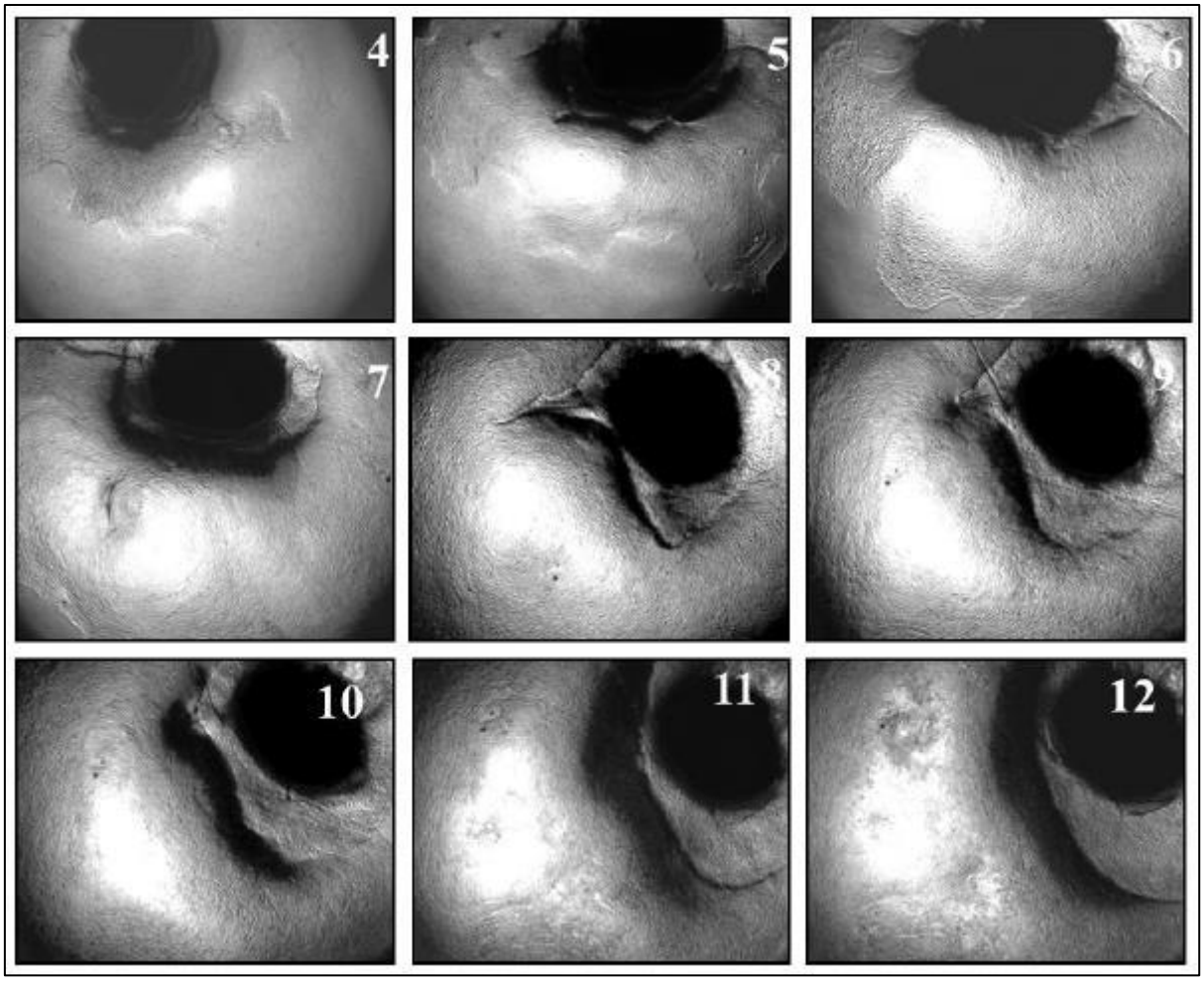

Fig.40: *First 12 days in culture. Phase contrast observation. There is a progressive outgrowth of cells from the central biopsy. Mesenchymal cells emerged first, followed by the epithelial ones. After the cells covered all the PET membrane of the insert, the growth started to develop three-dimensionally.*

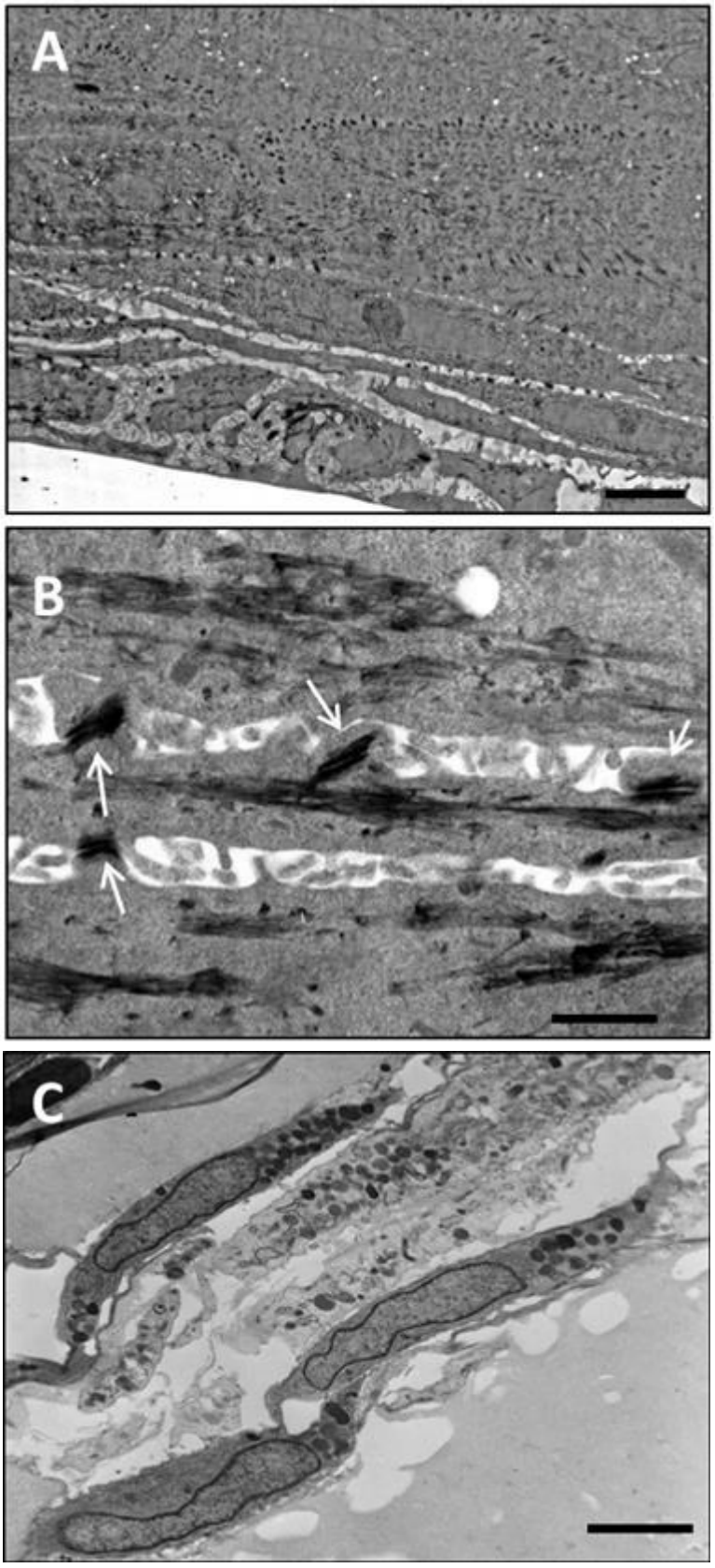

Fig.41: *Human Oral Outgrowth. Transmission Electron Microscopy. A: view of the outgrowth that shows, in particular, the lowest three strata of the epithelial layer. Epithelial cells exhibit a squamous non-keratinized phenotype, typical of the oral lining mucosa. B: Particular on desmosomes (white arrows). C: a particular of the fibroblast layer (lamina propria) that displays the characteristic spindly morphology of these cells and also the presence of an abundant extracellular matrix. Bars A-C: 10 µm, Bar B: 400nm*

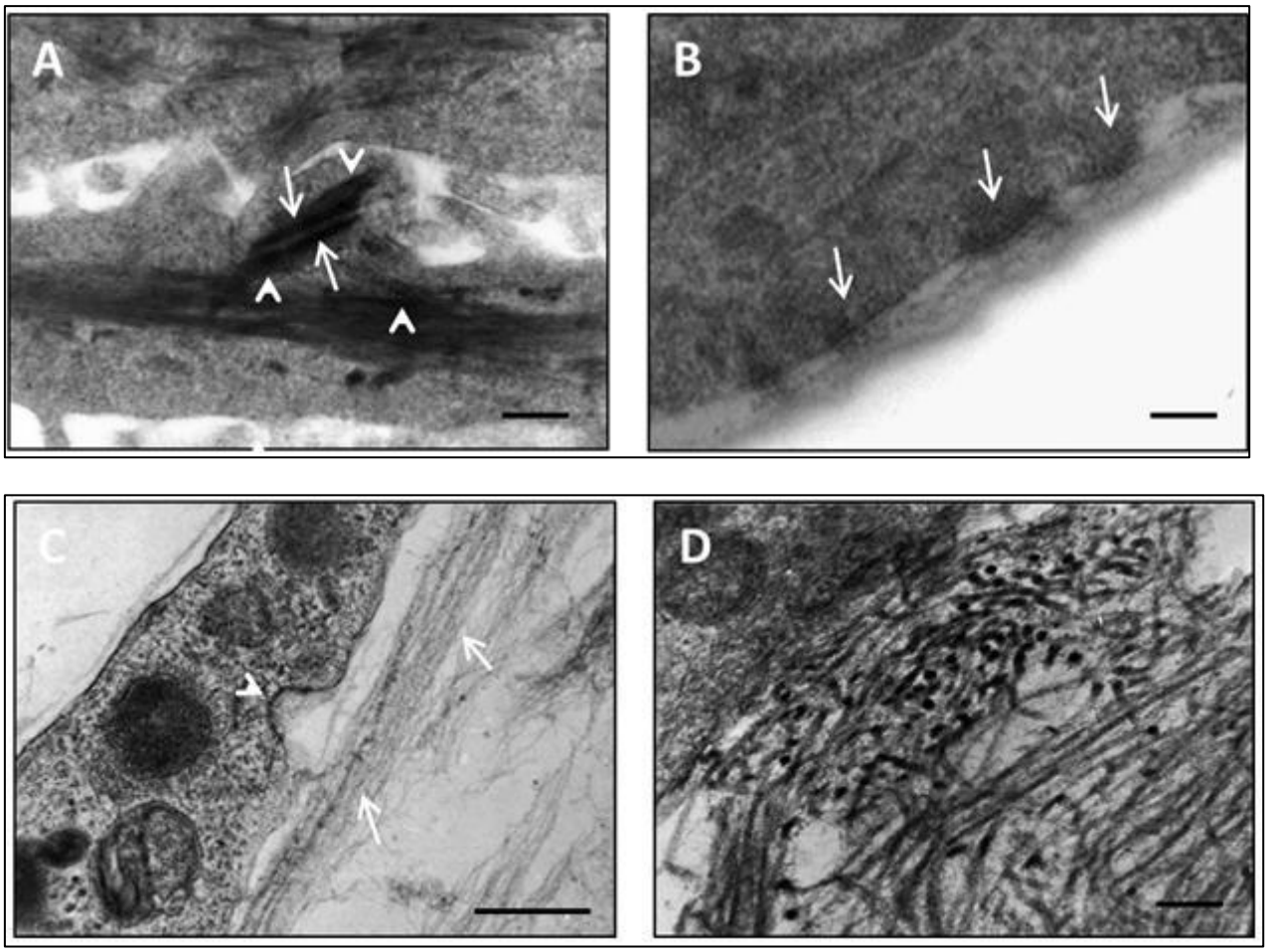

Fig.42: *Human Oral Outgrowth. Transmission Electron Microscopy. A: shows a highly magnified region of the interface between the basal and spinous layers, with the two adjacent cytoplasmic membranes of two keratinocytes tightly held together by a desmosome (white arrows) with both the attachment plaques well evident, B: it is possible to observe that the basal epithelial cells are separated from the underlaying fibroblast layer by a properly constituted basal membrane with which they both interact through hemidesmosomes (white arrows); in this micrograph it is only possible to observe the two most superficial regions of the basal membrane C: details of a cytoplasmic process of a fibroblast, proteic material (white arrows) that will eventually form the ECM is extruded into the extracellular space from caveolae-like structures (white arrowhead) present on the cytoplasmic membrane of the fibroblasts. This proteic material is mainly constituted by collagen proteins, as shown in fig.3 (D). Bars A-B-C: 200nm, Bar D: 50nm.*

3.3.2 Immunophenotypical characterization

Immunofluorescence: In order to properly characterize our 3D outgrowths, they were stained with a panel of antibodies directed towards some of the most common markers of the human oral mucosa components, and visualized by laser confocal microscopy in order to perform precise scans at the desired level of the different strata composing the outgrowth. Figure 43 shows four of the markers that were used to differentiate between the cell populations: CK5 and CK13 were employed to characterize basal and differentiated keratinocytes respectively (Fig.

43 A and B), whereas laminin (Fig. 43 C) and collagen type IV (Fig. 43 D) were used, together with fibronectin and collagen type I (not shown), to study the ECM. CK5 staining was limited to the basal layer and the positive cells had a distinctive rounded shape (Fig. 43 A), whereas CK13 staining, that was present throughout the whole epithelial stratum, was much stronger in the upper layers and positive cells had a typical squamous shape (Fig.43 B).

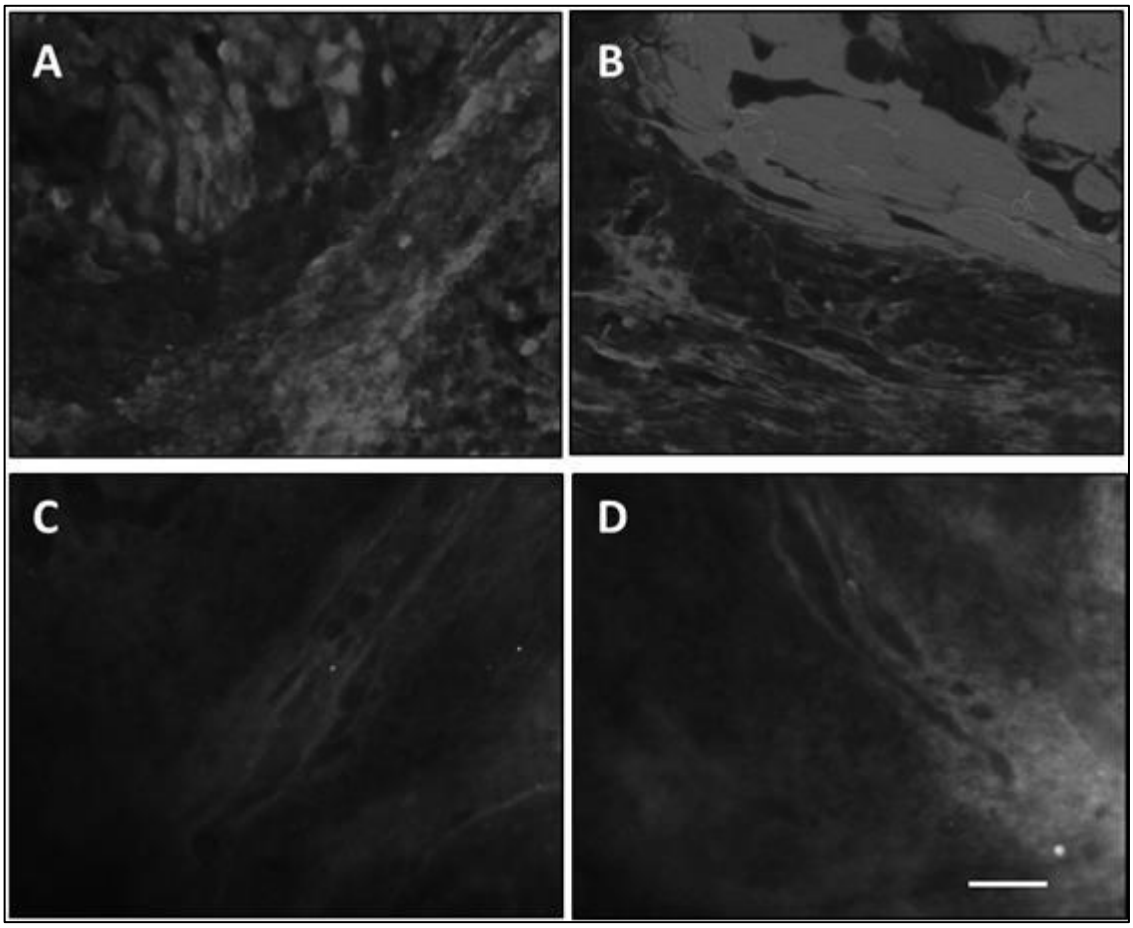

Fig.43: *Immunofluorescence staining of the epithelial (A and B) and fibroblast (C and D) layers in a 15 days old 3D outgrowth. The basal keratinocytes resulted positive for CK5 (A), whereas the more differentiated ones resulted positive for CK 13 (B); the fibroblast layer was positive for laminin (C) and collagen type IV (D). Bar: 40µm.*

Immunogold: In order to verify whether the ECM proteins that were found in the lamina propria of our 3D outgrowths with the immunofluorescent staining, had effectively been produced by the resident fibroblasts, these proteins were precisely localized inside the fibroblasts cytoplasm by TEM immunogold assay. Figure 44 shows representative micrographs of immunogold staining of fibroblasts of the lamina propria of the 3D outgrowth, with antibodies directed towards laminin (Fig.44 A), fibronectin (Fig.44 B) and collagen type IV (Fig.44

C). All proteins analyzed were found to be expressed in the cytoplasm of the fibroblasts, especially in the proximity of and within vacuolar cytoplasmic structures, with the exception of collagen type IV whose staining was diffuse.

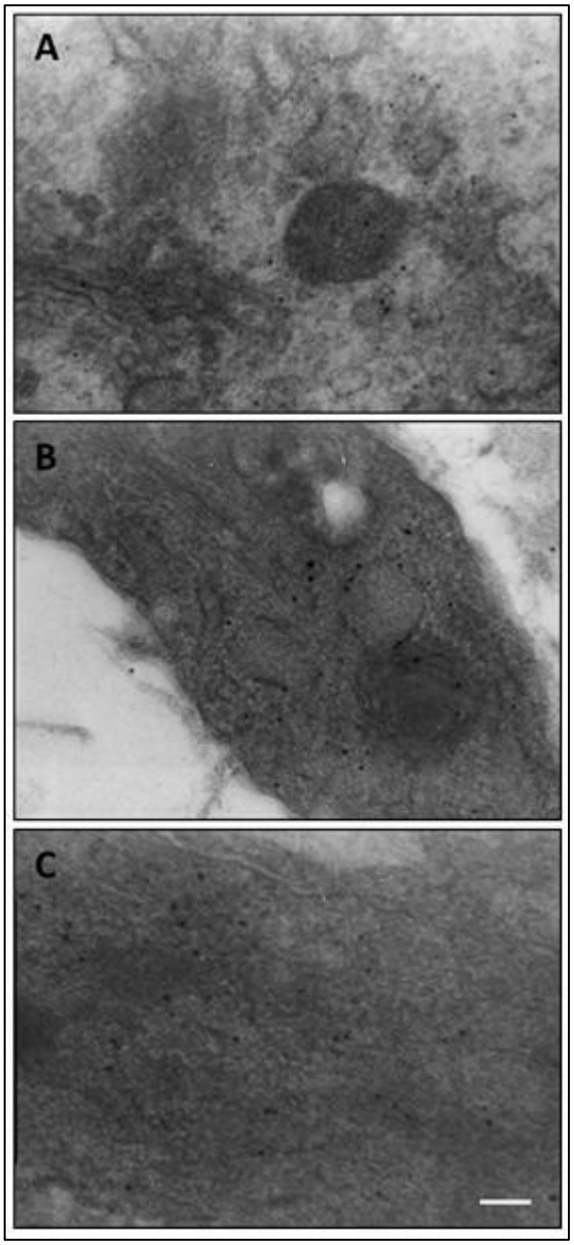

Fig.44: *Immunogold staining of fibroblast cytoplasmic proteins. A 15 days old 3D outgrowth of human oral mucosa was immunostained for laminin (A), fibronectin (B) and collagen type IV (C) using secondary antibodies labelled with colloidal gold particles 10nm in diameter and then analyzed by TEM. Bar = 50nm.*

3.3.3 Conclusions

The results that we have obtained during the development and characterization of our 3D model of the human oral mucosa clearly show that this system is a very good candidate for tissue-engineering the normal human oral mucosa. In our model, oral biopsies are placed directly on Matrigel in Transwells equipped with a PET membrane necessary to allow the passage of culture medium. Cells from our 3D outgrowth find in the Matrigel all the factors necessary to develop and to reconstitute the structures of the original tissue. However, after this initial phase, cells within the outgrowth start to demolish the Matrigel and begin to lay down their own ECM. This is a crucial moment in the development of the 3D outgrowth, resulting in a proper differentiation of the cell components (keratinocytes and fibroblasts) and in an in vitro reconstitution of the physiological architecture of human oral mucosa, including a stratified non-keratinized squamous layer composed of several layers, a proper basal membrane and a lamina propria where fibroblasts continue to produce ECM and biochemically signal with the layers above. Even if Matrigel is considered one of the most effective substrates for 3D cell culture, we believe that the strength of our outgrowth model is not so much in the culture medium used or in the matrix, but in the common source of fibroblasts and keratinocytes. In fact, fibroblasts and keratinocytes of our model are not separately isolated from the dermal layer or buccal mucosa respectively, and combined again in a scaffold of different materials, but they originate from the same biopsy. In this manner, the cultured tissue maintains the distinct characteristics of the single original source.

FINAL DISCUSSION

The main aim of this thesis was to apply novel 3D cell culture models to the study of chronic inflammatory diseases. To reach this goal, I employed a tissue-engineered human mucosal equivalent, the 3D mucosal outgrowth, that had been previously developed and characterised in our laboratories.

During the last few months of my PhD course, I had the possibility to spend part of my study period in the laboratories of Pulmonology Department of Leiden University Medical Center directed by Prof. Hiemstra, where I studied the potential protective effects of farm dust against inflammatory states such as those that take place in asthma and other chronic inflammatory diseases. The cell culture model used for this part of my studies was the ALI culture.

Giving the specific characteristics and developmental stages of these two, similar but quite distinct, cell culture models, I have preferred to present the results obtained during the latter part of my studies in Leiden in the initial chapters of this thesis, followed by the results of the earlier experiments using the 3D outgrowth models carried out in Palermo.

Primary cultures or cell lines still represent the most commonly used human *in vitro* culture models to study responses of cell systems to specific stimuli. However, the main limitations of these models are the absence of extracellular components and the loss of proper cell-cell communication that arises from the former characteristic.
The development of a model that involves the use of a culture medium conditioned with Pseudomonas Aeruginosa extracts permits to subject the cells to an external insult that mimics a natural insult *in vivo*. Furthermore, it is possible to modulate the dilution of the medium to support the specific requirements of different experimental conditions. I would like to to thank Dr. E. Van'Wout and Dr. A. Schadewijk for having perfected the method and shared and taught me this protocol. The studies conducted with Pseudomonas extracts have confirmed what had already been seen in previous works conducted on mice and also on human cells: Pseudomonas extracts cause diffuse cellular damage with a specific impact on tight junction proteins, defining them as ideal agents for use in studies that involve these proteins as their specific target. Numerous survey studies

have been conducted on the beneficial effects that living in a rural environment can have in protecting individuals from the onset of chronic inflammatory diseases of the airways (Korsal, 2008; Ege, 2011; Fishbein, 2012). The potential protective properties of farm dust have also been investigated in animal models (Hagner, 2013).

The use of the ALI cell culture model allows to obtain more accurate results since it is based on differentiated primary cells. Differentiated bronchial epithelial cells, such as those that are used in the ALI culture model, develop a complex polarized architecture offering the possibility to conduct TEER assessment.

The evaluation of the properties of farm dust produced interesting results: cells exposed to farm dust responded with an increased transcription of genes that encode for tight junction proteins. The transcription levels increased after 4 hours, that is probably the time necessary for the dust components to exert their effects. At the same time, the dust-exposed ALI samples displayed increased TEER levels. This is likely to be due to the fact that not only the RNA of tight junction proteins were transcribed, but active protein synthesis took place that determined the formation of functional tight junctions. On the other hand, the dust did not exhibit specific regenerative or protective abilities; in fact, in the samples exposed to dust when the damage had already taken place, we did not observe any protective effects. Moreover, as already reported in animal studies, the concomitant exposure to dust and an inflammatory agent did not inhibit the inflammatory process (as measured by IL-8 release). Therefore, while many studies have not been carried out to analyze dust properties *in vitro*, from the sample data of the two previous major projects (PARSIFAL and GABRIELA) and my preliminary *in vitro* results it would seem that farm dust components exert a protective effect again insults against respiratory mucosa (in both animal and human primary cell models). Hence the need for a more extensive and thorough analysis, especially of the single dust components to avoid eventual secondary consequences and, more importantly, to maximize the protective effects and their eventual therapeutic exploitation. Furthermore, the properties of farm dust (and its components) should be studied using a wider variety of stimuli in order to better characterize their effects.

Even though the primary cultures grown at the air-liquid interface represent an advanced *in vitro* human model to study responses of cell systems to specific

stimuli, they lack some of the fundamental components that constitute a normal mucosa: the ECM and connective cells.

The unavailability of suitable 3D cell culture models has inspired the researchers in our laboratories to develop and refine, with the application of tissue engineering techniques, an innovative three-dimensional culture model that is a faithful *in vitro* reconstruction of the human bronchial mucosa. In short, the model consists of an outgrowth of cells from a bronchial biopsy immersed in a three-dimensional gel (Matrigel™), in turn suspended using a Transwell system in a culture medium specific for the proliferation and differentiation of both epithelial cells and fibroblasts at the air-liquid interface. This model has proven to be an ideal tool to study medium- to long-term exposures to different stimuli, such as interleukins, CSE, oxidants etc.

One of the strengths of the model is the concurrent presence of epithelial and connective cells, that cooperate with each other by means of basement membrane-mediated cell-cell interaction, like in the normal mucosa. Many recent studies have focused on the interactions between the two cell populations, and finding a way to study them in a single model in a three-dimensional environment without the need to set up complicated co-culture systems or using conditioned media (where the lack of cell-cell interaction is a big limitation) definitely offers significant advantages.
Another key feature of the model is the deposition of neosynthesized ECM by the fibroblasts. Moreover, this model offers the possibility to conduct long-term experiments, to evaluate interactions and signaling between different cell populations, and it is an ideal setup for conducting drug administration studies. The complete absence of immune cells within the model is at the same time a limitation and an advantage, offering the opportunity to selectively add, whether in the epithelial or in the connective layer, cytokines, chemokines or any other factor whose effects one might want to research.
Another limiting aspect of this model is the lack of circulation; this, however, could be easily overcome by the employment of microfluidics, and in fact during the last two months of my PhD we started working on this in collaboration with some colleagues with a background in bioengineering.

One of the potential applications of this model includes the evaluation of the development of cell structures under normal conditions and when exposed to various stimuli. In particular, my interest was directed at the process of ciliogenesis since these specialized epithelial structures are damaged and dysfunctional in chronic inflammatory lung diseases and the major damaging agent affecting the cilia is thought to be cigarette smoke (Thomas B, 2010; Lam HC, 2013). Moreover, very little is still known about the mechanisms that are responsible for these alterations and traditional cell culture models do not permit the application of long-term cigarette smoke exposure. For example, primary bronchial epithelial cells treated with relatively low concentrations (10-20%) of CSE will usually undergo apoptosis within 48 hours. The bronchial outgrowth model instead can be exposed to such stimuli for prolonged periods of up to three to four weeks.

My experiments showed that when bronchial outgrowths were exposed to 20% CSE for 21 days, the ciliated epithelial cells lost their cilia within the first three days of exposure but remained viable until the end of the treatment period. Following the initial stress, epithelial cells started reorganizing their apical surface with newly developed elongated and protein-enriched microvilli and cilia-like structures. During the entire treatment period, these modified apical structures never regained their original architecture and function. The mucus that was produced by the Goblet cells was in fact gathering on top of the cells that were unable to get rid of it. This mucus layer was collected and stored for further analyses. The microvilli appeared hyper functional, probably in an effort to absorb the excess of mucus, while the cilia did not display the characteristic beating motion that could be observed in untreated outgrowths.

As already mentioned, these are just preliminary observations and further studies have already been started in order to evaluate the eventual recovery of the apical structures when the CSE stimulus is withdrawn, and to assess the expression of the main modulators of ciliogenesis at both RNA and protein level.

The last part of my thesis was focused on the efforts to apply this cell culture model to another human mucosa, the oral one.

Tissue-engineered oral mucosal equivalents have been developed for *in vitro* biocompatibility studies, as well as for mucosal irritation and oral disease studies

with the aim to better understand disease process and discover new treatments (Moharamzadeh, 2007; Kinikoglu, 2011). In 1975, Rheinwald and Green introduced a method to grow human keratinocytes in *in vitro* serial cultures, using a feeder layer composed of irradiated mouse fibroblasts and a specific culture medium (Rheinwald, 1975). This method is widely used for the culture of keratinocytes and single-layer epithelial sheets, but such sheets are fragile, difficult to handle and tend to contract (Moharamzadeh, 2007). Multilayer sheets of cultured epithelium were obtained by culturing oral keratinocytes and fibroblasts, crucial for the production of extracellular matrix, on permeable ethylene terephthalate cell culture membrane (PET) at the air/liquid interface (Moharamzadeh, 2008) or in polycarbonate cell culture inserts, developed by SkinEthic Laboratories (Nice, France). These models have the characteristic of being very similar to native epithelium and showing signs of differentiation, such as different cytokeratin expression and basement membrane formation, but not to the point of full differentiation because the cells used are derived from oral squamous carcinoma (Moharamzadeh, 2007). Moreover, epidermal differentiation of transformed keratinocytes is not perfect, and tumor derived cells are abnormal and not suitable for clinical use (Moharamzadeh, 2007).

In the oral outgrowth model, both keratinocytes and fibroblasts outgrow autonomously from an oral biopsy into a 3D gel (Matrigel^{TM}), whose composition is very similar to that of the normal ECM of the oral mucosa. Moreover, after the initial expansion phase, fibroblasts start to lay out a newly formed ECM that is architecturally and structurally compatible with that of the *in vivo* human oral mucosa. In the meantime, the keratinocytes start differentiating because of the air-liquid interface, and after around 15 days of culture the outgrowths present a properly differentiated oral epithelium separated, by a functional basal membrane, from a newly constituted *lamina propria* where fibroblasts lay the ECM. In our opinion, this constitutes a valid model where to study the responses of the human oral mucosa as a whole, to the administration of drugs and other exogenous substances.

REFERENCES

Murray JF. The normal lung. WB Sanders, Philadelphia, 1986

Kuhn C. Ultrastructure and cellular function in the distal lung. In: Thurlbeck WM Abell MR. The lung, Williams & Wilkins, Baltimore,1978

Jeffrey PK. Microscopic structure of the lung. In: Gibson GJ, GeddesJM, Costabel V, Stok PJ, Corrin B (Eds): Respiratory medicine,Elsevier Science, London, 2003; pp. 34-50

Gail DB, Lenfant CJM. Cells of the lung: Biology ad clinical implications. Am Rev Respir Dis 1983; 127: 366-87

Standring S. Gray's Anatomy. Elsevier Churchill Livingstone, Philadelphia, 2005; Chap. 62: pp. 1057-62

© 2011 STCC Foundation Press written by Dawn A. Tamarkin, Ph.D.

Friedl, P. Prespecification and plasticity: shifting mechanisms of cell migration. Curr. Opin. Cell Biol. 16(1), 14–23 (2004).

Boushey, H.A., Holtzman, M.J., Sheller, J.R., Nadel, J.A. 1980. Bronchial hyperreactivity. Am Rev Respir Dis. 121:389-413.

Chung, K.F., Adcock, I.M. 2001. Pathophysiological mechanisms of asthma. Mol. Biotech. 18:213-232.

Cockcroft, D.W., Davis, B.E. 2006. Mechanisms of airway hyperresponsiveness. Chest. 118:551-559.

Dahl, R. 2006. "Systemic side effects of inhaled corticosteroids in patients with asthma". Respir Med. 100(8):1307-1317.

From the Global Strategy for Asthma Management and Prevention, Global Initiative for Asthma (GINA), 2008.

Hargreave, F.E., Nair, P. 2009. The definition and diagnosis of asthma. Clin Exp Allergy. 39:1652-1658.

Jeffrey, P.K., Haahtela, T. 2006. Allergic rhinitis and asthma: inflammation in a one-airway condition.BMC Pulm Med. 30(6 Suppl) 1:S5.

Pawankar, R., Baena-Cagnani, C.E., Bousquet, J., Canonica, G.W., Cruz, A.A., Kaliner, M.A., Lanier, B.Q. 2008. "State of World Allergy Report 2008: Allergy and Chronic Respiratory Diseases". WAO Journal. Supplement S4-S17.

World Health Organization publication. 2003. Prevention of allergy and allergic asthma. Based on the WHO/WAO meeting on the prevention of allergy and allergic asthma. Geneva, 8-9 January 2002.

J. Bousquet, P. K. Jeffery, W. W. Busse, M. Johnson, and A. M. Vignola: "Asthma: from bronchoconstriction to airways inflammation and remodeling," American Journal of Respiratory and Critical CareMedicine, vol. 161, no. 5, pp. 1720–1745, 2000.

S. T. Holgate, "Epithelium dysfunction in asthma: "Journal of Allergy and Clinical Immunology, vol. 120, no. 6, pp. 1233– 1244, 2007.

T. L. Hackett, G. K. Singhera, F. Shaheen et al.: "Intrinsic phenotypic differences of asthmatic epithelium and its inflammatory responses to RSV and air pollution," American Journal of Respiratory Cell and Molecular Biology, vol. 45, no. 5, pp. 1090–1100, 2011.

C. Xiao, S.M. Puddicombe, S. Field et al.: "Defective epithelial barrier function in asthma," Journal of Allergy and Clinical Immunology, vol. 128, no. 3, pp. 549.e12–556.e12, 2011.

E. Stewart, Torr E., Jamili N., Bosquillon et al.: "Evaluation of differentiated human bronchial epithelial cell culture systems for asthma research", Journal of Allergy, vol.2012, article ID 943982.

H. Wan, H. L. Winton, C. Soeller et al.: "Quantitative structural and biochemical analyses of tight junction dynamics following exposure of epithelial cells to house dust mite allergen Der p 1," Clinical and Experimental Allergy, vol. 30, no. 5, pp. 685–698, 2000.

Holgate ST: "The airway epithelium is central to the pathogenesis of asthma". Allergol Int 2008, 57:1-10.

Yamaya M, Finkbeiner WE, Chun SY, Widdicombe JH: "Differentiated structure and function of cultures from human tracheal epithelium". Am J Physiol 1992, 262:L713-724.

Cunningham F, et al. : "Use of large animal models of obstructive lung disease to identify novel therapeutic targets". J Vet Pharmacol Therap 2009, 32(Suppl 1):31-33.

Karp PH, Moniger TO, Weber SP, Nesselhauf TS, Launspach JL, Zabner J, Welsh MJ: "An in vitro model of differentiated human airway epithelia Methods for establishing primary cultures". Methods Mol Biol 2002, 188:115-137.

Fulcher ML, Gabriel S, Burns KA, Yankaskas JR, Randell SH: "Well-differentiated human airway epithelial cell cultures". Meth Mol Med 2005, 107:183-206.

Widdicombe JH, Sachs LA, Morrow JL, Finkbeiner WE: "Expansion of cultures of human tracheal epithelium with maintenance of differentiated structure and function". BioTechniques 2005, 39:249-255.

Coyne CB, Gambling TM, Boucher RC, Carson JL, Johnson LG: "Role of claudin interactions in airway tight junctional permeability". Am J Physiol Lung Cell Mol Physiol 2003, 285:L1166-L1178.

Lee MK, Yoo JW, Lin H, Kim YS, Kim DD, Choi YM, Park SK, Lee CH, Roh HJ: "Air-liquid interface culture of serially passaged human nasal epithelial cell monolayer for in vitro drug transport studies". Drug Delivery 2005, 12:305-311.

E. F.A. van't Wout, A. van Schadewijk, J. Stolk, P. S. Hiemstra: "Pseudomonas AerugINOSa Causes Endoplasmic Reticulum Stress In Primary Bronchial Epithelial Cells Which Is Associated With Disruption Of Tight Junctions". Am J Respir Crit Care Med 185;2012:A1068.

S. Hagner, H. Harb, M. Zhao et al.: "Farmderived Gram-positive bacterium Staphylococcus sciuri W620 prevents asthma phenotype in HDM- and OVA-exposed mice". Allergy 2013; 68: 322–329.

Ege MJ, Mayer M, Normand AC, Genuneit J, Cookson WO, Braun-Fahrl€ander C et al.: "Exposure to environmental microorganisms and childhood asthma". N Engl J Med 2011;364:701–709.

Ege MJ, Mayer M, Schwaiger K, Mattes J, Pershagen G, van Hage Met al.: "Environmental bacteria and childhood asthma". Allergy 2012;67:1565–1571.

Korthals M, Ege MJ, Tebbe CC, von Mutius E, Bauer J: "Application of PCR-SSCP for molecular epidemiological studies on the exposure of farm children to bacteria in environmental dust". J Microbiol Methods 2008;73:49–56.

Schneeberger EE, Lynch RD et al.: "The tight junction: a multifunctional complex".
Am J Physiol Cell Physiol 2004;286:C1213–C1228.

Hartsock A, Nelson WJ: "Adherens and tight junctions: structure, function and connections to the actin cytoskeleton". Biochim Biophys Acta 2008;1778:660–669.

Shin K, Fogg VC, Margolis B: "Tight junctions and cell polarity". Annu Rev Cell Dev Biol 2006;22:207–235.

Knight DA, Holgate ST : "The airway epithelium: structural and functional properties in health and disease". Respirology 2003;8:432–446.

Crystal RG, Randell SH, Engelhardt JF, Voynow J, Sunday ME: "Airway epithelial cells: current concepts and challenges". Proc Am Thorac Soc 2008;5:772–777.

Rabe KF, Hurd S, Anzueto A, Barnes PJ, Buist SA, Calverley P, Fukuchi Y, Jenkins C, Rodriguez-Roisin R, van Weel WC, 890 R. Shaykhiev et al. Zielinski J: "Global strategy for the diagnosis, management, and prevention of chronic obstructive pulmonary disease: GOLD executive summary". Am J Respir Crit Care Med 2007;176:532–555.

Lee G, Walser TC, Dubinett SM: "Chronic inflammation, chronic obstructive pulmonary disease, and lung cancer". Curr Opin Pulm Med 2009;15:303–307.

Sun W, Wu R, Last JA: "Effects of exposure to environmental tobacco smoke on a human tracheobronchial epithelial cell line". Toxicology 1995;100:163–174.

Balda MS, Matter K: “Tight junctions and the regulation of gene expression”. Biochim Biophys Acta 2009;1788:761–767.

Zeisberg M, Neilson EG: “Biomarkers for epithelial-mesenchymal transitions”. J Clin Invest 2009;119:1429–1437.

Vincent T, Neve EP, Johnson JR, Kukalev A, Rojo F, Albanell J, Pietras K, Virtanen I, Philipson L, Leopold PL, Crystal RG, de Herreros AG, Moustakas A, Pettersson RF, Fuxe J: “A SNAIL1-SMAD3/4 transcriptional repressor complex promotes TGF-beta mediated epithelial-mesenchymal transition”. Nat Cell Biol 2009;11:943–950

Reid L, Meyrick B, Antony V, Chang L, Crapo J, Reynolds H: "The Mysterious Pulmonary Brush Cell". American Journal of Respiratory and Critical Care Medicine 2005; Vol. 172, pp. 136-139.

Poole CA, Jensen CG, Snyder JA, Gray CG, Hermanutz VL, Wheatley DN: “Confocal analysis of primary cilia structure and colocalization with the Golgi apparatus in chondrocytes and aortic smooth muscle cells”. Cell Biol Int 1997;21(8):483–494.

Plotnikova O, Golemis E, Pugacheva E: “Cell Cycle-Dependent Ciliogenesis and Cancer”. Cancer Res. 2008; 68(7): 2058–2061.

Santos N, Reiter J: “Building It Up and Taking It Down: the Regulation of Vertebrate Ciliogenesis”. Developmental Dynamics. 2008; 237:1972-1981.

Dawe H, Farr H, Gull K: “Centiole/basal body morphogenesis and migration during ciliogenesis in animal cells”. Journal of Science, 2006; 120, 7-15.

Di Cello et al.: “Cigarette smoke induces epithelial to mesenchymal transition and increases the metastatic ability of breast cancer cells”. Molecular Cancer 2013 12:90.

Zhang H, Liu H, Borok Z, Ursini F: “Cigarette smoke extract-stimulated epithelial-mesenchymal transition through Src activation”. Free Radic Biol Med. 2012 April 15; 52(8): 1437–1442.

Iwahashi H, Iimura S: "Enhancement by cigarette smoke extract of the radical formation in a reaction mixture of 13-hydroperoxide octadecadienoic acid and ferric ions". J Biochem. 2006 Apr;139(4):671-6.

Yamamoto ML, Chapman AM, Schiestl RH: "Effects of side-stream tobacco smoke and smoke extract on glutathione- and oxidative DNA damage repair-deficient mice and blood cells". Mutat Res. 2013;749(1-2):58-65

Mortaz E, Kraneveld AD, Smit JJ, Kool M, Lambrecht BN: "Effect of Cigarette Smoke Extract on Dendritic Cells and Their Impact on T-Cell Proliferation". PLoS ONE 2009; 4(3): e4946.

Hoshino Y, Mio T, Nagai S, Miki H, Ito I, Izumi T: "Cytotoxic effects of cigarette smoke extract on an alveolar type II cell-derived cell line". American Journal of Physiology - Lung Cellular and Molecular Physiology 2001;Vol. 281no. L509-L516.

Park JW, Ryter SW, Kyung SY, Lee SP, Jeong SH: "The phosphodiesterase 4 inhibitor rolipram protects against cigarette smoke extract-induced apoptosis in human lung fibroblasts". European Journal of Pharmacology 2013; Volume 706, Issues 1–3, 76-83.

Moharamzadeh K, Brook IM, Van Noort R, Scutt AM, Thornhill MH: "Tissue-engineered oral mucosa: a review of the scientific literature". J Dent Res 2007; 86(2): 115-24.

Kinikoglu B, Rodríguez-Cabello JC, Damour O, Hasirci V: "The influence of elastin-like recombinant polymer on the self-renewing potential of a 3D tissue equivalent derived from human lamina propria fibroblasts and oral epithelial cells". Biomaterials 2011; 32(25):5756-64.

Rheinwald JG, Green H: "Serial cultivation of strains of human epidermal keratinocytes: the formation of keratinizing colonies from single cells". Cell, 1975;6:331-343.

Moharamzadeh K, Brook IM, Van Noort R, Scutt AM, Smith KG, Thornhill MH: "Development, optimization and characterization of a full-thickness tissue engineered human oral mucosal model for biological assessment of dental biomaterials". J Mater Sci Mater Med. 2008;19(4):1793-801.

Hughes CS, Postovit LM, Lajoie GA: "Matrigel: a complex protein mixture required for optimal growth of cell culture". Proteomics. 2010;10(9):1886-90.

Campisi G, Giannola LI, Fucarino A, Marino Gammazza A, Pitruzzella A, Marciano V, De Caro V, Siragusa MG, Giandalia G, Compilato D, Holgate ST, Davies DE, Farina F, Zummo G, Paderni C, Bucchieri F: "Medium-term culture of primary oral squamous cell carcinoma in a three- dimensional model: effects on cell survival following topical 5-fluororacile delivery by drug-loaded matrix tablets". Curr Pharm Des. 2012;18(34):5411-20.

Hylkema M, Blacquiere M, Geerlings M, Peters M, Timens W, Bufe A, Holst O, Postma D: "Farm Dust Downregulates Th2-Driven Allergic Airway Inflammation In Mice; A Role For Epithelial TLR Expression And Chemokine Production". AIRWAY IMMUNE MECHANISMS AND INFLAMMATION: ANIMAL MODELS. 2011; A2865-A2865

Robbe P: "Farm dust protects against allergic asthma but Induces IL-17-Mediated Airway Inflammation". ATS 2012; 3.2.12.101CO

Richter, Patricia, Hodge, Knachelle, Stanfill, Stephen, Zhang, Liqin and Watson, Clifford: "Surveillance of moist snuff: total nicotine, moisture, pH, un-ionized nicotine, and tobacco-specific nitrosamines". Nicotine & Tobacco Research. 2008; 10:11

Funk, G. F., Karnell, L. H., Robinson, R. A., Zhen, W. K., Trask, D. K. and Hoffman: "Presentation, treatment, and outcome of oral cavity cancer: A national cancer data base report". Head Neck. 2002; 24: 165–180

Faux SP, Tai T, Thorne D, Xu Y, Breheny D, Gaca M: "The role of oxidative stress in the biological responses of lung epithelial cells to cigarette smoke". Biomarkers. 2009;14 Suppl 1:90-6

Howard, D.J., Briggs: "Oxidative DNA damage in mouse heart, liver, and lung tissue due to acute side-stream tobacco smoke exposure". Arch. Biochem. Biophys 1998; 352, 293-297.

Thomas B, Rutman A, Hirst RA, Haldar P, Wardlaw AJ, Bankart J, Brightling CE, O'Callaghan C: "Ciliary dysfunction and ultrastructural abnormalities are features of severe asthma". J Allergy Clin Immunol. 2010;126(4):722-729.e2. doi:

10.1016/j.jaci.2010.05.046. Epub 20 J Clin Invest. 2013 ;123(12):5212-30. doi: 10.1172/JCI69636. Epub 2013.

Lam HC, Cloonan SM, Bhashyam AR, Haspel JA, Singh A, Sathirapongsasuti JF, Cervo M, Yao H, Chung AL, Mizumura K, An CH, Shan B, Franks JM, Haley KJ, Owen CA, Tesfaigzi Y, Washko GR, Quackenbush J, Silverman EK, Rahman I, Kim HP, Mahmood A, Biswal SS, Ryter SW, Choi AM: "Histone deacetylase 6-mediated selective autophagy regulates COPD-associated cilia dysfunction". J Clin Invest. 2013;123(12):5212-30. doi: 10.1172/JCI69636. Epub 2013.

Fishbein AB, Fuleihan RL: "The hygiene hypothesis revisited: does exposure to infectious agents protect us from allergy?". Curr Opin Pediatr. 2012; 24(1):98-102.